University of Stellenbosch

CONCRETE WIND TURBINE TOWERS IN SOUTHERN AFRICA

by

Willem Sternberg van Zyl

Thesis presented in fulfilment of the requirements for the degree Master of Engineering (Research) in the Faculty of Engineering at Stellenbosch University

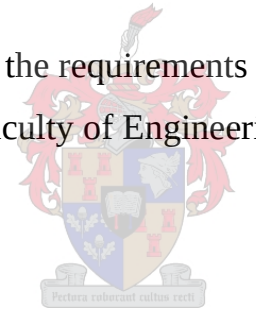

Supervisor: Prof G.P.A.G. van Zijl

Department of Structural Engineering

December 2014

Declaration

By submitting this thesis electronically, I declare that the entirety of the work contained therein is my own original work, that I am the authorship owner thereof (unless to the extent explicitly otherwise stated) and that I have not previously in its entirety or in part submitted it for obtaining any qualification.

December 2014

Abstract

Exponential growth of the global wind turbine market has led to a significant increase in the capacity of wind turbine generators. Modern turbines require higher support structures as higher wind speeds combined with longer blades are necessary to increase their generating capacity. The standard 80-90 m tower is thus not economically viable anymore. Transportation logistics of large steel towers has led to concrete towers becoming a viable option. There are currently no design codes dealing exclusively with the design of concrete wind turbine towers. The aim of this project is to investigate and highlight important aspects of the design process of a normally reinforced high strength concrete wind turbine tower. The tower was designed using nonlinear finite element modelling as a design tool to accurately design the tower for various loads and load cases. An analytical design method was developed that can be used in the preliminary design stage. Finally, the importance of the soil-structure interaction was investigated through a sensitivity analysis.

It was found that the formation of cracks greatly affected the stiffness of the structure and that the reduction in stiffness increased the deflection significantly. It was also found that a structure that has sufficient strength to resist the ULS loads may not necessarily comply with the maximum deflection limit for the SLS. The concrete strength class required was not only determined by the maximum compression stress the concrete would experience, but also by the stiffness required to ensure that the tower frequency is within the turbine's working frequency. The dynamic behaviour of the tower was also affected by the formation of cracks. The fundamental frequency of the tower was reduced by 46% after the SLS loads were applied. It was found that the soil preparation for the foundation plays a vital role in ensuring that the tower frequency is not reduced to a level where it falls outside the turbine working frequency.

Samevatting

Die eksponensiële groei van die globale wind turbine mark het gelei tot ’n beduidende toename in die opwekkingskapasiteit van wind turbine kragopwekkers. Moderne turbines benodig hoër ondersteuningstrukture om hulle opwekkingskapasiteit te verhoog en daarom is die standaard 80-90 m toring nie meer geskik nie. Die vervoer logistiek van groot staal torings het daartoe gelei dat beton torings ’n lewensvatbare opsie geword het. Daar is huidiglik geen ontwerpkodes wat uitsluitlik handel met die ontwerp van beton wind turbine torings nie. Die doel van hierdie projek is om die ontwerp proses van ’n bewapende hoë sterkte beton wind turbine toring te ondersoek en belangrike aspekte uit te lig. Die toring word ontwerp deur ’n nie-liniêre eindige element model te gebruik as ’n ontwerp hulpmiddel, om die toring akkuraat te ontwerp vir verskeie laste en lasgevalle. ’n Analitiese ontwerpmetode is ontwikkel wat gebruik kan word in die voorlopige ontwerpfase. Laastens is die grond-struktuur interaksie ondersoek deur ’n sensitiwiteitsanalise.

Daar is gevind dat die vorming van krake die styfheid van die struktuur aansienlik beïnvloed en dat die vermindering in styfheid die defleksie beduidend vermeerder. Daar is ook gevind dat ’n struktuur wat voldoende sterkte het om die uiterste lastoestande te weerstaan, nie noodwendig voldoen aan die maksimum defleksiegrens vir die diens lastoestande nie. Die beton sterkte klas wat benodig is, is nie net bepaal deur die maksimum druk spanning wat die beton sal ondervind nie, maar ook deur die styfheid wat vereis word om te verseker dat die toring se frekwensie binne die turbine se werksfrekwensie val. Die dinamiese gedrag van die toring is ook beïnvloed deur die vorming van krake. Die fundamentele frekwensie van die toring is verlaag met 46% nadat die diens lastoestande toegepas is. Daar is gevind dat die grond voorbereiding vir die fondasie ’n belangrike rol speel om te verseker dat die toring se frekwensie nie verlaag word tot ’n vlak waar dit buite die turbine se werksfrekwensie val nie.

Acknowledgements

I would sincerely like to thank the following people for their assistance and time. Without their help this project would not have been possible:

- Professor GPAG van Zijl, my supervisor, for his support and guidance throughout the project and for always taking time to share his knowledge.

- Dr JAVB Strasheim for his help with DIANA

- The Department of Structural Engineering at the University of Stellenbosch for the necessary funds to do the study

Table of Contents

List of Figures

List of Tables

List of Abbreviations

ACI	American Concrete Institute
ASCE	American Society of Civil Engineers
ASR	Alkali-aggregate reaction
CSF	Condensed silica fume
DEL	Damage equivalent load
EOG	Extreme operating gust
EWM	Extreme wind model
FA	Fly ash
FEM	Finite element model
GFM	Gust factor method
GGBS	Ground granulated blast furnace slag
GGCS	Ground granulated Corex Slag
GWEC	Global Wind Energy Council
HPC	High performance concrete
HSC	High strength concrete
IEC	International Electrotechnical Commission
IRP	Integrated Resource Plan
NREL	National Renewable Energy Laboratory
NSC	Normal strength concrete
REIPPPP	Renewable Energy Independent Power Producer Procurement Program
SA	South Africa
SANS	South African National Standards
SCMs	Supplementary cementitious materials
SLS	Serviceability limit state
ULS	Ultimate limit state
W/B	Water-binder ratio
WASA	Wind Atlas of South Africa
WTG	Wind turbine generator

Chapter 1: Introduction

1.1. Background

Modern civilization is dependent on energy. The global energy demand is steadily rising each year and is accompanied by rising greenhouse gas emissions. Global Warming is a real danger and worldwide governments are implementing goals for generating large percentages of their countries' energy needs with renewable energy. The Global Wind Energy Council (GWEC) predicts that by 2035 renewable energy will be generating more than 25% of the world's electricity needs, with a quarter of this coming from wind energy (GWEC, 2013). Wind energy is currently the second largest renewable energy source, after hydro power, and it has been growing exponentially over the last decade. In Figure 1-1 the global cumulative installed wind capacity is shown.

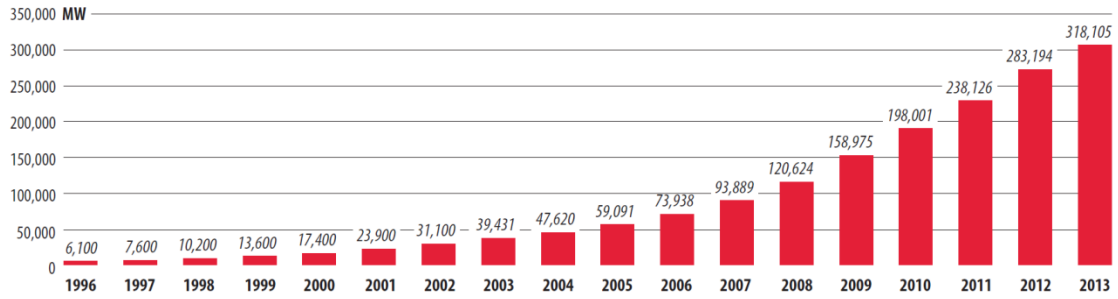

Figure 1-1: Global cumulative installed wind capacity (GWEC, 2013)

South Africa (SA) has the seventh largest coal reserve in the world. In 2012, 72% of the country's electricity was being produced by coal, 24% by oil and natural gas, 3% by nuclear, and less than 1% by renewable energy. This dependence on hydrocarbons, particularly coal, has made SA the 12th largest CO_2 emitter in the world (GWEC, 2013).

The Renewable Energy Independent Power Producer Procurement Program (REIPPPP) was created to encourage the exploitation of SA's vast renewable energy reserves. SA's long-term energy blueprint, the Integrated Resource Plan (IRP), specifies that about 9,000 MW of electricity must be produced by wind energy by 2030. The first phase of 634 MW of wind energy is currently in operation and is connected to the national electricity grid. The second phase of 562 MW is currently under construction.

A Wind Turbine Generator (WTG) mainly consists out of 6 components, namely: Foundation, Tower, Hub, Nacelle, Rotor blades and Transformer. The different components are shown in Figure 1-2. The structural engineer has the ability to influence the design of the tower and foundation. These two components make up a significant part of the total cost. For a typical onshore wind turbine, the tower will account for 17% of the total cost and the foundation will account for 16% of the total cost (IRENA, 2012). The cost is, however, strongly influenced by the specific site and specific turbine. Large savings can thus be achieved by optimizing the design of the tower and foundation.

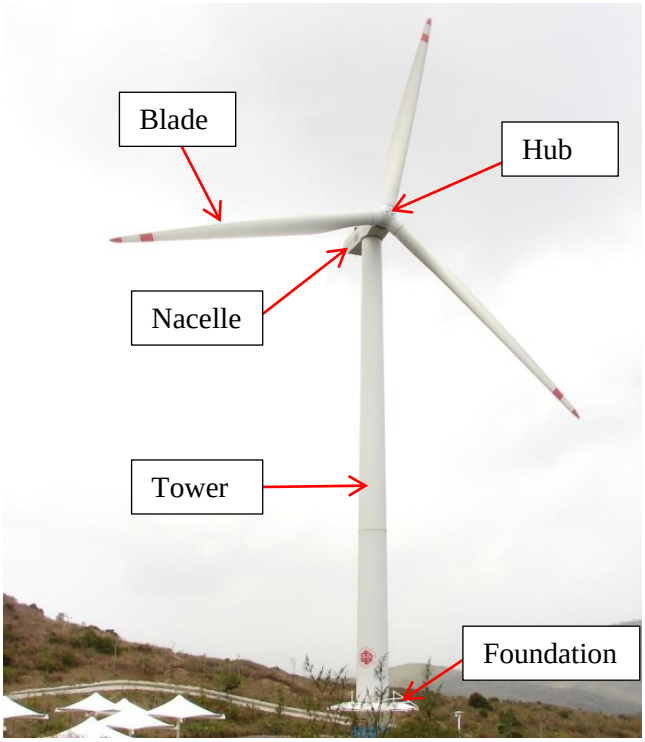

Figure 1-2: WTG components

The worldwide movement to generate large amounts of electricity with wind turbines has led to an significant increase in wind turbine size. Turbine sizes have increased from a couple of kilowatts in the 1970's to anything between 2000 and 7500 kilowatt turbines today. One method of increasing the capacity of wind turbines, is to increase the annual average wind speed that the turbine will be exposed to. This can be achieved by choosing a site with a high annual average wind speed, as well as increasing the hub height of the turbine. The effect of surface roughness decreases with height, thus a more constant wind speed can be achieved by placing the turbine higher.

Low wind speed sites can be utilized by increasing the rotor blade diameter. Onshore wind turbine rotor diameters of up to 126 m are being used in low wind speed sites. The rule of thumb is that the tower must be at least the height of the blade diameter, thus requiring the towers to increase in height.

The standard 80-90 m tower is therefore not suitable anymore if the capacity of the turbine is to be increased. A steel tower's base diameter is limited to approximately 4.2 m due to transportation logistics. The diameter limitations make steel towers uneconomical at hub heights greater than approximately 80-90 m. One solution to the height limitation is to use concrete towers. Concrete wind turbine towers can either be pre-cast and assembled on site, or slip-formed. This has the advantage that the tower segments can either be made small enough to transport by normal truck or the tower can be produced on site. This overcomes the limitation on the diameter of the tower and therefore there is no limitation on the height that is possible.

There are currently no structural design codes that specifically give design guidelines for the design of concrete wind turbine towers. This has resulted in a handful of companies worldwide, which have the

knowledge to design these towers, having a monopoly in the industry. It is therefore of paramount importance to develop a design process that will enable countries like SA, to design their own concrete towers. This will have great economic benefits. It is estimated that the cost of wind turbines in SA is 18 million ZAR per MW (Szewczuk , 2012). The first two phases of wind farms currently in progress make up 1196 MW and thus have an approximate cost of 21.5 Billion ZAR. Currently almost all the design work, apart from foundation design, is done by engineers from abroad. The structural consulting industry of SA can significantly benefit from doing the structural design work of SA and even other African countries' wind farms.

1.2. Layout and objectives of this study

The overall objective of this study is to investigate the design process required to design a concrete wind turbine tower. A nonlinear Finite Element Model (FEM) is used as a design tool to evaluate the tower. Focus is put on determining the appropriate wind models and wind loads to accurately model the tower. The FEM is then used to study the behaviour of the tower under different loading conditions to determine the critical design load case. The effect that crack formation has on the tower's stiffness and dynamic behaviour is studied and a sensitivity analysis is done to determine the effect that soil stiffness has on the fundamental frequency of the tower. Different structural design codes are then used to create an analytical design method that can primarily be used in the preliminary design stage - but in certain cases may even be appropriate to use in the final design stage. The analytical design method is compared to the FEM to determine its accuracy. The aim of the project is to provide the structural engineer with a basic design process that can be followed when designing a concrete wind turbine tower and to highlight important design considerations.

1.3. Scope

The scope of this investigation is large onshore wind turbines, as this seems to be the trend of the SA wind industry. A tower height of 100 m is used, as this is the approximate height limit of cost effective steel towers. High strength concrete (HSC) with normal reinforcing steel is used for the design of the tower. A traditional concrete gravity spread foundation is used to support the tower. The standard wind speeds given by the International Electrotechnical Commission (IEC) are used, but are compared to actual site wind conditions. Generic soil conditions are investigated to determine the effect it has on the fundamental frequency of the tower.

1.4. Outcome of investigation

- Verify structural strength of large concrete turbine towers
- Verify stability of large concrete turbines towers
- Determine accuracy of analytical design methods when compared to FEM
- Determine the effect different soil conditions have on the dynamic behaviour of the tower.
- Determine the loss of stiffness due to cracking and evaluate the effect that it has on the dynamic behaviour of the tower

Chapter 2: Literature review

2.1. Introduction

Primitive versions of wind turbines have been around for decades. It is estimated that there are approximately 22,000 borehole windmills in SA (Szewczuk , 2012). Modern turbines evolved from earlier concepts like the one and two bladed horizontal axis wind turbines, the upwind turbine, as well as the vertical axis turbine. Today the three bladed horizontal axis wind turbine dominates the wind energy industry.

Over the years there have been numerous different wind turbine tower concepts. Many early wind turbines used lattice towers. The highest lattice tower is in Germany and has a hub height of 141 m. These towers consist out of normal steel profiles bolted together in a truss configuration. The main advantage of lattice towers is that they use much less steel to achieve the same strength and stiffness as normal monopole towers and are thus cheaper. The major disadvantage of lattice towers is their visual appearance and large number of joints. Guy-wired towers and three-legged towers are primarily used for small scale wind turbines. Today steel and concrete monopole towers are used almost exclusively. The different tower concepts discussed are shown in Figure 2-1.

Figure 2-1: Different tower concepts (DNV & Riso, 2002)

2.2. Steel monopole towers

Today the most common turbine tower is the steel monopole. Traditionally steel has been used because of its excellent strength to weight ratio. Steel is also a ductile material and thus allows large deformations to take place before failure occurs. The tubes forming the tower are manufactured out of rolled steel plates. The tower outside diameter tapers from the bottom, where the most strength is

required, to the top. The wall thickness also varies with height to create an economical structure. The conical sections forming the tower have flanges at both ends so they can be bolted together on site, ensuring a short erection time. The tower is normally manufactured in sections varying from 20-30 m in length, depending on the means of transport to site. Transportation of the tower segments is the main disadvantage of steel towers. All steel towers must be manufactured at a steel mill which is normally situated on the outskirts of large cities. Wind farms require unobstructed wind flow to be efficient and therefore are normally constructed in rural areas. This causes the steel sections to be transported over long distances by road. In SA the maximum height of a truck from the road surface to the top of the load is 4.3 m (TRH 11, 2009). The tower sections are transported on special trucks that optimize this usable height and can thus carry a tower with maximum diameter of approximately 4.2m, allowing for space between the road and load. One of these special trailers is shown in Figure 2-2.

Figure 2-2: Special tower transport trailer (Dvorak, 2011)

As a result, this transportation limit puts a practical limit on hub heights for steel of around 100 m (Brughuis, 2004). Due to this limitation it is estimated that concrete towers become cheaper than steel towers at a height of 80-100m. It is possible that in SA concrete towers are cheaper at even lower hub heights due to long transport distances and a relatively small steel tower manufacturing industry compared to the concrete tower industry. Until recently, SA imported all steel towers from abroad. In January 2014 the DCD Group's steel tower factory began production in Coega, Port Elizabeth. A second steel tower factory is currently under construction in Atlantis in the Western Cape. This will certainly reduce the transportation distance to certain sites, but wind farms not close to one of these two factories will still require that tower sections be transported over long distances. Another disadvantage of steel towers is that the world steel price is quite volatile. This can make it difficult to determine the cost of a wind farm at tender time, which can be months or even years before the project will be executed. In Figure 2-3 the historical evolution of the US iron ore and precast concrete prices are shown (Gaspar, 2012).

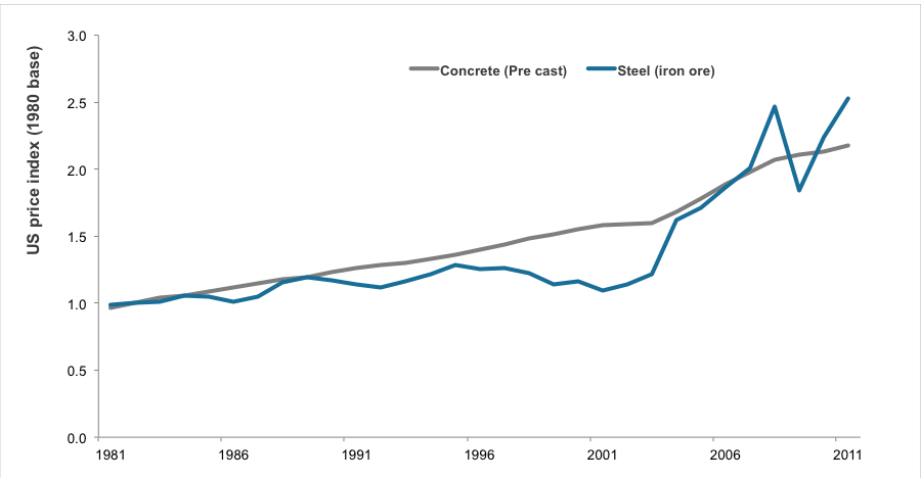

Figure 2-3: Fluctuation of steel and precast concrete price (Gaspar, 2012)

Wind turbine structures are exposed to dynamic loading not typically found in normal civil engineering structures. Winds are often turbulent and can fluctuate with time, this will cause the wind load on the blades, and in turn on the tower, to fluctuate. Steel's most valuable asset, its high strength, makes it vulnerable to fatigue. Fatigue life governs the design of steel towers (LaNier, 2004). A material's fatigue life is directly proportional to the stress range the material will be exposed to. Therefore, by increasing the thickness of the steel shell of the tower, the stresses are lowered and the fatigue life increased, but this also increases the cost of the tower. Steel towers are commonly designed only for an operational life span of 20 years.

2.3. Concrete wind turbine towers

Concrete is the single most widely used construction material in the world and until recently completely absent in the wind turbine tower industry. Although in recent years the concrete tower industry has grown fast, steel towers still dominate the industry. One of the biggest advantages of concrete is that it is readily available, especially in SA. Concrete towers can be cast on site or in a factory in the form of precast concrete segments. These segments are similar to the conical sections used for steel towers, with the main difference being that the segments can be broken up into sections in the circumferential direction. Concrete towers can be reinforced with normal reinforcing steel consisting out of four layers of steel. Two vertical layers of steel are placed just inside the wall, and a further two layers of horizontal steel are placed aside each vertical layer. This is shown in Figure 2-4. The whole tower can also be post-tensioned. The normal reinforcing layout is then still used, but the percentage vertical steel is significantly reduced. Both the precast segments and cast on site construction methods have the advantage that there is no transportation limit placed on the diameter of the tower and thus no limit on the height of the tower. Concrete is a durable material and, if properly designed, can survive extreme conditions for 50-100 years. Concrete towers have a long fatigue life that makes it possible to retrofit the tower with a new turbine after the turbine's 20 year design life. A concrete tower's self-weight is significantly larger than that of a steel tower which helps to resist the

large overturning moment induced by wind forces. The foundation of a concrete tower can be up to 30-40% lighter than that of a steel tower thus reducing the cost of the foundation.

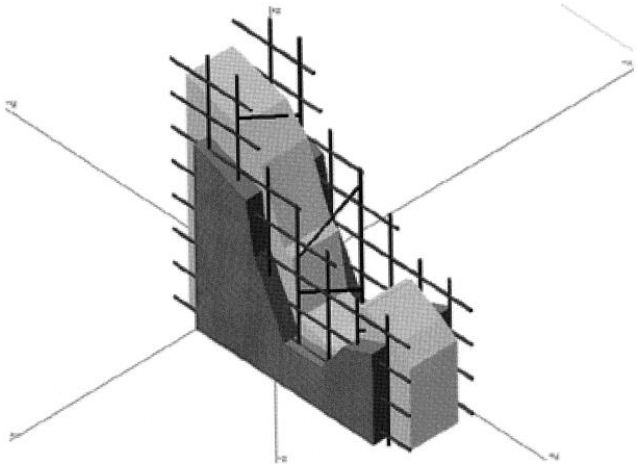

Figure 2-4: Reinforcing layout of concrete tower

There are mainly three different concrete tower designs concepts currently available. They are:

- Slipform
- Large and small precast segments
- Hybrid

2.3.1. Slipform

Slipforming is a method for constructing vertical concrete structures using a self-climbing formwork system. In slipform construction, the formwork is constantly moving upwards as the structure is cast. The concrete is thus cast continuously until the required height is reached. The technology is well established in SA's concrete chimney industry. The advantages and disadvantages are given below:

Advantages:

- No need for transport of precast units to wind farm
- Monolithic concrete structures with no cold joints
- Crane cost and logistic problems are reduced
- Construction in remote areas is possible

Disadvantages:

- Longer construction period than precast construction (Construction rate approximately 250 mm per hour)
- Possible higher cost than precast construction depending on the specific construction site
- Custom formwork required for each tower if more than one tower is constructed simultaneously
- Minimum wall thickness in the range of 150–175 mm

The main disadvantage of slipform construction is the construction time. At a rate of 250 mm per hour it will take 16.7 days to complete one tower, if construction continues 24 hour a day. The number of towers constructed simultaneously can be increased by increasing the number of formwork platforms, but this will increase the cost significantly. A slipform concrete tower construction is shown in Figure 2-5.

Figure 2-5: Typical slipform tower (NorthField)

2.3.2.Large and small precast segments

Precast concrete is no new concept and it has been used for years in the construction of floor slabs, stairs, retaining walls and various other structural elements. There are mainly two types of precast construction used for wind turbine towers. The tower can either be built using large segments with a height of 20-25 m or small ring segments approximately 3 m high.

The large precast segments concept involves using long curved concrete panels. The tower diameter is divided into segments to reduce the size of the panels. Normally for large towers the base is divided into three panels, 120 degrees each. This ensures that the segments can be transported on normal roads without exceeding the height limit. Due to the fact that the tower diameter reduces with height, it is possible to divide the middle section of the tower in 180 degree segments and the top section of the tower can be cast as a cylinder. This will however depend strongly on the height and dimensions of the specific tower. The segments are then connected on site to form a tubular section 20-25m long -as shown in Figure 2-6. The joints are a crucial part of precast construction, because they ensure that the tower behaves like a monolithically cast structure. Various joint configurations are available - one solution is to cast a groove opening at the side of each section. Reinforcing steel is extended out of the segment and into the groove to ensure a rigid connection. Rubber seals are placed at the edges where

the segments will be connected. The two segments are then aligned with their grooves facing each other with the steel reinforcing of the two panels overlapping in the opening. Finally the joint is filled with grout to ensure the panels are bonded. A typical vertical joint is shown in Figure 2-7.

Figure 2-6: Assembled tower pieces (de Rábago, 2011)

Figure 2-7: Vertical joint detail (de Rábago, 2011)

The panels can be connected to form the tubular sections using a smaller crane, than is needed to erect the nacelle and for placing the tubular sections on top of each other. At the base of the tower the tubular section will typically be constructed from three panels. The crane used, can thus be a third of the size needed to place the tubular sections on top of each other. By reducing the time a large crane

spends on site, overall construction cost can be reduced, as these cranes typically account for a large percentage of the construction cost.

This precast concept is already a well-established technology in countries like Spain, Germany and some parts of the USA. The first SA wind farm to use this technology is currently under construction at Gouda in the Western Cape. The farm will consist of 46 ACCIONA 3 MW wind turbines totalling 138 MW of installed capacity. The towers are precast concrete with a hub height of 100 m.

Small precast segmental construction uses the same concept as large segments with the main difference being that the segments' height is considerably less. Typical small segments are 3m in height compared to the 20-25m of large segments. One advantage of the smaller sections is that it can be transported on normal trucks and lifted into place with relatively small cranes. The large number of segments significantly increases the number of joints which in turn increases the cost. The choice between large and small precast segments will be strongly influenced by the specific site.

Transportation cost of tower segments can account for a large percentage of the total cost of the tower, particularly when wind sites are remote or served by poor transportation networks. Companies like Enercon regularly use mobile precast concrete factories for the production of tower segments. This has two advantages, firstly transportation cost is reduced significantly and secondly local labour can be used. One of Enercon's mobile precast factories used in Gujarat in India, is shown in Figure 2-8. The advantages and disadvantages of precast segmental construction are given below:

Advantages:

- Fast production due to industrialized production process
- High quality due to efficient quality control
- No need for abnormal transport to the construction site
- Construction time equivalent to that of existing steel towers is reported by companies

Disadvantages:

- Large crane is required for final erection
- Precast factory is required
- Connection design can be complex

Figure 2-8: Mobile precast factory (Gaspar, 2012)

2.3.3.Hybrid

The third tower concept currently utilized by the wind industry is hybrid towers. Hybrid towers combine concrete and steel towers. As mentioned earlier, the height of steel towers is limited by transportation logistics of the base part of the tower. Hybrid towers overcome this problem by using a concrete base with a normal tubular steel part mounted on top of the concrete. A typical hybrid tower is shown in Figure 2-9. The tower thus has no height limit due to transportation limits, as the concrete base can be made to any diameter. Hybrid towers can achieve heights of 140 m and higher. Compared to full concrete towers, the hybrid solution is much lighter which in some cases may be beneficial. The construction time of hybrid towers may be less than full concrete towers, depending on the height of the tower and the site location. The main disadvantage of hybrid towers is that they still use tubular steel sections that must be manufactured at a steel mill. This results in the steel sections to be transported long distances and therefore increases the cost of the tower.

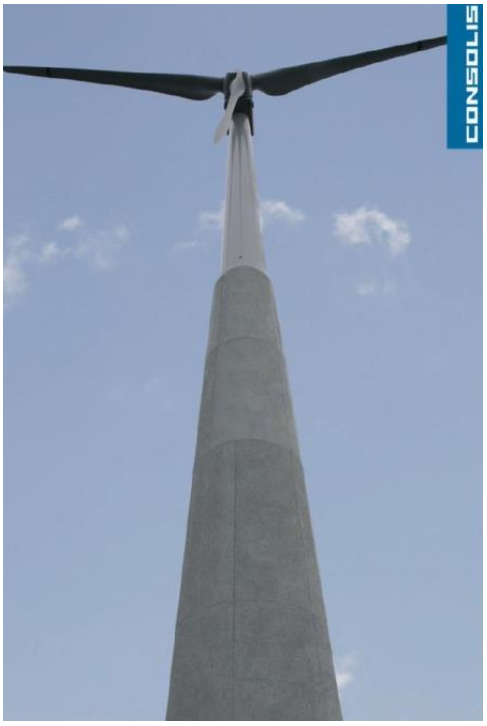

Figure 2-9: Hybrid tower solution (de Rábago, 2011)

2.4. Wind loads

Wind is the predominate loading on tall freestanding towers like wind turbines. Wind is unsteady and exhibits random fluctuations in both the time and space domains. Because wind can be considered to possess stationary characteristics, it is possible to describe its functions in statistical terms. Advances in computational techniques have made it possible to generate wind histories and wind fields with the same statistical characteristics as real wind. Generally it is assumed that the wind velocity is made up of a constant or mean wind speed component, and a fluctuating velocity component due to turbulence or gusting, caused by the ground roughness (Buchholdt & Moossavi Nejad, 2012). The flow of air close to the surface of the earth is disturbed by drag forces caused by the roughness of the ground. This surface roughness can be a result of mountains, vegetation and manmade objects obstructing the flow of the wind. The drag force caused by surface roughness will decrease the wind speed near the surface and can cause random variations in magnitude and direction. The effect of surface roughness increases as the roughness of the terrain increases. The influence of surface roughness decreases with height. At approximately 300 – 600 m above the ground the effect of surface roughness is negligible. This height is called the gradient height. The gradient height will vary depending on the surface roughness of the specific terrain. It has been established that recording periods between 10 minutes and 2 hours provide reasonably stable values for the mean component of the wind speed (Buchholdt & Moossavi Nejad, 2012). Most structural design codes use a 10 minute mean wind speed at a height of 10 m for a reference wind speed to calculate wind loads on structures. There are various models describing the change in mean wind speed with height. Two of the most used are the power law and the logarithmic law.

Power law:

$$V(z) = V_{ref}\left(\frac{z}{z_{ref}}\right)^{\alpha} \tag{2.1}$$

Where,

V_{ref} is the 10 minute average wind speed at a height of 10 m

z_{ref} is the reference height of 10 m

z is the height above the ground where the wind speed is required

α is the power law exponent and is a function of the ground roughness

Logarithmic law:

$$V(z) = 2.5U_{*}ln\left(\frac{z}{z_0}\right) \tag{2.2}$$

Where,

$$U_{*} = \frac{V_{ref}}{2.5\ ln\left(\frac{10}{z_0}\right)} \tag{2.3}$$

and

z_0 is the roughness length

u_* is the shear velocity or friction velocity

The wind turbine industry generally uses the power law to describe the variation in mean wind speed with height. Table 2-1 gives power law exponents for different terrain types. A typical power law wind profile is given in Figure 2-10 ($\alpha = 0.2$, $V_{ref} = 30$ m/s, $z_{ref} = 10$ m).

Table 2-1: Typical power law exponents for different terrain types (Ray, 2006)

Terrain Description	Power law exponent, α
Smooth, hard ground, lake or ocean	0.10
Short grass on untilled ground	0.14
Level country with foot-high grass, occasional tree	0.16
Tall row crops, hedges, a few trees	0.20
Many trees and occasional buildings	0.22 – 0.24
Wooded country – small towns and suburbs	0.28 – 0.30
Urban areas with tall buildings	0.4

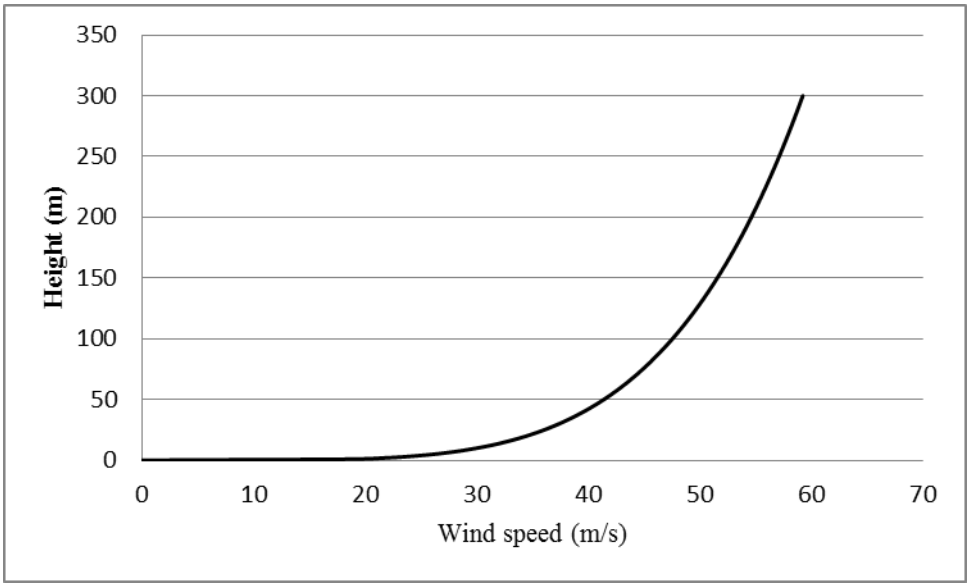

Figure 2-10: Power law wind profile

Flexible structures, like wind turbine support structures, experience wind induced loading in the along-wind and across-wind direction. Along-wind loading is caused by the drag component of the wind and is in the direction of the mean wind flow. Across-wind loading is caused by the "lift" component of the wind and acts perpendicular to the mean wind flow direction.

2.4.1. Along-wind loading

The along-wind loading consists of two parts - a static constant wind pressure, as well as a variable dynamic part due to the gust buffeting effect of turbulent wind flow. The gust buffeting effect causes a dynamic response in the direction of the mean wind flow and can only accurately be modelled using a dynamic analysis. In practice structural engineers rarely use dynamic analyses to design structures due to their timely and costly nature. The gust factor method (GFM) was developed to solve this problem

and enable engineers to estimate the equivalent static load induced by a dynamic wind load. The method involves the use of a gust effect factor that increases the static wind load to account for additional dynamic loading due to wind turbulence and structure interaction. The fluctuation of the mean wind speed due to turbulence is shown in Figure 2-11. The GFM method does not account for across-wind loading. These effects should still be checked. The gust effect factor accounts for the increase in the mean wind loads due to the following factors (Adhikari, 2010):

- Random wind gusts acting for short durations over the entire structure or sections of the structure.
- Fluctuating pressures induced in the wake of the structure, including vortex shedding forces.
- Fluctuating forces induced by the motion of the structure.

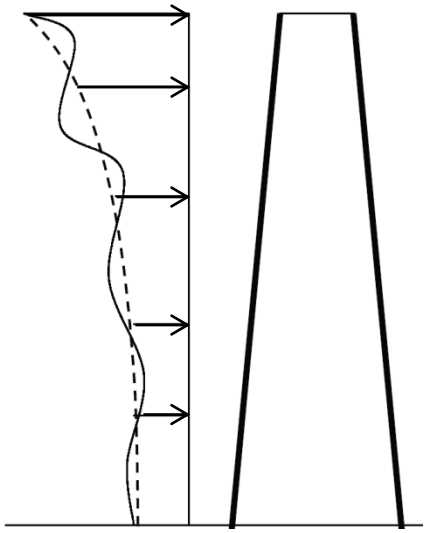

Figure 2-11: Fluctuation of mean wind speed with height

2.4.2. Across-wind loading

Across-wind loading refers to oscillating movement of a structure in the direction perpendicular to that of the mean wind flow direction. This movement induces dynamic forces in the structure perpendicular to the main wind force direction. A cylindrical structure like a wind turbine tower can be classified as a bluff body. A bluff body is one in which the length in the flow direction, is close to or equal to the length perpendicular to the flow direction. Air moving past a bluff body separates from the body as it moves past. This separated flow causes high negative pressures in the wake region behind the body. The wake region is highly turbulent and this causes the formation of eddies or vortices behind the bluff body. At a certain velocity for a specific bluff body, vortices are shed alternately from opposite sides of the bluff body - this is known as alternate vortex shedding. When a vortex is formed on one side of the body, the wind velocity increases on the opposite side. This increase in velocity causes the pressure to decrease, which in turn results in a pressure difference between the two sides that creates a force away from the side where the vortex is formed. This effect is

illustrated in Figure 2-12 where the blue areas are low pressure zones and the red areas are high pressure zones.

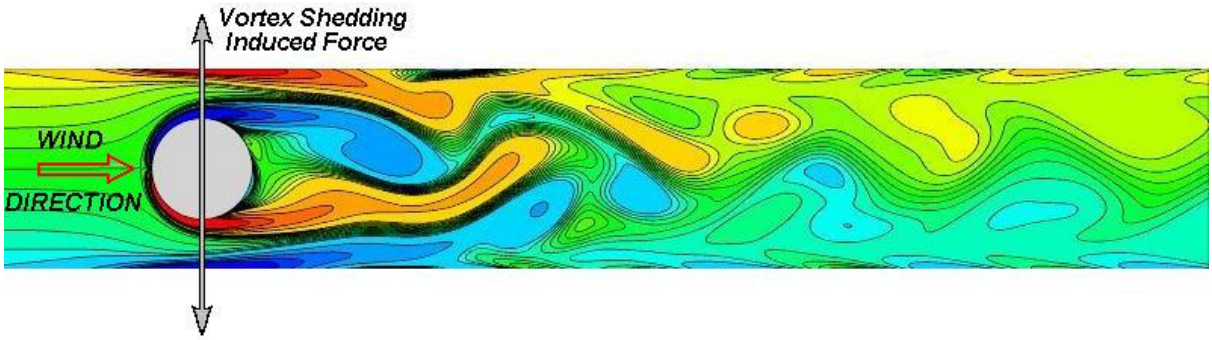

Figure 2-12: Vortex Shedding phenomenon induced by wind flowing over a cylinder (Giosan)

This organized pattern of vortices is referred to as Von Karman's vortex street. A cylinder is said to be "locked in" when the structure's fundamental frequency is equal to the vortex shedding frequency. This causes the structure to resonate and can even cause structural failure due to excessive deformation. The vortex shedding mode for a cylindrical structure depends on the Reynolds number. The Reynolds number is given by:

$$Re(z) = \frac{V(z)D}{v} \tag{2.4}$$

Where,

V(z) is the wind speed at the height of interest

D is the diameter of the structure

v is the kinematic viscosity of air taken as 15×10^{-6} m^2/s

Vortex shedding tends to occur with steady continuous winds at a specific velocity. The velocity does not have to be very high, but it has been found that significant vibration does not occur unless the velocity is greater than 5 m/s. Turbulent winds, which might occur in a fifty year storm, typically will not cause vortex shedding. In fact, if the wind velocity is greater than 15 m/s, the wind is generally too turbulent for vortex shedding to occur. Thus winds that are dangerous for vortex shedding are steady winds in the velocity range 5 to 15 m/s (Giosan). Vortex shedding can be described by the dimensionless number called the Strouhal number (St). The Strouhal number is given by the equation below:

$$St = \frac{f.L}{V} \tag{2.5}$$

Where,

f is the vortex shedding frequency

L is the characteristic length

V is the wind speed

The Strouhal number has been experimentally determined for various bluff shapes and Reynolds numbers and is given in Figure 2-13. In practice, the Strouhal number is generally taken as 0.2 for the design of normal structures. This is due to the fact that usually not all the necessary parameters for calculating the Strouhal number, are known at the design stage. It can be seen in the Figure 2-13 that 0.2 is a good first assumption at the preliminary design stage, but it may be necessary to do a more accurate calculation in certain cases if the Reynolds number is extremely large or small.

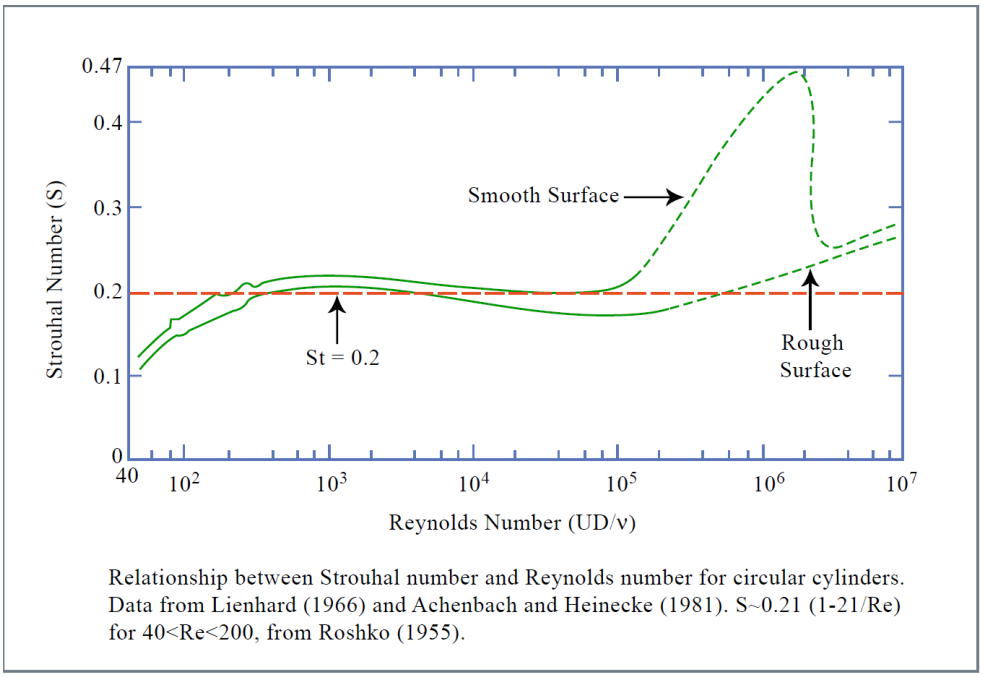

Relationship between Strouhal number and Reynolds number for circular cylinders. Data from Lienhard (1966) and Achenbach and Heinecke (1981). S~0.21 (1-21/Re) for 40<Re<200, from Roshko (1955).

Figure 2-13: Strouhal number of circular cylinders (Techet, 2005)

Usually the critical wind speed at which vortex shedding will cause resonance, is of importance. Equation 2.5 can be rewritten in terms of the critical wind speed by setting the characteristic length equal to the tower diameter. At resonance, the tower's fundamental frequency is equal to the vortex shedding frequency. The critical wind speed at which locking will occur is then given by:

$$V = \frac{f.D}{St} \tag{2.6}$$

Where,

f is the fundamental frequency of the tower

D is the tower diameter

St is the Strouhal number

2.5. Temperature load effects

Temperature differences between the inside of the tower and the outside can cause significant temperature loads to arise inside the concrete shell. During the day when the tower is exposed to solar radiation, the outside concrete's temperature rises. The temperature inside the tower stays almost constant due to no direct solar radiation. This difference in temperature causes a temperature gradient between the outside surface and inside surface of the concrete shell. The outside surface concrete wants to expand relative to the inside surface concrete. Due to monolithic action this is not possible and thus equal expansion takes place. The equal expansion causes horizontal and vertical tensile stresses to arise at the inside surface of the concrete. At night there is no direct solar radiation on the outside surface and as the outside air cools down, the temperature gradient is reversed. Tensile stress will now arise at the outside surface of the concrete shell.

Horizontal reinforcing steel is thus required to resist the horizontal temperature tensile forces at the outside and inside surface. Reinforcing hoops are usually placed around the vertical reinforcing steel. The vertical reinforcing steel must be designed to resist the temperature tensile forces in addition to the normal stresses caused by the overturning moment.

2.6. Ovalization of tower walls

When air moves past a circular bluff body, like a wind turbine tower, it causes positive pressure on the upwind side of the tower and negative pressure at the sides and downwind side of the tower. The negative pressure at the sides of the tower, in combination with the positive pressure at the upwind side of the tower, may cause ovalization of the circular tower. Ovalization causes horizontal bending moments inside the walls of the tower. The horizontal normal stresses caused by the ovalization moment must be taken into account when designing the horizontal reinforcing steel. Ovalization usually occurs at the open end of concrete chimneys. It can also occur at other positions if the structure's walls are very slender. An example of such slender structures is cooling towers used by coal power plants.

The turbine structure at the top of a concrete wind turbine tower will prevent ovalization from occurring. The walls of concrete wind turbine towers are designed to resist large overturning moments and gravity loads caused by the turbine, and thus these structures are usually not slender enough to make them prone to ovalization.

2.7. Fatigue

Wind turbine components are subjected to variable loads due to the variable nature of the wind. These cyclic loads cause cumulative damage in materials and can lead to structural failure over time. The magnitude of fatigue loads are usually far below the static failure load of the material and thus fatigue failure will only occur after a large number of load cycles. This is known as high cycle fatigue. The first step in a fatigue analysis, is to convert the time stress history of the wind turbine to a specified number of stress ranges, each occurring a certain number of times. This is known as cycle counting. There are several methods available for cycle counting - three of them are (DNV & Riso, 2002):

- Peak counting
- Range counting
- Rain-flow counting

Rain-flow counting is the most used cycle counting method for wind turbines. The results of the Rain-flow counting method is usually provided by the wind turbine manufacturer. The data is given in the form of stress bins, each occurring a number of times, or as a stress range histogram. The stress range histogram is then converted to a constant amplitude stress, occurring a certain number of cycles. This constant stress at a certain number of cycles, causes the same fatigue damage as the original stress range. The method is known as the Damage Equivalent Load (DEL) method. The DEL is commonly determined using the Palmgren-Miner rule. The process by which a variable-amplitude cyclic stress time series is converted into a DEL, is schematically shown in Figure 2-14.

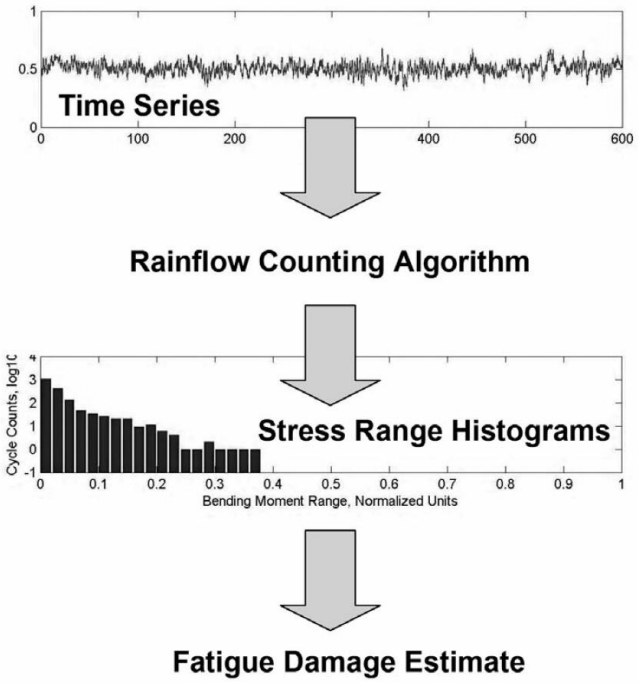

Figure 2-14: Fatigue load methods (Ragan & Manuel, 2007)

2.8. Dynamic behaviour

The fundamental frequency of structures exposed to dynamic loading is of vital importance as to avoid resonance. Resonance happens when an external dynamic force is applied to a structure at the same frequency as the structure's natural frequency. This causes the structure to undergo large displacements and can cause immediate failure or fatigue failure over time. There are mainly two methods to ensure that a structure is dynamically safe. The first is to ensure that the structure's fundamental frequency does not coincide with any external vibration frequency that the structure may experience in its life. The second method uses damping to decrease the dynamic amplification of an external vibration force. The dynamic amplification factor relates the maximum static displacement to the maximum dynamic displacement. A lightly damped structure can experience a dynamic displacement up to 10 times the static displacement, thus giving it a dynamic amplification factor of 10. Damping is the absorption of energy by the structure itself or some external object. In order for a structure to vibrate, the structure's stiffness must be overcome to enable the structure to displace. This requires energy. During the motion some energy is absorbed by the structure, normally in the form of heat, which is known as damping. The amount of damping mainly depends on the structure's geometry and material properties. The damping characteristics of various materials have been experimentally determined over years of research, some damping ratios are given in Table 2-2. Extreme care should be taken not to overestimate the damping characteristics of a material, as this can lead to underestimating the dynamic amplification factor of a structure and ultimately lead to structural failure due to resonance. The dynamic amplification factor for various damping ratios are given in Figure 2-15. The ratio of the applied vibration frequency to that of the structure, is given on the x-axis. When this ratio is equal to one, resonance takes place. The figure emphasizes the influence the damping ratio has on the dynamic amplification factor. Concrete structures are normally assumed to have a damping ratio of 0.02.

Table 2-2: Material damping ratio (Bare structure) (Bachmann et al, 1995)

System	Viscous Damping Ratio ξ
Reinforced Concrete	
Small Stress Intensity (uncracked)	0.007 to 0.010
Medium Stress Intensity (fully cracked)	0.010 to 0.040
High Stress Intensity (fully cracked but no yielding of reinforcement)	0.005 to 0.008
Prestressed Concrete (uncracked)	0.04 to 0.07
Partially Prestressed Concrete (slightly cracked)	0.008 to 0.012
Composite	0.002 to 0.003
Steel	0.001 to 0.002

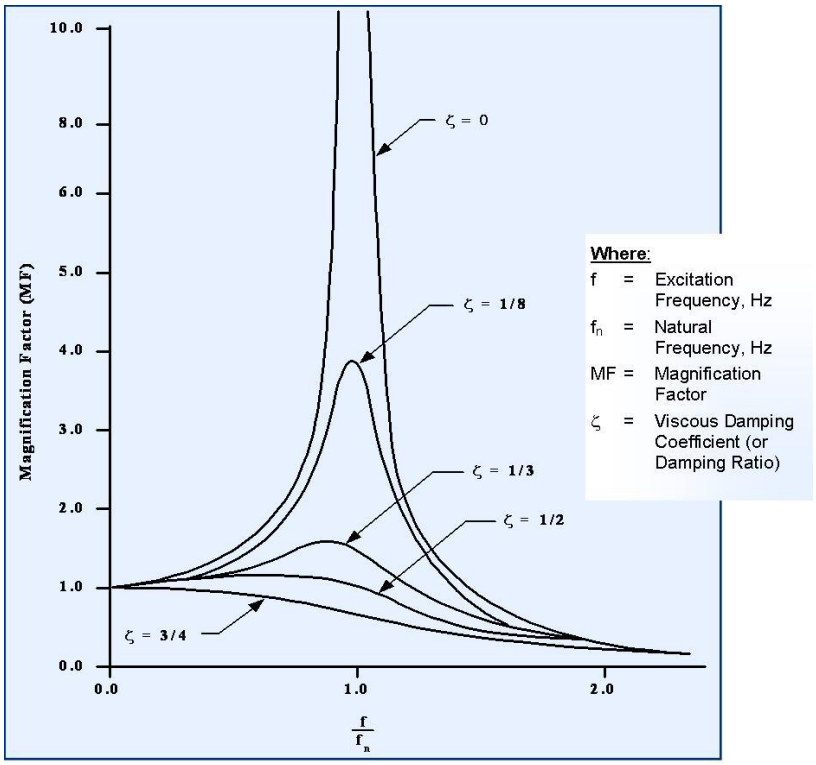

Figure 2-15: Dynamic amplification factor (Carucci, 2010)

Wind turbine structures are exposed to multiple excitation frequencies that can cause the structure to vibrate. The most important of these excitation frequencies, are the blade rotational frequency, known as the 1P frequency, and the blade passing frequency, known as the 3P frequency. The 1P, or rotor revolution frequency, is caused by the unbalanced weight of the rotor, wind shear and tower shadow (DNV & Riso, 2002). Modern wind turbines are variable speed turbines, thus the 1P and 3P frequencies are not single frequencies but a frequency interval. There are three different design options: First to design a structure with a fundamental frequency higher than the 3P frequency interval, called a stiff-stiff structure. The second option is to design a structure with fundamental frequency between the 1P and 3P frequency intervals, called a soft-stiff structure and finally to design a structure with fundamental frequency below the 1P frequency known as a soft-soft structure. This concept is illustrated in Figure 2-16. It has been shown that a soft-stiff structure is the most economical for wind turbine towers. It is difficult to calculate the exact fundamental frequency of a structure at the design stage as there are various factors that may influence the frequency. Due to this uncertainty, the tower's frequency is kept out of ±10% of the 1P and 3P frequency intervals (DNV/RISO, 2002). The frequency between the 1.1P and 2.7P frequencies, is known as the working frequency.

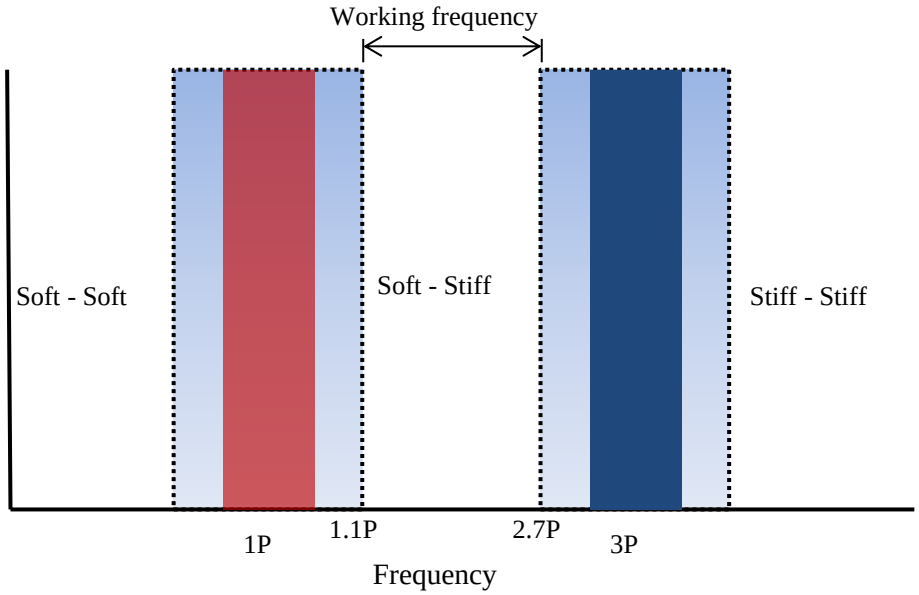

Figure 2-16: Excitation frequency

Normally, as the turbine's generating capacity increases, the blade length increases. The rotor's rotational speed decreases as the blade length increases. This lowers the working frequency range. Therefore, for larger turbines the tower's fundamental frequency lies closer to the edge of the working frequency. This can be seen in Figure 2-17. The fundamental frequency of the tower is strongly influenced by the boundary conditions of the foundation. It is estimated that by assuming the foundation is fully fixed, the error in the tower's fundamental frequency can be up to 20% (DNV/RISO, 2002). Wind turbine codes generally propose that elastic springs are used to simulate the soil stiffness.

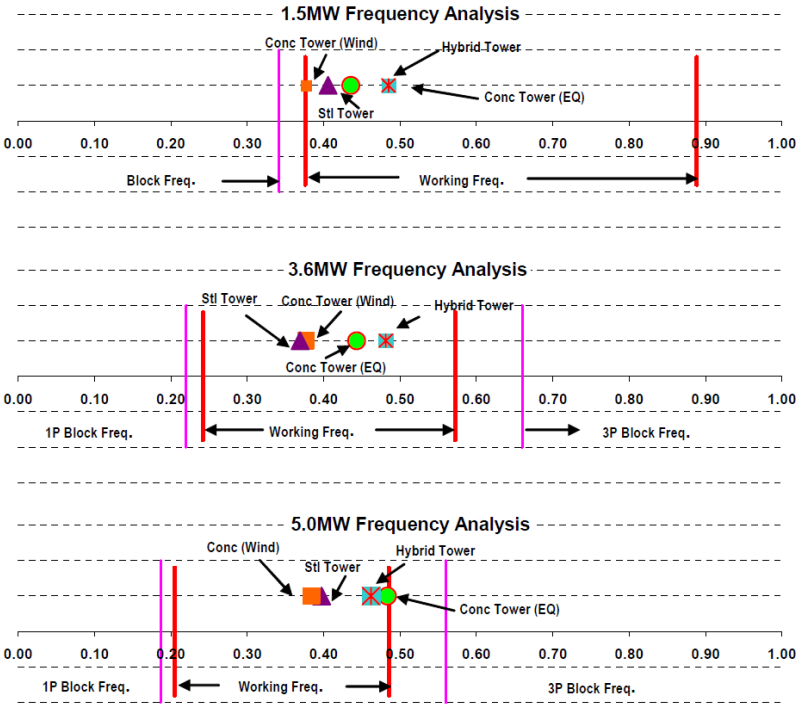

Figure 2-17: Working frequency range for various turbine sizes and towers (LaNier, 2004)

2.9. High strength concrete (HSC)

2.9.1. Introduction

HSC, as the name suggests, has a high compressive strength. There is however not one numerical strength limit that can be used to classify concrete as normal strength concrete (NSC) or HSC. The numerical strength limit used to classify concrete as HSC, strongly depends on the geographic area where the concrete is being manufactured and used. North America classifies concrete with a cylinder compression strength of higher than approximately 50 MPa as HSC, in Europe concrete with cylinder strength higher than approximately 70 MPa is classified as HSC. In SA HSC is still a new technology and is not frequently used. The main reason is that SA's concrete design codes do not yet make provision for HSC. SA is currently adopting the Eurocode 2 for the design of reinforced concrete structures. This will allow SA's engineers to fully exploit the advantages of HSC. Concrete with a cylinder strength above approximately 30 - 40 MPa can be seen as HSC in SA. The fast development of commercially available HSC is largely due to the advances in chemical admixtures, especially water reducing admixture. HSC not only has the advantage of a high compressive stress, but due to the low permeability it can be an extremely durable material. It is important to realize that HSC is not automatically durable - special care has to be taken in the design of HSC. The terms high strength concrete (HSC) and high performance concrete (HPC) are frequently misunderstood as being synonyms for the same material. Correctly designed HSC can be categorized as a type of HPC. HPC is a broad term used for any concrete exhibiting characteristics not found in normal concrete. All HPC must be constructible and durable. As mentioned earlier, concrete having a high compressive strength does not guarantee durability. For this reason, high strength concrete should not automatically be classified as being high performance concrete. In addition to HSC, other examples of HPC include (Caldarone, 2009):

- Flowing concrete
- Self-consolidating concrete (SCC)
- Lightweight concrete
- Heavyweight concrete
- Pervious (no-fines concrete)
- Low permeability concrete
- Shrinkage compensating concrete

Concrete is generally seen as a single material but when designing HSC, it is sometimes beneficial to view it as a composite material consisting of filler (aggregate) and binder (paste). The term water-cement ratio is exchanged for the term water-binder (W/B) ratio. The reason is that HSC frequently replaces a significant part of the concrete's cement requirements with supplementary cementitious materials. The significance of different materials used for HSC is discussed below:

2.9.2.Binder material

The W/B ratio is the single most important factor when it comes to increasing concrete's strength. HSC has a much lower W/B ratio than NSC. HSC typically has a W/B ratio of less than 0.4 and can have a cement content ranging from 400 kg/m^3 to 1000 kg/m^3 of concrete. Compressive strength compared to W/B ratio is given in Figure 2-18. The high cement content increases the heat of hydration. This can lead to cracking due to a high thermal gradient in the concrete. One method of solving this problem is to use the correct cement replacement material. This is discussed in section 2.9.3.

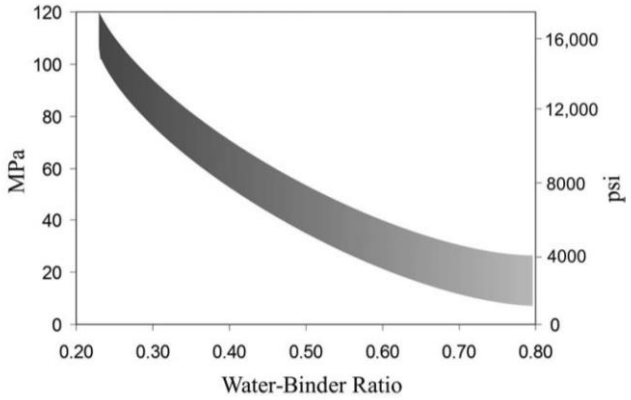

Figure 2-18: Compression stress vs W/B ratio (Caldarone, 2009)

The high cement content also means that the concrete mix contains a large amount of fine material. This increases the water demand of the mix and causes the concrete to have a poor workability or even clot. The workability can be improved by adding water to the mix, but this will increase the W/B ratio and thus decrease the strength. This problem is solved by the use of chemical admixtures. These admixtures have the ability to alter various properties of concrete without changing the materials used for the concrete. The following are typical chemical admixtures:

- Plasticizers – Reduces water demand of mix
- Superplasticizers - Significantly reduces water demand of mix
- Air entrainers - Increases the air in concrete (lightweight concrete)
- Accelerators - Accelerates setting time
- Retarders - Retards setting time

HSC is not possible without the use of superplasticizers. During the concrete mixing process the cement grains flocculate to some degree and trap some of the water. Superplasticizers disperse the cement particles, ensuring that the water in the mix is free to move through the whole mix. The water demand for the mix is thus reduced and the workability increased. In some cases the strength can also be increased by the use of Superplasticizers.

2.9.3. Supplementary cementitious materials (SCMs)

Caldarone (2009) gives the following definition for SCMs: "SCMs are important materials that contribute to the properties of concrete when used in conjunction with Portland cement by reacting either hydraulically or pozzolanically. Pozzolans are siliceous or alumino-siliceous materials that, by themselves, possess no hydraulic (cementing) value, but will, in finely divided form and in the presence of water, chemically react with calcium hydroxide to form compounds having cementitious properties." Depending on the specific SCM used the following may be achieved:

- Higher early age strength
- Higher strength over time
- Permeability reduction
- Reduction in alkali-aggregate reaction
- Reduction in heat of hydration
- Reduction in overall cost of concrete mix

Four of the most commonly used SCMs in SA are: Ground granulated blast furnace slag (GGBS), Ground granulated Corex Slag (GGCS), Condensed silica fume (CSF) and Fly ash (FA).

Slag

When steel is manufactured, slag is produced as a byproduct of the smelting process. Slag is a white powder and is normally ground to the same fineness as Portland cement. Up to 90% of Portland cement can be replaced by slag in a concrete mix. Two different types of slags are found in SA, namely GGBS and GGCS. GGCS is produced at Saldanha steel in the Western Cape and is finer than normal GGBS. This has the advantage that it is more reactive than GGBS. Slag is a valuable SCM and has the advantage that when used in HSC it reduces the risk of alkali-silicate reaction, sulfate attack, and chloride-induced corrosion (Caldarone, 2009). Slag increases the setting time of concrete and can thus reduce the heat of hydration, preventing the concrete from cracking due to a high thermal gradient. The sufficient use of slag can improve the long term strength of concrete.

Condensed silica fume (CSF)

CSF is a byproduct of silicon metals produced in an electric arc furnace. CSF is a dark gray powder with an average particle size of 0.1 - 0.3 μm, approximately 100 times smaller than the particle size of normal Portland cement (Caldarone, 2009). CSF can increase the strength of concrete. It also increases the permeability creating a durable concrete. The fine particles of CSF dramatically increases the water demand of the mix, and thus a high volume water reducing admixtures are always required. Due to the very fine particle size, the cohesion of the mix is increased which has the advantage that segregation and bleeding is prevented. CSF has the ability to increase the concrete's strength by increasing the bond between the aggregate and paste. A maximum of 20 - 30% CSF can be used in a mix before the concrete's water demand becomes too high, even with the use of chemical admixtures.

CSF accelerates the curing process and can achieve higher early age strength than normal Portland cement, making it ideal for the pre-cast industry. CSF is normally more expensive than Portland cement.

Fly ash (FA)

Coal power stations produce FA as a byproduct when coal is burned in the furnace. The quality and specific characteristics of FA are strongly influenced by the quality of the coal used in the power station. FA is one of the most common SCMs and can normally replace up to 30 - 40 % of the cement content of a mix. High percentages of FA reduce the risk of the alkali-silicate reaction and sulfate attack (Caldarone, 2009). FA retards the setting time of concrete and this is beneficial for reducing the heat of hydration. FA improves the workability and reduces the water demand of a mix due to its spherical shape.

2.9.4.Fine aggregate

Aggregate makes up the largest part of concrete's volume and has a significant influence on its properties in the hardened and fresh state. When at least 90% of a representative sample of aggregate passes through a 4.75 mm sieve and is retained by a 75 µm sieve, the sample is defined as a fine aggregate or sand. The remaining aggregate that does not pass through the 4.75 mm sieve is classified as coarse aggregate or stone. Aggregate that is suitable for NSC, is not necessarily suitable for HSC. One of the main criteria used to determine if a certain type of sand is suitable for NSC, is its particle size distribution. A good particle size distribution will ensure good packing of the particles. HSC has an abundance of very fine particles and thus the size distribution of the sand is not as important as the fineness modulus of the sand. Fine sand tends to cause HSC to become sticky and thus coarse sand is more suitable. Sand with a fineness modulus between 2.3 and 3.1 is seen as ideal for NSC, whereas for HSC a fineness modulus of 3.0 gives the best workability and compression strength (Caldarone, 2009).

2.9.5.Coarse aggregate

The properties of the coarse aggregate become more important as the strength of the concrete increases. In NSC the aggregate is almost always stronger than that of the cement paste. This is not the case for HSC, where the cement paste's strength may be close to, or even higher than, the aggregate strength. The aggregate can thus fail before the cement paste fails. Choosing the correct aggregate for a specific strength of concrete, plays a vital role in ensuring that the concrete meets its design strength. Using a strong, stiff aggregate can actually in some cases cause the concrete to have a lower compression strength. If the stiffness of the aggregate is significantly higher than that of the cement paste, stress concentrations will occur. These stress concentrations can exceed the compression strength of the aggregate and cause the concrete to fail. A study on HSC done by Van Zyl (2012), found that cracks formed through the aggregate at a compression stress well below the aggregate's compression strength. The Greywacke stone used in this experiment had a high stiffness compared to

that of the cement paste. This led to the stone failing at a compression stress of approximately a third of the compression strength of the stone. Figure 2-19 shows a specimen with a crack going through the stone rather than around it.

Figure 2-19: Crack through 13mm Greywacke stone (van Zyl, 2012)

The second important factor when choosing a suitable coarse aggregate for HSC is the interface zone between the aggregate and cement paste. As the target strength increases, water-demand of aggregates become less relevant, and the properties that relate to interfacial bond, become more important. Smaller aggregate has a larger surface area increasing the interface area between the aggregate and paste. Aggregate that has an angular shape with a coarse texture, provide greater mechanical bond and is generally more suitable for use in HSC than smooth textured aggregates (Caldarone, 2009).

2.9.6. Alkali-aggregate reaction

There are two types of alkali-aggregate reactions: alkali-silica and alkali-carbonate. Alkali-carbonate reactions are not very common and will not be discussed further. Certain aggregates contain reactive silica that can react with the alkaline hydroxides in the pore water. The reaction causes a gel to form between the aggregate and cement paste, breaking their bond. The gel can only form if active silica and alkalis are present. When the gel comes into contact with water it absorbs it and expands, this is known as the alkali-silica reaction (ASR). This expansion normally leads to cracking of the concrete. The following factors are required for ASR to take place:

- Reactive aggregate (containing active silica)
- High alkaline content
- Water

The process is slow and can take up to ten years before cracking takes place. ASR normally forms a crocodile skin cracking pattern on the surface of the concrete. Research has found that limiting the alkaline content of the concrete to less than 3 kg/m^3 can significantly reduce the risk of ASR (Illston & Domone, 2009). The concrete does not have to come into direct contact with water, a relative humidity of approximately 85% can be sufficient to start the ASR process. The following methods are generally used to effectively reduce the risk of ASR:

- Avoid the use of reactive aggregates
- Low alkaline cement with alkali content less than 0.6% (Illston & Domone, 2009)
- Supplementary cementitious materials (Reduces active alkaline content and permeability)
- Limiting the active alkaline content to less than 3 kg/m^3
- Admixtures containing Lithium salts

2.10. Wind turbine foundations

Wind turbine towers are essentially large cantilever columns and thus the foundation must resist large overturning moments. These moments cause large eccentricities in the foundation. In addition to the large overturning moments, the foundation also has to resist horizontal shear forces, vertical axial force and torsion moments. There are mainly two types of foundation systems used for onshore wind turbine towers namely, gravity spread foundations and pile foundations.

2.10.1. Gravity spread foundations

Gravity spread foundations are the most common foundation system used for wind turbines. They are used when the top soil has sufficient bearing capacity and stiffness to support the structure. They resist the overturning moment by an eccentric reaction to the weight of the turbine, tower, foundation, and backfill soil. The shear force is resisted through direct soil pressure on the sides of the foundation and friction forces between the soil and base of the foundation. A typical gravity spread foundation is shown in Figure 2-20.

Figure 2-20: Gravity spread foundation

2.10.2. Pile foundations

Pile foundations are used when the top soil is too soft to support the turbine loads. Piles transfer the loads deep into the ground to stronger soils or even bedrock. The turbine forces are mainly resisted by friction forces between the soil and the piles. In recent years monopoles have been used for wind turbines. Monopiles use the same system as normal pile foundation but instead of a large number of piles, only one large pile is used. This system mainly resists horizontal loads and moments through horizontal soil pressure and, to a lesser extent, soil friction. The different pile systems are shown in Figure 2-21.

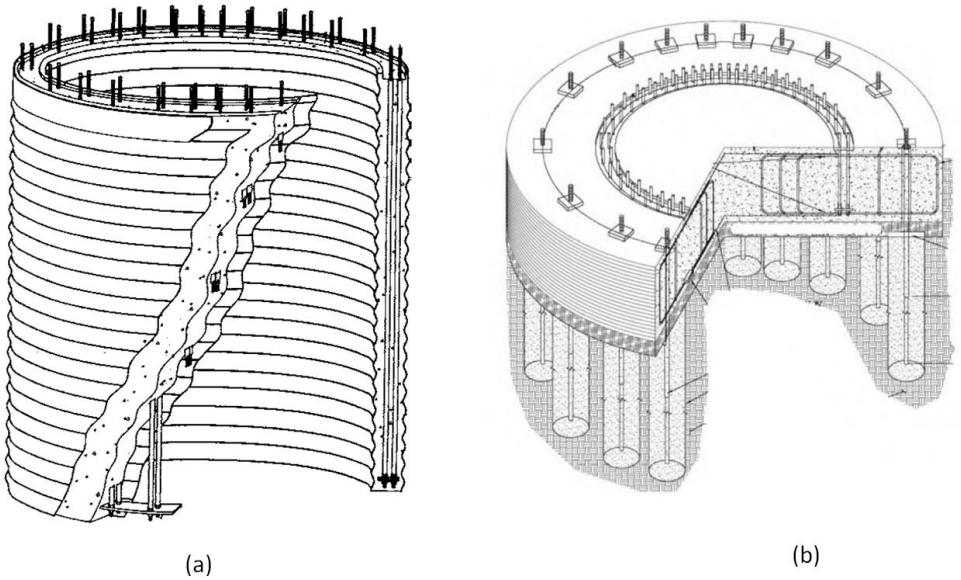

Figure 2-21: (a) Monopile foundation (b) Normal pile foundation (P&H, 2012)

2.11. Limit state design

Structures are designed to be safe, durable, economical and must be able to resist the worst possible loading and must not undergo excessive deformation under normal service conditions. The most used design method for accomplishing this is the limit state design method. For this method, the design loads are calculated by multiplying the nominal loads by a partial factor of safety. The design strength of the material is calculated by dividing the characteristic strength of the material with a partial factor of safety. The magnitude of these factors may vary, depending on the type of material and the type of stress the material will be exposed to. There are two limit states namely, Ultimate Limit State (ULS) and Serviceability Limit State (SLS). The ULS concerns the maximum load a structure can resist before structural failure occurs. Excessive deformation may in some cases cause ULS failure. SLS concerns the normal use of the structure and is usually governed by deformation and concrete cracking which may impair the normal operation of the structure. The limit state method ensures that the risk of reaching a limit state in the structure's design life is reduced to an acceptable level. A risk of 1 in 10^6 is

typically acceptable for the ULS and a risk of 1 in 10^2 is typically acceptable for the SLS (Robberts & Marshall, 2010).

2.11.1. Ultimate limit state

The major ultimate limit states are (Robberts & Marshall, 2010):

- Loss of equilibrium - overturning, sliding
- Rupture - a part of the structure or the whole structure reaches its ultimate strength.
- Formation of a mechanism – a part of the structure reaches yielding and forms a plastic hinge leading to instability. (reinforcement yielding)
- Instability - buckling of a column
- Progressive collapse - a localized failure causing a domino effect, ultimately leading to complete structural failure.
- Fatigue - cyclic loading causing material failure. SLS loads are used for fatigue calculations although fatigue failure is a ULS failure.

2.11.2. Serviceability limit state

A structure reaches its serviceability limit state when it is not fit for its intended use. The following may cause the structure to become unfit for its intended use (Robberts & Marshall, 2010):

- Excessive deformation (not causing ULS failure) - the deformation may be visually unacceptable or lead to damage to nonstructural components (tiles). Sensitive equipment may malfunction.
- Cracking - this can cause poor durability and unacceptable visual appearance
- Poor durability of structure
- Excessive vibration - can cause discomfort to people in the structure

Both limit states have the same governing equation:
(Design load effects, Q_d) ≤ (Design resistance, R_d)
Or mathematically:

$$\gamma_f Q_n \leq \frac{f_k}{\gamma_m} \tag{2.7}$$

The different variables in this governing equation will now be discussed.

2.11.3. Characteristic material strength (f_k) and characteristic loads (Q_n)

In normal structural design a 95% probability of exceedance is used to describe the characteristic strength of a material. Thus, if a large number of specimens are tested, only 5% of the specimens will have a strength lower than the characteristic strength. If the strength of the specimens follows a normal distribution, the characteristic strength is given by the graph shown in Figure 2-22. A characteristic

load on the other hand has a 5% probability of exceedance, thus 95% of the loads will be smaller or equal to the characteristic load.

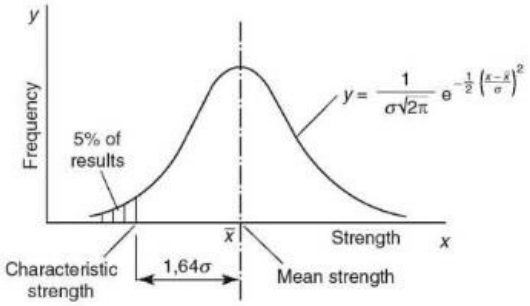

Figure 2-22: Characteristic strength of a material

2.11.4. Partial factors of safety for materials (γ_m) and loads (γ_f)

The material strength in a structure is usually less than the strength obtained in the laboratory. Concrete's strength development is sensitive to placing, curing and compacting conditions on site. Partial factors for materials are used to take account of the difference in strength. The material partial factor for concrete and steel, prescribed by the SANS10100 (2000), is given in Table 2-3. Equation 2.8 is then used to calculate the design strength of the concrete and tension steel. Equation 2.9 is used for steel reinforcing in compression.

Table 2-3: Partial factors of safety for materials

Limit state		Concrete	Steel
Ultimate:	Flexure and axial	1.5	1.15
	Shear	1.4	1.15
	Bond	1.4	
Serviceability:		1.0	1.0

$$R_d = \frac{f_k}{\gamma_m} \tag{2.8}$$

$$R_{comp\ steel} = \frac{f_y}{\gamma_m + \frac{f_y}{2000}} \tag{2.9}$$

Where,

f_k is the characteristic material strength

R_d is the design strength

γ_m is the material partial factor from Table 2-3

Just as for the characteristic strength of a material, the characteristic load has to be increased by a partial factor for loads. This is to account for any uncertainties in the characteristic load applied to the structure. The design load is given by:

$$Q_d = \gamma_f Q_n \tag{2.10}$$

Where,

γ_f is the partial factor for loads

Q_n is the nominal or characteristic load

2.12. Case study: Largest wind turbine in the world

The German company called Enercon, manufactures the largest onshore wind turbine in the world. The turbine is called the E-126 and has a power generating capacity of 7.5 MW with a 127 m rotor diameter. The nacelle has a circular form and has a diameter of 12 m. The tower is manufactured out of pre-cast concrete rings and has a hub height of 135 m. It consists of 35 tapering concrete rings with a steel connector at the top of the tower. The tower has a base diameter of 14.5 m and narrows to 4.1 m at the top with a maximum wall thickness of 450 mm. The tower is shown in Figure 2-23 and the segments are shown in Figure 2-24. A spiral staircase fitted alongside the inner tower wall is used for reaching the first floor, from where there is an elevator capable of transporting four people to the top. The last 15 – 20 m into the nacelle has to be climbed by a traditional ladder (de Vries, 2012). Due to the enormous base diameter the first 8 rings are divided into 3 segments of 120 degrees. The next 22 rings are divided into two segments and the last 5 are manufactured as complete rings. The pre-cast segments are manufactured in a controlled environment, using steel moulds to ensure a high level of accuracy. The tower is vertically post tensioned using steel cables that run from the top of the tower to the foundation. The cables run through prefabricated ducts at the center line of the walls. The cables are tensioned from the bottom and the ducts are filled with quick setting grout after the cables have been tensioned. The foundation of the tower has a diameter of 29 m and consists of more than 1400 m³ of concrete and more than 120 tons of reinforcing steel. The foundation's total weight is approximately 3500 tons.

Figure 2-23: Enercon E-126 (Deep Resource, 2013)

Figure 2-24: Pre-cast segments (Deep Resource, 2013)

Chapter 3: Loads

3.1. Introduction

The loading on wind turbine structures is very unique when compared to normal concrete structures. Structural engineers are used to working with building structures, of which the loading is dominated by the structure's own weight and live loads such as people and moveable loads in the building. Provision for wind loads is usually made by incorporating shear walls into the building frame. What makes wind turbine towers unique is that the live loads on these types of structures are negligibly small. Instead, the tower's loading is dominated by wind loading and the own weight of the structure is actually beneficial for resisting the wind loads. As mentioned earlier, there is currently not a design code describing the design process of wind turbine towers. This chapter describes the process followed in this investigation to obtain the wind loads imposed on the tower structure. Various design codes are used to obtain the final wind loads that are used for the design of the tower. The wind loads are translated into direct wind pressure on the tower and turbine loads.

3.2. Direct wind pressure on tower

This section describes a method often used for calculating the direct wind pressure on a wind turbine tower. There are other approaches - not discussed here - that may also be sufficient. The direct wind pressure acting on the tower itself, is calculated by using three different design codes. The basic wind speed is calculated according to the IEC 61400-1. The wind pressure is then calculated using the ASCE 7-10 and finally the circumference pressure distribution is calculated according to SANS 10160-3. Ideally, wind tunnel test data specific for wind turbine towers, would enable accurate derivation of pressures on these structures due to wind. However, the vast pool of data on wind pressure distributions for various Reynolds numbers of wind, acting on cylindrical structures like chimneys, is exploited.

3.2.1. Basic wind speed according to the IEC 61400-1

The IEC 61400-1 is a design standard published by the International Electrotechnical Commission (IEC). The IEC gives "minimum design requirements for wind turbines and is not intended for use as a complete design specification or instruction manual" (IEC, 2005). The standard is especially useful for obtaining the design wind speed and appropriate wind model for a WTG. This is done by categorizing wind turbines into three classes (Class I, II, III), based on the typical wind environment that they will be exposed to. Depending on the specific site, the classes can be further sub-divided into categories A, B and C according to the turbulence characteristics of the wind. The turbine classes do not describe a specific site but rather describe a generic type of site for a specific type of turbine. In addition to the three standard wind turbine classes, a fourth class is specified, class S. This class must be used when the turbine is exposed to wind conditions not covered by the standard, like hurricanes. The standard wind turbine classes are given in Table 3-1.

Table 3-1 Standard wind turbine classes (IEC, 2005)

Wind turbine class	I	II	III	S
V_{ref} (m/s)	50	42.5	37.5	Values specified by the designer
I_{ref} - A	0.16			
I_{ref} - B	0.14			
I_{ref} - C	0.12			

*All values apply at **hub height**

Where,

V_{ref} is the reference wind speed average over 10 minutes

A designates the category for higher turbulence characteristics

B designates the category for medium turbulence characteristics

C designates the category for lower turbulence characteristics

I_{ref} is the expected value of the turbulence intensity at 15 m/s

The reference wind speed and turbulence intensity are then used in wind models to describe different wind conditions. The wind regime for load and safety considerations is divided into the normal wind conditions, which will occur frequently during normal operation of a wind turbine, and the extreme wind conditions that are defined as having a 1-year or 50-year recurrence period. The IEC describes 8 different wind models, which are: Normal Wind Profile (NWP), Normal Turbulence Model (NTM), Extreme Wind Model (EWM), Extreme Operating Gust (EOG), Extreme Turbulence Model (ETM), Extreme Direction Change (EDC), Extreme Coherent Gust with Direction Change (ECD), and Extreme Wind Shear (EWS). Currently the turbine manufacturers only provide turbine loads for the EWM and EOG model. The EWM and EOG models, and the wind models used by them, will now be discussed.

The normal wind profile model (NWP)

The IEC uses the power law to describe the variation in average wind speed with height.

$$V(z) = V_{hub}\left(\frac{z}{z_{hub}}\right)^{\alpha} \tag{3.1}$$

Where,

V_{hub} is the reference wind speed from Table 3-1

z_{hub} is the hub height

z is the height above the ground where the wind speed is required

α is the power law exponent that is a function of the ground roughness. The IEC uses a power of 0.1 for extreme conditions and 0.2 for normal conditions.

Normal turbulence model (NTM)

The representative value of the turbulence standard deviation, σ_1, is given by the 90% quantile for a given wind speed at hub height (IEC, 2005). The turbulence standard deviation for the standard turbine classes is given by the following equation:

$$\sigma_1 = I_{ref}(0.75V_{out} + b) \tag{3.2}$$

Where,

b = 5.6 m/s

I_{ref} is the turbulence intensity given in Table 3-1

V_{out} is the cut-out wind speed, specified by the turbine manufacturers

Extreme wind speed model (EWM)

The EWM model is a non-operating condition, therefore the turbine is stationary. The EWM can either be a steady or a turbulent wind model. The turbulent wind model is used when a dynamic analysis is required. The steady extreme wind speeds, V_{e50} and V_{e1} have recurrence periods of 50 years and 1 year respectively. The steady extreme wind speeds are calculated by the following equations:

$$V_{e50}(z) = 1.4V_{ref}\left(\frac{z}{z_{hub}}\right)^{0.11} \tag{3.3}$$

$$V_{e1}(z) = 0.8V_{e50}(z) \tag{3.4}$$

Where,

V_{ref} is the reference wind speed for the standard wind turbine classes

z is the height of interest

It is important to note that the V_{e50} and the V_{e1} wind speeds are both **3 second gust** wind speeds.

Extreme operating gust (EOG)

The hub height gust magnitude V_{gust} is given for the standard wind turbine classes by the following relationship:

$$V_{gust} = Min\begin{cases}1.35(V_{e1} - V_{hub}) \\ 3.3\left(\frac{\sigma_1}{1+0.1\left(\frac{D}{\Lambda_1}\right)}\right)\end{cases} \tag{3.5}$$

Where,

V_{hub} is the cut-out wind speed of the turbine

σ_1 is given in equation 3.2

Λ_1 is the longitudinal turbulence scale parameter and is assumed to be 42 m when $z_{hub} \geq 60$ m

D is the turbine rotor diameter

The wind speed is then defined by the following equation:

$$V(z,t) = \begin{cases} V(z) - 0.37V_{gust}\sin\left(\frac{3\pi t}{T}\right)\left(1 - cos\left(\frac{2\pi t}{T}\right)\right) & for\ 0 \le t \le T \\ V(z) & t > T \end{cases} \quad (3.6)$$

Where,

$V(z)$ is defined in equation 3.1

T = 10.5 s

The EOG model can be used as a static model by using the maximum peak value obtained by equation 3.6. The value obtained is the static 3 second gust wind speed for the EOG model. An example of the extreme operating gust wind profile (V_{out} = 25 m/s, Class I_B, D = 113 m) is shown in Figure 3-1.

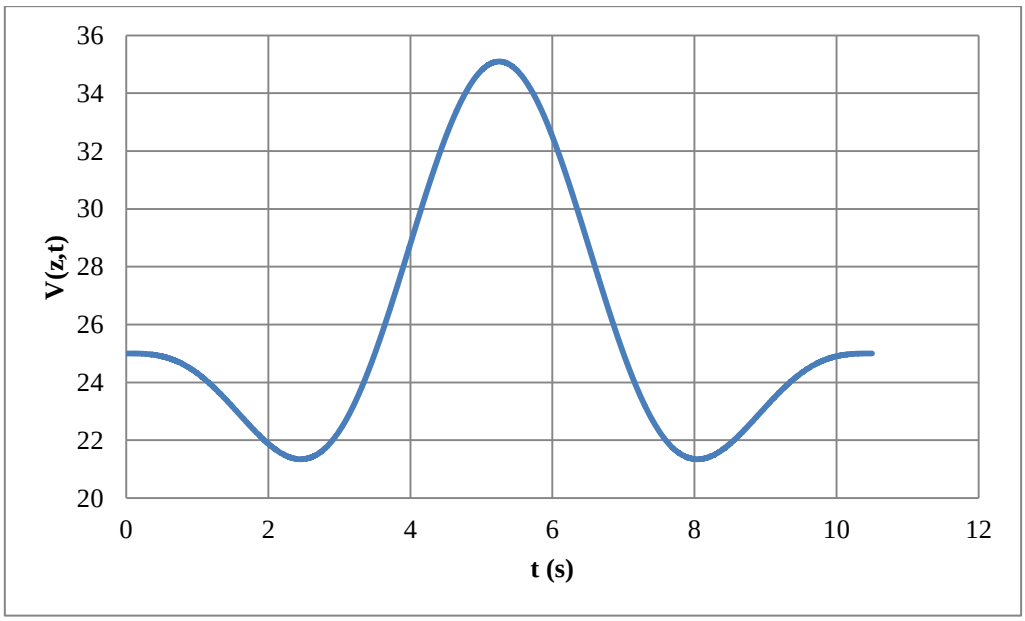

Figure 3-1: EOG wind speed profile

3.2.2.Wind pressure according to ASCE 7-10

The ASCE 7-10 is published by the American Society of Civil Engineers and is a design standard accredited by the American National Standards Institute (ANSI). It gives guidance for the minimum design loads for buildings and other structures. SANS 10160-3 is not used for determining the wind loading, due to the fact that it does not take into account the dynamic interaction between a slender structure and the wind. The ASCE 7-10 takes this into account by using the gust factor method discussed in section 2.4.1. The code distinguishes between stiff structures ($f_n > 1$ Hz) and slender structures having a natural frequency below 1 Hz. Concrete wind turbine towers of 100 m height normally have a first natural frequency in the range of 0.4 Hz.

The code states that the wind calculations stipulated in the code are applicable to the following type of structures:

- *"The building or other structure is a regular shaped building or structure."*
- *"The building or other structure does not have response characteristics making it subject to across-wind loading,* ***vortex shedding****, instability due to galloping or flutter"* (ASCE 7-10, 2010).

It further states that chapter 29 of the code applies to the following types of structures:

> *"Use Chapter 29 to determine wind pressures on the Main Wind-Force Resisting System of solid freestanding walls, freestanding solid signs,* ***chimneys****, tanks, open signs, lattice frameworks and trussed towers"* (ASCE 7-10, 2010).

Concrete chimney design codes are often used for the design of concrete wind turbine towers because of the similarities in the geometry and slenderness of the structures. The code statements above indicate that the code is applicable to wind turbine towers if the necessary design checks are done to ensure that the structures are not prone to any of the wind phenomena described.

It is common in the wind turbine industry to give the reference wind speed at the hub height of the turbine. The ASCE 7-10, like most other design codes, uses a reference wind speed or basic wind speed at a height of 10 m. The basic wind speed is also required to be a 3 second gust wind speed. The reference wind speed calculated using the IEC is a 3 second gust wind speed at hub height and therefore has to be converted to a wind speed at 10 m. The power law given in equation 3.1, is used to convert the wind speed.

The process given by the ASCE 7-10 for calculating the design wind pressure on the wind turbine tower is given below.

The velocity wind pressure as a function of tower height is given by:

$$q_z(z) = 0.613 K_z K_{zt} K_d V^2 I G \tag{3.7}$$

K_z is a velocity pressure exposure coefficient and is a function of surface roughness and the height of the structure.

$$K_z = \begin{cases} 2.01\left(\frac{z}{z_g}\right)^{\frac{2}{\alpha}} \; for \; 4.6\,m < z < z_g \\ 2.01\left(\frac{4.6}{z_g}\right)^{\frac{2}{\alpha}} \; for \; z < 4.6\,m \end{cases} \quad (3.8)$$

Where,

z is the height of interest

α = 11.5 for exposure category D

z_g = 213.36 m and is the gradient height of exposure category D

The exposure categories used by the ASCE 7-10 are similar to the categories used by SANS 10160-3. Exposure category D is used for open unobstructed terrains. This is deemed appropriate for this investigation as wind turbines are usually constructed in sites with few obstructions to the wind to optimize the electricity generated by the turbine. Other categories may be appropriate for some wind turbine sites. Each site must be examined to determine the appropriate exposure category.

K_{zt} is the topographic factor and takes account of the wind speed-up effect at hills and ridges where the topography of the landscape changes abruptly. K_{zt} can be taken as 1.0 for flat terrains.

K_d is the directionality factor and takes into account the shape of the structure. K_d for round towers is 0.95.

V is the basic wind speed (m/s) with a 3 second averaging time at a height of 10 m. This is calculated according to the IEC wind models that are discussed in section 3.2.1.

I is the importance factor and takes into account the risk to humans in the case of structural failure. The importance factor is taken as one, because wind turbines are usually constructed in open rural areas where humans are not in close proximity to the structure.

G is the gust effect factor that for flexible or dynamic sensitive structures is calculated with the following equation:

$$G_f = 0.925\left(\frac{1+1.7I_{\bar{z}}\sqrt{g_Q{}^2Q^2+g_R^2R^2}}{1+1.7g_vI_{\bar{z}}}\right) \quad (3.9)$$

g_Q = 3.4 (Peak factor for background response)

q_v = 3.4 (Peak factor for wind response)

g_R, the peak factor for resonance is given by:

$$g_R = \sqrt{2\ln(3600n_1)} + \frac{0.577}{\sqrt{2\ln(3600n_1)}} \tag{3.10}$$

R, the resonant response factor is given by:

$$R = \sqrt{\frac{1}{\beta} R_n R_h R_B (0.53 + 0.47 R_L)} \tag{3.11}$$

$$N_1 = \frac{n_1 L_{\bar{z}}}{\bar{V}_{\bar{z}}} \tag{3.12}$$

$$R_n = \frac{7.47 N_1}{(1+10.3N_1)^{\frac{5}{3}}} \tag{3.13}$$

$$L_{\bar{z}} = l\left(\frac{\bar{z}}{10}\right)^{\bar{\epsilon}} \tag{3.14}$$

$$R_h = \frac{1}{4.6n_1\frac{h}{\bar{V}_{\bar{z}}}} - \frac{\left(1-e^{-2\left(4.6n_1\frac{h}{\bar{V}_{\bar{z}}}\right)}\right)}{2\left(4.6n_1\frac{h}{\bar{V}_{\bar{z}}}\right)^2} \tag{3.15}$$

$$R_B = \frac{1}{4.6n_1\frac{B}{\bar{V}_{\bar{z}}}} - \frac{\left(1-e^{-2\left(4.6n_1\frac{B}{\bar{V}_{\bar{z}}}\right)}\right)}{2\left(4.6n_1\frac{B}{\bar{V}_{\bar{z}}}\right)^2} \tag{3.16}$$

$$R_L = \frac{1}{15.4n_1\frac{L}{\bar{V}_{\bar{z}}}} - \frac{\left(1-e^{-2\left(15.4n_1\frac{L}{\bar{V}_{\bar{z}}}\right)}\right)}{2\left(15.4n_1\frac{L}{\bar{V}_{\bar{z}}}\right)^2} \tag{3.17}$$

The turbulence intensity at height $\bar{z}$ is given by:

$$I_{\bar{z}} = c\left(\frac{10}{\bar{z}}\right)^{\frac{1}{6}} \tag{3.18}$$

$$Q = \sqrt{\frac{1}{1+0.63\left(\frac{B+h}{L_{\bar{z}}}\right)^{0.63}}} \tag{3.19}$$

$$\bar{V}_{\bar{z}} = \bar{b}\left(\frac{\bar{z}}{10}\right)^{\bar{\alpha}} V \tag{3.20}$$

n_1 is the fundamental frequency of the tower in Hz

$\bar{z}$ = 0.6h

h= tower height

V is the basic wind speed (m/s)

B is the width of the tower measured perpendicular to the wind direction, thus equal to the tower diameter

L is tower dimension parallel to the wind direction, thus equal to the tower diameter.

All constants used are given in Table 3-2.

Table 3-2: Wind constants (ASCE 7-10, 2010)

In metric

Exposure	α	z_g (m)	$\hat{a}$	$\hat{b}$	$\bar{\alpha}$	$\bar{b}$	c	ℓ (m)	$\bar{\epsilon}$	z_{min} (m)*
B	7.0	365.76	1/7	0.84	1/4.0	0.45	0.30	97.54	1/3.0	9.14
C	9.5	274.32	1/9.5	1.00	1/6.5	0.65	0.20	152.4	1/5.0	4.57
D	11.5	213.36	1/11.5	1.07	1/9.0	0.80	0.15	198.12	1/8.0	2.13

*z_{min} = minimum height used to ensure that the equivalent height $\bar{z}$ is greater of $0.6h$ or z_{min}.
For buildings with $h \le z_{min}$, $\bar{z}$ shall be taken as z_{min}.

3.2.3.Circumferential pressure distribution according to SANS 10160-3

SANS 10160-3 is published by the South African Bureau of Standards (SABS) and gives guidance on the determination of natural wind actions for the structural design of buildings and industrial structures (SANS 10160-3, 2011). The circumference pressure distribution is strongly influenced by the Reynolds number describing the flow regime of the wind. SANS gives the external pressure coefficients for various Reynolds numbers. Figure 3-2 is based on an equivalent roughness of k/b < $5x10^{-4}$, where k is the roughness protrusion and b the diameter of the cylinder. The concrete wind turbine tower used in this investigation complies with this limit. The critical pressure coefficients of Figure 3-2 are given in Table 3-3.

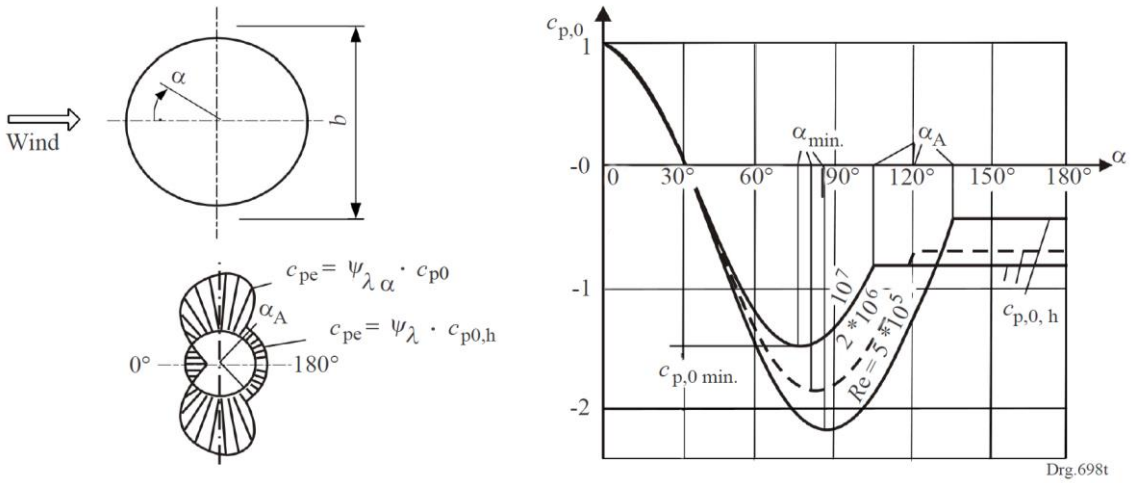

Figure 3-2: Pressure distribution for cylinders with different Reynolds numbers (SANS 10160-3, 2011)

Table 3-3: External pressure coefficient (SANS 10160-3, 2011)

1	2	3	4	5
Re	α_{min} [a]	$c_{p,0min}$ [b]	α_A [c]	$c_{p,0,h}$ [d]
5×10^5	85	−2,2	135	−0,4
2×10^6	80	−1,9	120	−0,7
10^7	75	−1,5	105	−0,8

[a] α_{min} is the position of the minimum pressure, expressed in degrees.
[b] $c_{p,0min}$ is the value of the minimum pressure coefficient.
[c] α_A is the position of the flow separation, expressed in degrees.
[d] $c_{p,0,h}$ is the base pressure coefficient.

3.2.4. Direct wind pressure design procedure

Step 1) Calculate the basic wind speed according to the IEC:

- Choose wind turbine class according to turbine specifications
- Choose wind turbulence category according to turbine specifications
- Calculate EWM wind speed
- Calculate EOG wind speed

Step 2) Calculate the wind pressure over the height of the structure according to the ASCE 7-10:

- Convert IEC hub height wind speed to wind speed at 10 m
- Determine risk category of tower
- Determine exposure category B, C or D according to the ground roughness of the site
- Choose wind directionality factor, K_d according to the shape of the structure
- If wind speed-up effects are present, calculate the topographic factor, K_{zt}
- Determine velocity pressure exposure coefficient, K_z
- Calculate the gust effect factor, G – to take into account the slenderness of the structure
- Calculate velocity pressure q_z at required height

Step 3) Calculate circumference pressure distribution according to SANS 10160-3:

- Calculate Reynolds number for the design wind speed used in Step 2
- Choose correct curve on Figure 3-2 according to Reynolds number
- Use Table 3-3 to accurately determine critical values of the chosen curve
- Multiply the external pressure coefficients with the design velocity pressure, q_z.

3.3. Turbine loads

Wind pressure on the blades, hub and nacelle is transferred to the top of the tower. These forces are known as turbine loads and are the largest loads imposed on the tower. The determination of turbine loads are complex and require in depth knowledge of aerodynamics. For this reason, the turbine loads are given by the turbine manufacturers for a specific turbine in a specific wind environment. These loads are regarded as trade secrets and are thus not freely available. A study done by Berger-Abam

engineers for the National Renewable Energy Laboratory (NREL) in Colorado, lists turbine loads, obtained by the use of computational fluid dynamics (CFD). These loads are used in this report because actual turbine loads are protected by copyright. The specifications of the turbine used by the NREL, are given in Table 3-4. The turbine loads are given for two IEC wind conditions namely: EWM and EOG. The 3 second gust wind speeds used for the EWM and EOG models were 59.5 m/s and 35.1 m/s respectively. The turbine loads at a hub height of 100 m are given in Table 3-5.

Table 3-4: Turbine specifications (LaNier, 2004)

Power output	3.6 MW
Rotor Speed	13.2 rpm
Rotor Diameter	108.4 m
Head Mass (incl. nacelle, hub and blades)	314 912 kg
Hub Height:	100 m
IEC class	IIB

Table 3-5: Turbine loads (LaNier, 2004)

	Thrust force (kN)	Over turning Moment (kNm)	Tower Axial Force - Causing tower compression (kN)	Torsional Moment - About tower longitudinal axis (kNm)
EWM	1 086	16 767	3 155	5 961
EOG	1 199	9 913	3 129	1 597
Fatigue Load	143	2213	-	2220

3.4. Load factors and load combinations

Limit state design as discussed in section 2.11 is used for the design of the tower. The ultimate limit state partial load factors prescribed by the ASCE, are primarily used but modifications are made to comply with the IEC. The IEC specifies a partial safety factor of 1.35 on wind induced turbine loads. The ASCE uses a partial load factor of 1.6 on all wind induced loads. The design wind pressure on the tower is calculated according to the ASCE and thus, to be consistent with the code, a factor of 1.6 was used for the direct wind pressure on the tower. In the industry the turbine loads are calculated according to the IEC and therefore a partial load factor of 1.35 was used for all the wind induced turbine loads.

The serviceability limit state for a wind turbine must be an operating condition under normal wind conditions. The EOG model is the only operational wind model for which turbine loads are available.

The model simulates an extreme condition with a reoccurrence period of 1 year. Using the EOG turbine loads will greatly overestimate the normal operational loads of the turbine and will lead to an uneconomical design. Turbine manufacturers recommend that in the absence of operational loads, 60% of the extreme characteristic load may be used.

Ultimate Limit State (ULS):

0.9D + 1.6W + 1.35TWL

Serviceability Limit State (SLS):

0.6(1.0D + 1.0W + 1.0TWL)

Fatigue design:

1.0SLS – 1.0ΔTWL

Where,

D is the dead load

W is the direct wind load on the tower

TWL is the wind induced turbine loads

ΔTWL is the variation in turbine loads, causing fatigue

The variation in turbine loads is a result of the operation of the turbine. This load is thus applied to the SLS loads to accurately predict the stress variation the fatigue load will cause. Berger-Abam engineers recommend that a partial load factor of one be used for fatigue calculations as codes dealing with fatigue usually incorporate their own load factors (LaNier, 2004). This is checked when material fatigue is calculated.

3.5. Vortex shedding

The procedure described in section 3.2 for calculating the direct wind pressure acting on the tower is only valid if the tower is not prone to vortex shedding. The ASCE 7-10 does not cover vortex shedding and thus the ACI 307-98 design standard is used. The design standard gives guidelines for the design of reinforced concrete chimneys. As previously mentioned, the geometry and slenderness of concrete chimneys and concrete wind turbine towers are similar. It is thus deemed to be acceptable to use some guidelines given for concrete chimneys and apply them on wind turbine towers. The code gives a procedure to follow, to check if vortex shedding should be considered as a design load. The procedure is given below:

"Across-wind loads due to vortex shedding in the first and second modes will be considered in the design of all chimney shells when the critical wind speed V_{cr} is between 0.50 and 1.30 times $V(z_{cr})$." (ACI 307, 1998) Thus Vortex shedding must be considered as a design criterion if the following is true:

$0.5V(z_{cr}) \leq V_{cr} \leq 1.30V(z_{cr})$ (3.21)

Where,

$z_{cr} = 5/6h$

$V(z_{cr})$ is the mean design wind speed at z_{cr}

V_{cr} is the critical speed at z_{cr}

$$V_{cr} = \frac{fd(u)}{S_t} \quad (3.22)$$

Where,

f is the fundamental frequency of the tower (Hz)

S_t is the Strouhal number

$S_t = 0.25F_1(A)$ (3.23)

Where,

$$F_1(A) = 0.333 + 0.206ln\left(\frac{h}{d(u)}\right) \text{ but } 0.6 < F_1(A) < 1.0 \quad (3.24)$$

And,

d(u) is the mean outside diameter of the upper third of the tower (m)

h is the tower height above ground level (m)

The results of the above calculations for the tower designed in this report, are given in Table 3-6. It was found that for the EWM it is not necessary to design for vortex shedding. The normal operating wind speed of the turbine was also checked. The operating wind speed is significantly lower than the EWM wind speed and thus causes the tower to fall within the vortex shedding range. A critical vortex shedding wind speed that falls within the working range of the turbine, is normally acceptable, as the blades causes turbulence around the tower that obstructs the formation of vortices (DNV/RISO, 2002).

Table 3-6: Summary of vortex shedding calculations

Wind Model:	**EWM**	**Typical operating wind speed**
f =	0.42 Hz	0.42 Hz
$F_1(A)$ =	0.971	0.971
S_t =	0.243	0.243
V_{cr} =	7.807 m/s	7.807 m/s
$V(z_{cr})$=	41.66 m/s	11.0 m/s
$0.5V(z_{cr})$=	20.83 m/s	5.5 m/s
$1.3V(z_{cr})$=	54.16 m/s	14.3 m/s

3.6. Validation of IEC reference wind speeds for SA

The wind loads used in this report uses the IEC reference wind speed. The reference wind speed is an important parameter when estimating wind loads as it directly influences the magnitude of the wind loads. It is thus important to verify if the generic wind speed from the standard wind turbine classes accurately describes the actual wind conditions in SA. Two different methods that can be used to verify the IEC reference wind speed are discussed below.

3.6.1. WASA wind speeds

The Wind Atlas of South Africa (WASA) is a programme that aims to map SA's wind resources. The programme uses actual wind speed readings obtained from various wind masts. WASA produced maps of the yearly average wind speed, as well as the extreme wind speed for SA. The 1 in 50 year 10 minute average wind speed is shown in Figure 3-3.

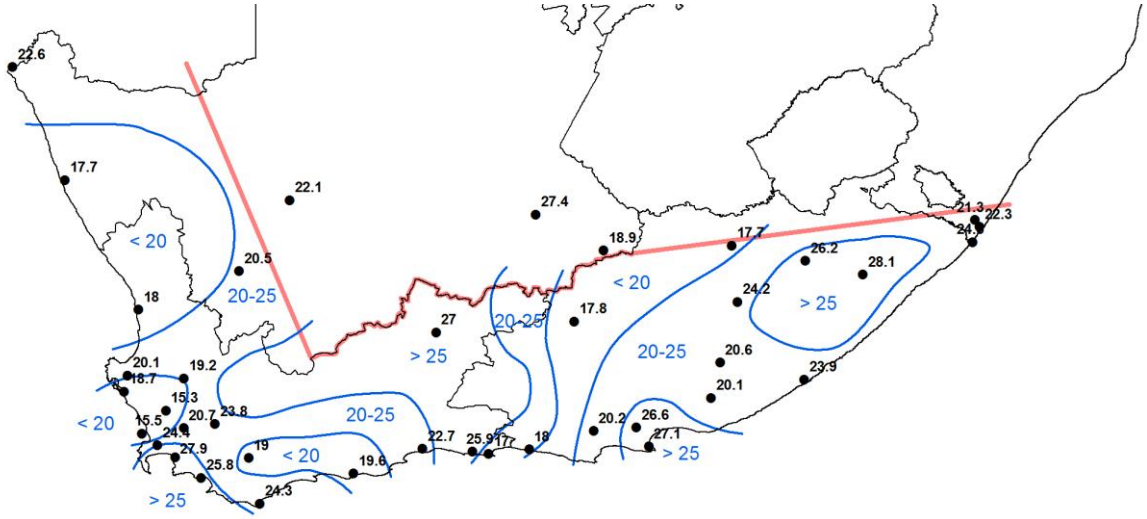

Figure 3-3: 1:50 year 10 minute wind speed of WASA (m/s)

3.6.2. 3TIER global wind dataset

3TIER is an International company specializing in wind and solar prospecting. "The 3TIER global wind dataset is the first high-resolution, methodologically consistent wind resource assessment of global extent. Computer simulations using a mesoscale numerical weather prediction model form the basis of the dataset. The dataset contains hourly values over a 10-year period, on a 2-arcminute (approximately 5 km) resolution grid covering all continental and near-shore areas between 60°S and 70°N" (3TIER, 2009). 3Tier wind data is primarily used to estimate wind speeds at sites where direct wind measurement is not available. 3Tier assessed the accuracy of their wind speed predictions by comparing it to 194 meteorological stations within Africa. They found that the difference between the observed annual wind speed and the 3Tier annual wind speed is less than 0.5 m/s at 35% of the stations, and the difference is less than 1 m/s at 66% of the stations. The overall bias is +0.35 m/s relative to the actual measurements, and the root mean square error (RMSE) is 1.13 m/s (3TIER, 2009).

Chapter 4: Finite Element model (FEM)

4.1. Introduction

The tower is modelled in a finite element package called Diana. Diana is a product of the company TNO, which specializes in the nonlinear analysis of concrete and masonry structures. Full scale or even scale modelling of a structure is extremely expensive. The FEM is a cost effective method for accurately modelling a structure. In this project the FEM is used to accurately design the reinforced concrete tower and to determine the accuracy of some analytical design techniques. The FEM is also used to do a sensitivity analysis of various design factors to determine the importance of these factors to the whole design. The different components of the FEM used in this project, are discussed in this chapter.

4.2. Geometry

The tower has a conical profile, with the diameter and wall thickness reducing with height. This is due to the fact that the bending moment and shear force are at a maximum at foundation level and then reduces to the top. Reducing the diameter and wall thickness saves unnecessary weight and costs. The tower is modelled with a steel ring at the top. The ring prevents ovalization of the tower's top and forms a platform to which the turbine loads can be applied. This is a simple method for modelling the effect that the steel turbine structure has on top of the tower. The steel ring has the same diameter and thickness as the tower, with a height of 0.5 m. The center line diameter and wall thickness of the tower is given in Table 4-1. The FEM is divided into five reinforcing sections to have the ability to reduce the steel reinforcing in certain sections where the forces are smaller. The sections are shown in Figure 4-6.

Table 4-1: Tower Dimensions

	H=0m	H=50m	H=100m
Outside Diameter (m)*	6.70	5.20	3.70
Wall thickness (m)*	0.40	0.35	0.30

*Diameter and wall thickness vary linearly between H=0 m and H=100 m

4.3. Material

In this section the material properties are divided into the physical properties of the material and the finite element material models used to model the physical material. Internationally HSC is commonly used in high rise buildings because of its ability to reduce the size and weight of structural elements. In recent years, HSC has also been used in some buildings in SA. The high compression strength and high stiffness of HSC makes it ideal for concrete wind turbine towers. The use of HSC is not yet a

well-established technology in South Africa and thus the strength was limited to the C80/95 strength class.

4.3.1. Physical material properties - Model Code 2010

The Model Code for concrete structures is published by the CEB and FIB, two large international bodies aimed at synthesizing research findings, defining new research directions and producing design recommendations (CEB-FIB, 2010). The first Model Code was published in 1978, the Model Code 1990 was the next publication and recently the Model Code 2010 was published. The Model codes form the bases of many of today's concrete design codes, including the Eurocode. The 2010 edition of the Model Code includes material properties for HSC. The code is used to compute the physical material properties of the tower:

Table 4-2: Concrete Strength

Strength class – C80/95	
Characteristic cube compression strength- $f_{ck,\ cube}$	95 MPa
Characteristic cylinder compression strength- f_{ck}	80 MPa

Mean strength

For some concrete properties the **mean compression strength** is required:

$$f_{cm} = f_{ck} + \Delta f \tag{4.1}$$

Where,

Δf = 8 MPa

Tensile strength

The tensile strength for normal weight concrete may be calculated using the characteristic compression strength.

The **mean tensile** strength is given by:

$$f_{ctm} = 2.12 \ln(1 + 0.1(f_{ck} + \Delta f)) \quad \text{for concrete grades} > C50 \tag{4.2}$$

Where,

f_{ck} is the characteristic compressive strength (MPa)

The lower and upper bound values of the characteristic tensile strength $f_{ctk,max}$ and $f_{ctk,min}$ are given by:

$$f_{ctk,min} = 0.7 \cdot f_{ctm} \tag{4.3}$$

$$f_{ctk,max} = 1.3 \cdot f_{ctm} \tag{4.4}$$

Fracture energy

The fracture energy of concrete, G_F (N/m), is defined as the energy required to propagate a tensile crack of unit area. For ordinary normal weight concrete, the fracture energy may be calculated using the following formula:

$$G_F = 73 f_{cm}^{0.18} \quad (4.5)$$

Where,

f_{cm} is the mean compressive strength in MPa

Modulus of elasticity

The modulus of elasticity E_{ci} obtained from equation 4.6, is defined as the tangent modulus of elasticity at the origin of the stress-strain diagram. Values for the modulus of elasticity for normal weight concrete with natural sand and gravel, can be estimated from the characteristic compression strength using equation 4.6.

$$E_{ci} = E_{c0}\, \alpha_E \left(\frac{f_{ck}+\Delta f}{10}\right)^{1/3} \quad (4.6)$$

Where,

E_{ci} is the modulus of elasticity in MPa at a concrete age of 28 days

f_{ck} is the characteristic compression strength in MPa

E_{c0} = 21.5 GPa

α_E is 1.0 for quartzite aggregates. For different types of aggregate, qualitative values for α_E can be found in Table 4-3.

Table 4-3: Alpha values for different types of aggregate

Type of aggregate	α_E
Basalt, dense limestone aggregates	1.2
Quartzite aggregates	1.0
Limestone aggregates	0.9
Sandstone aggregates	0.7

Poisson's ratio

For the range of stresses $-0.6f_{ck} < \nu_c < 0.8f_{ctk}$ the Poisson's ratio of concrete ν_c ranges between 0.14 and 0.26. Regarding the significance of ν_c for the design of members, especially the influence of crack formation at the ultimate limit state, the estimation of ν_c = 0.20 meets the required accuracy (CEB-FIB, 2010).

The calculated physical characteristics of the concrete used for the tower are summarized in Table 4-4.

Table 4-4: Summary of concrete properties obtained using the Model code 2010

f_{ck}=	80 MPa
$f_{ctk,min}$=	3.4 MPa
G_F=	163.4 N/m
E_{ci}=	44.4 GPa
ν_c=	0.2

4.3.2.Diana material models

Diana offers various predefined finite element material models. Different material models are used for the concrete and reinforcing steel. The concrete's material behaviour is further divided into concrete failing in compression (Crushing) and concrete failing in tension (Cracking).The models used in the FEM for the different materials, are now discussed.

A plasticity model is used to describe the concrete's behaviour in compression. When comparing elastic and plastic material behaviour, the main difference is that an elastic material will undergo no permanent deformation and a plastic material will undergo permanent or irreversible deformations. The mathematical formulation of plasticity can be applied to all materials showing irreversible deformations (Diana 9.4.4, 2012). In the event of small strains the total strain can be decomposed into an elastic part and an irreversible plastic part:

$$\varepsilon^{Total} = \varepsilon^{Elastic} + \varepsilon^{Plastic} \tag{4.7}$$

The formulation of plasticity can be used for concrete reaching its crushing strength. The concrete will become plastic if the principal stress exceeds the compressive elastic limit of the concrete. When this happens, the concrete can then either exhibit hardening or softening behaviour depending on the type of concrete being modelled. Diana offers various different stress strain diagrams to describe a material's strain hardening or softening behaviour. In Figure 4-1 the predefined compression behaviour for total strain models available in Diana, is shown. HSC is notorious for being a brittle material and thus the Thorenfeldt curve was chosen for the compression behaviour of the concrete. The Thorenfeldt model reduces the stiffness of the material rapidly when the principal stress reaches the maximum compression strength, thus accurately describing the behaviour of HSC.

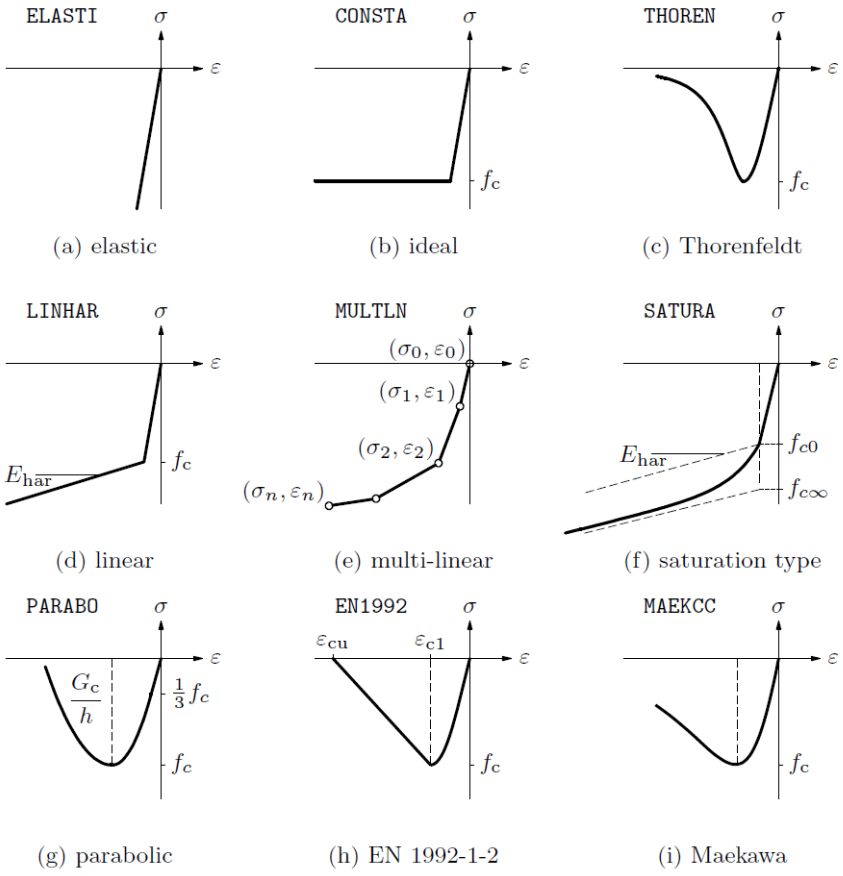

Figure 4-1: Predefined compression behavior for Total Strain model (Diana 9.4.4, 2012)

A smeared cracking model is used to describe the concrete's behaviour in tension. One of the most significant nonlinearities of concrete happens when the tensile strength is exceeded and crack formation occurs. Diana specifies cracking as a combination of tension cut-off, tension softening and shear retention (Diana 9.4.4, 2012). A total strain based smeared cracking model is used to model the crack behaviour of concrete in Diana. As the name suggests, the crack width is smeared out or averaged over an element. This is different to a discrete cracking model, where two or more elements lose contact with each other and a physical gap occurs. The total strain of the smeared cracking model is decomposed into an elastic strain component and a crack strain component:

$$\varepsilon_{Total} = \varepsilon^{elastic} + \varepsilon^{crack} \tag{4.8}$$

A crack is formed when the principal tensile stress violates the maximum tensile strength condition. The tensile strength of the material can then either be reduced to zero immediately or it can gradually decrease to zero - the latter is known as tension softening and is governed by fracture energy. A rotating crack model that reorients the crack direction, so that it will always coincide with the principal stress direction, is used. If the stress in a crack is reversed the crack will close and the material will still have its full compression strength. The tensile strength however is lost and the crack will reopen the moment tensile stresses reoccur. In Figure 4-2 the predefined tension softening behaviour for total

strain models available in Diana, is shown. The exponential curve is used for the FEM in this research project.

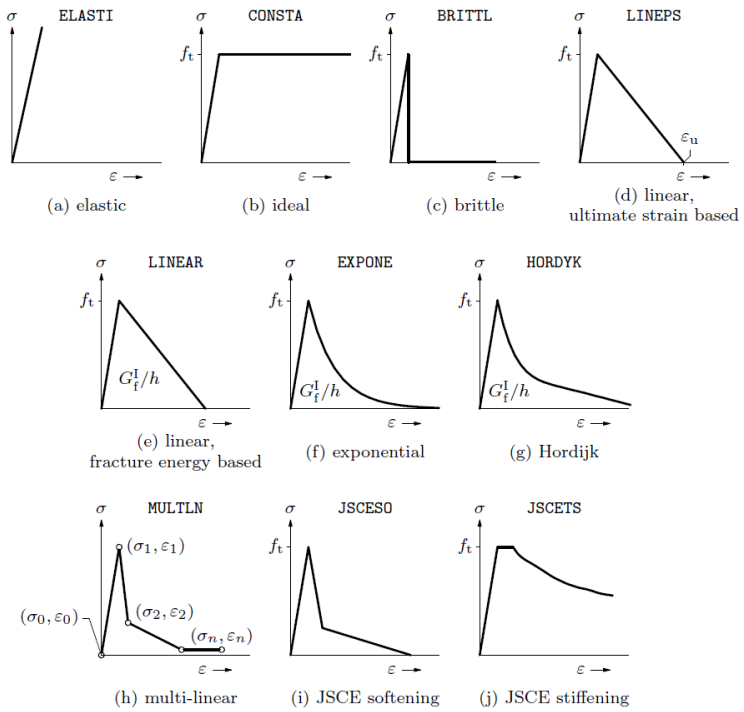

Figure 4-2: Predefined tension softening for Total Strain crack model (Diana 9.4.4, 2012)

There are mainly three models available in Diana for describing the stress strain behaviour of the reinforcing steel. They are: linear elasticity, ideal plasticity and hardening plasticity. The ideal plasticity model (Figure 4-3b) is used for this project. The hardening of the reinforcing steel is not taken into account in the FEM. Large strains are required before hardening takes place, this will lead to large deformation in the structure. Out of a design perspective, it will thus not be conservative to take into account the hardening of the steel reinforcing. The reinforcing steel properties of the tower are given in Table 4-5. The amount of reinforcing is kept constant through the height of the tower. For optimization purposes the amount of reinforcing should obviously be reduced with height when the forces in the tower are known. The five reinforcing zones discussed above can be used to optimize the FEM model.

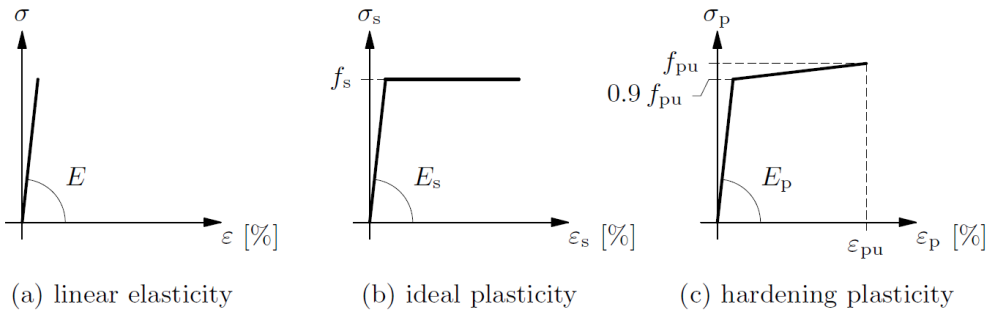

Figure 4-3: Reinforcement steel material models

Table 4-5: Reinforcing steel properties

Density	7850 kg/m^3
Modulus of elasticity	200 GPa
Poisson's ratio	0.3
Yield strength	450 MPa
Diana material model	Ideal plasticity
Vertical reinforcing steel	5068 mm^2/m per layer*
Horizontal reinforcing steel	1636 mm^2/m per layer*
Concrete cover	40 mm

*2 layers each horizontally and vertically as discussed in section 2.3.

4.4. Loads

The tower loads are calculated as described in Chapter 3. Four load cases are investigated, namely: EWM, EOG, SLS and Fatigue. The turbine loads are applied to the steel ring at the top of the tower. The thrust force and turbine weight are applied as a series of point loads at each node of the ring. Both the overturning and torsion moments are applied as a series of couple forces at each node of the ring. The direct wind pressure is applied as a pressure force on the whole tower. The pressure of each element is calculated according to the element's height above the ground, as well as its radial position. Thus all 7200 elements forming the tower shell, have a unique wind pressure according to its position.

4.5. Mesh and element type

There are mainly two types of elements available in Diana for describing the geometry of a tower - they are flat shells and curved shells. Flat shells do not allow for reinforcement to be placed in the shell and thus cannot be used for a reinforced concrete structure. Curved shell elements are used to model the tower structure. A normal curved shell element has five degrees of freedom in every element node, three translations and two rotations. Thus the basic variables of the curved shell elements are the translations u_X, u_Y and u_Z in the global XYZ directions, and the rotations ϕ_x and ϕ_y respectively around the local x and y axes in the tangent plane. Normal curved shell elements do not have a rotational drilling degree of freedom (ϕ_z). A moment force around an axis normal to the surface of the shell element will be lost due to the fact that ϕ_z does not exist. Curved shell elements that have a drilling degree of freedom, do exist, but are not required in this model and will only increase computational time. Eight node and four node quadrilateral curved shell elements are used to model the tower. A comparison is then made between the accuracy of the two element types. The degrees of freedom for 8 node quadrilateral curved shell element are shown in Figure 4-4.

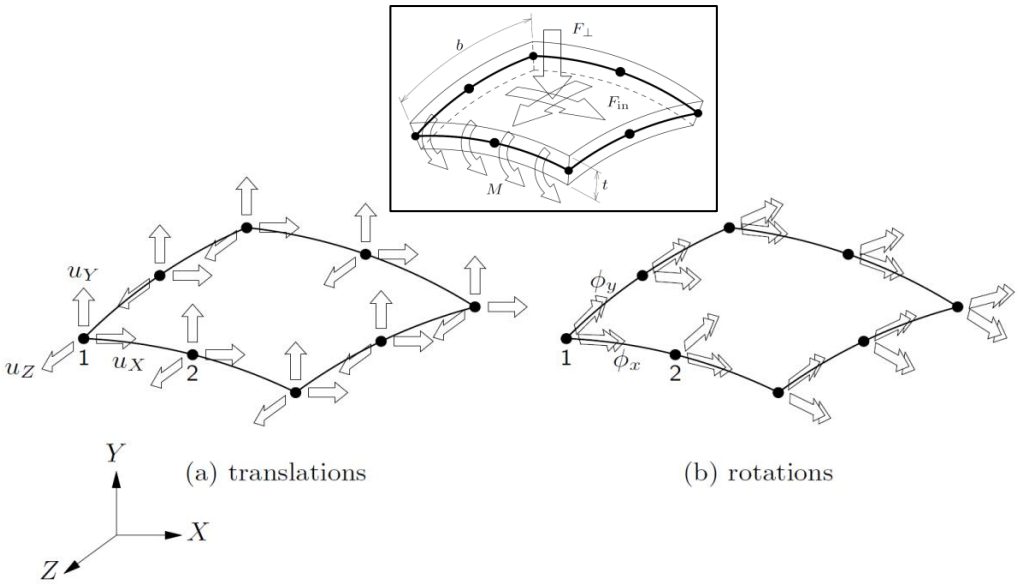

Figure 4-4: DOF for 8 node quadrilateral curved shell element (Diana 9.4.4, 2012)

The mesh size of a FEM model has a significant effect on the accuracy of the model. Smaller element sizes usually give more accurate results, but computational time can quickly limit the size of the elements. The computation time of an analysis increases approximately quadratically with the number of elements in the model (Hendriks, 2012). The maximum element size is limited to ensure that the material model does not exhibit a "snap-back" in the stress-strain relationship. The following equation serves as a guideline for the maximum element size (Hendriks, 2012):

$$h \leq \frac{EG_F}{f_t^2} \tag{4.9}$$

Where,

E is Young's modulus of the concrete

G_f is the fracture energy

f_t is the tensile strength of the concrete

The tower is meshed with a 0.5 m mesh size in the vertical direction and a 10 degree size in the circumference direction. This ensures an economic analysis time, while not exceeding the maximum element size. The element size at different positions on the tower is given in Table 4-6.

Table 4-6: Element size

	H = 0 m (Base)	**H = 50 m**	**H = 100 m**
Vertical size (m)	0.50	0.50	0.50
Horizontal size (m)	0.59	0.45	0.32

*Maximum element size limit = 0.63 m

Diana has two different types of reinforcing elements for curved shells- bar elements and grid elements. Reinforcing elements do not have their own degrees of freedom. When embedded, the displacements and strains of the reinforcing element is fully coupled to that of the element in which it is embedded. The reinforcing element adds stiffness to the elements in which it is embedded. Bar and grid reinforcing elements are available in Diana. Grid reinforcing uses an equivalent thickness method. This method involves calculating the equivalent thickness of the reinforcing bars over a unit area. A grid can provide stiffness in two orthogonal directions. A bar element is modelled using individual bars that add stiffness only in the axial direction of the bar. Four layers of bar elements are used for the tower. The vertical and horizontal bars are placed at a spacing of 300 mm at the base of the tower. The number of bars is kept constant throughout the height of the tower. The spacing thus reduces with height. This was only done to simplify the FEM. In practice, the spacing of the reinforcing bars will be kept approximately the same and the bar diameter will decrease with height to account for the bending moment that decreases with height.

4.6. Stability analysis

The stability of the tower is checked using Diana's Euler stability analysis. The implementation of Euler's method in Diana is given below:

$$\left[K_{tb} + (\lambda_i - \lambda_b)[K_D(q_b, \dot{q}_b) + K_G(\dot{\sigma}_b)]\right]q_i = 0 \tag{4.10}$$

Where,

K_{tb} is the tangent stiffness matrix

K_D is the initial displacement matrix

K_G is the geometric stiffness matrix

q_b is the nodal displacements

$\dot{q}_b$ is the derivative of the nodal displacements

$\dot{\sigma}_b$ is the derivative of the stress function

λ_i is the buckling loads

q_i is the buckling modes

The equation is solved by first using a standard nonlinear analysis to reach as close as possible to the critical (bifurcation buckling) point, without encountering any negative diagonal term in the system stiffness matrix. This state is defined as the base state which occurs at $\lambda=\lambda_b$, with the corresponding displacement and stress states q_b, σ_b and tangent stiffness matrix K_{tb} . Then, a linearized buckling analysis is done at the base state, which is nothing but the solution of the eigenvalue problem (Diana 9.4.4, 2012).

4.7. Foundation

The foundation is a vital part of a wind turbine tower design. The design of the foundation itself falls outside the scope of this investigation. The foundation can however not be assumed to be fixed when the fundamental frequency of the tower is computed. Studies have shown that the effect the stiffness of the foundation itself has on the fundamental frequency of the tower, is small when compared to the effect of the soil stiffness (DNV/RISO, 2002).

The soil stiffness and soil-foundation interaction can be modelled through the use of soil elements and interface elements respectively, but this is a time consuming and computationally expensive procedure. Another method that is commonly used, involves the use of linear springs to represent the soil stiffness. This method is a simple and cost effective method to simulate the effect the soil stiffness will have on the dynamic behaviour of the tower. The soil stiffness is uncoupled into a vertical, horizontal, rotational and torsional stiffness component. The foundation itself is then assumed to be rigid and supported on the appropriate springs. One of the most used models for representing the stiffness of the soil through linear springs, is the method described by George Gazetas in his 1983 paper on machine foundation vibrations. The equations for calculating the soil stiffness of a foundation on a homogeneous half space is given in Table 4-7. These equations do not take into account that the foundation is embedded into the soil. Embedment factors can be multiplied with the stiffness obtained with the equations in Table 4-7 to account for the embedment depth. These factors are given in Table 4-8. The added stiffness due to the embedment depth, will only be accurate if there is complete contact between the foundation sides and the soil surrounding it. Various factors like poor soil compacting and concrete shrinkage may cause the foundation sides to lose contact with the soil. For this reason it was considered that is would not be conservative to take into account the embedment effects. The soil stiffness obtained by the equations in Table 4-7 was used for all foundation calculations.

Table 4-7: Soil stiffness for circular foundation (Gazetas, 1983)

Mode of motion	Circular foundation stiffness
Vertical	$K_v = \frac{4GR}{1-\nu}$
Horizontal	$K_H = \frac{8GR}{2-\upsilon}$
Rocking	$K_R = \frac{8GR^3}{3(1-\upsilon)}$
Torsion	$K_T = \frac{16GR^3}{3}$
Where, R is the radius of the foundation G is the dynamic shear modulus of the soil ν is Poisson's ratio of the soil	

Table 4-8: Embedment depth factors

Mode of motion	Embedment factor for circular foundation
Vertical	$\eta_V = 1 + 0.6(1-\nu)\left(\frac{h}{R}\right)$
Horizontal	$\eta_H = 1 + 0.55(2-\nu)\left(\frac{h}{R}\right)$
Rocking	$\eta_R = 1 + 1.2(1-\nu)\left(\frac{h}{R}\right) + 0.2(2-\nu)\left(\frac{h}{R}\right)^3$
Torsion	-
Where, h is the embedment depth	

The rocking motion is the dominant mode for the tower. The foundation is thus supported on vertical springs that give the same rocking stiffness as the stiffness calculated by Gazetas' method. A sensitivity analysis was done to determine the effect soil stiffness has on the fundamental frequency of the tower. Typical soil types and their properties are given in Table 4-9. These generic soil types were used for the sensitivity analysis. A typical foundation size for a 3.6 MW turbine supported on a concrete tower is used. It is justified to use a generic foundation due to the fact that the foundation is only used for a sensitivity analysis of the soil stiffness. The foundation should, however, be designed according to the specific turbine and tower if the foundation is used in the deflection calculations. The dimensions for the foundation used are given in Figure 4-5.

Table 4-9: Properties of typical soil types

Soil type	Dynamic Young's modulus (MPa)	Dynamic shear modulus (MPa)*
Fine Sand	110	41
Sand	170	63
Coarse Sand	200	74
Gravel	300	111
Soft Clay	35	13
Clay	70	25
Stiff Clay	140	50
* Poisson's ratio for sand is taken as 0.40 and for clay it is taken as 0.35.		

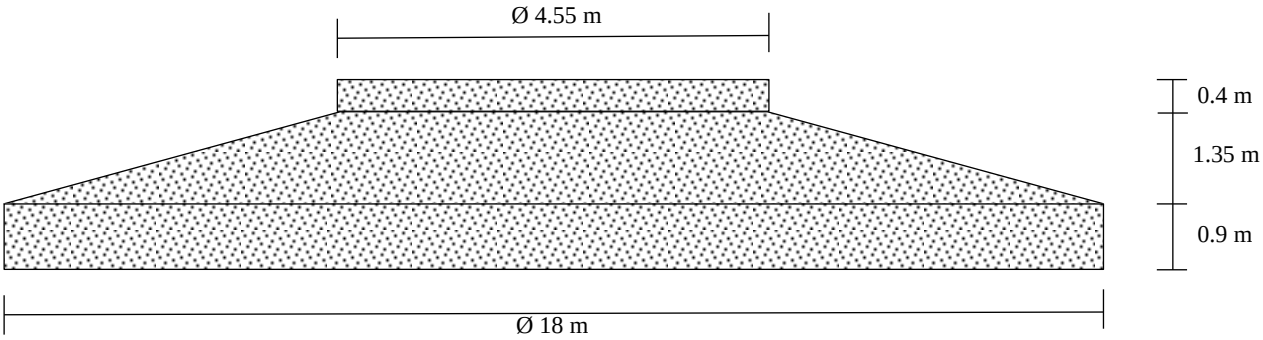

Figure 4-5: Foundation dimensions

4.8. FEM Schematization

The schematizing in Figure 4-6 shows how all the different components discussed in this section.

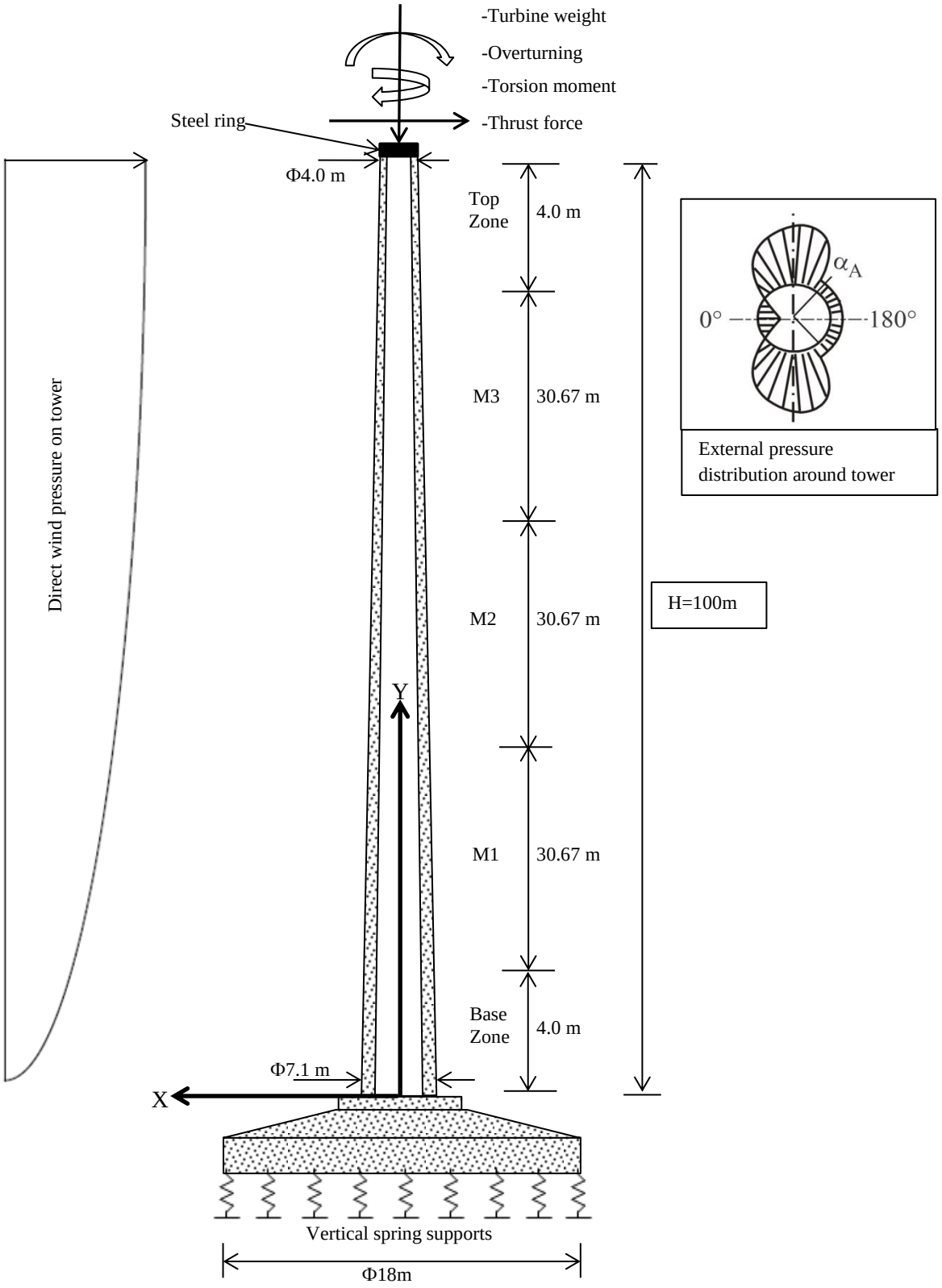

Figure 4-6: FEM Schematization

Chapter 5: Analytical design methods

5.1. Introduction

The finite element method is an excellent method for designing complex structures, but it can be a time consuming and expensive method. The results of a finite element analysis can also be difficult to interpret, as the method produces a vast amount of data. Analytical design methods can sometimes produce accurate results in a time and cost effective manner. In this chapter various codes are used to design and analyze different aspects of the tower. The methods described, are mainly used in the preliminary design stage, but some may even be used in the detailed design stage. Microsoft Excel is used for all the calculations and therefore the methods described in this chapter, can be done on any computer without additional software.

In this chapter the reinforcing steel requirements and the shear resistance of the tower, are calculated according to the strength method. Design codes from North America use the strength design method and not the limit state design method used in SA. The main difference between the two design methods is that the strength method does not reduce the material strength with a partial safety factor. The nominal section strength (calculated without partial material factors) is reduced by a strength reduction factor to calculate the design strength of the section. The design loads used in the strength method is calculated using the same methodology used by the limit state design method.

American design codes are used in this report to design certain aspects of the tower as it is often used in literature. It is thus valuable to compare these methods to the FEM to verify their accuracy. The European equivalents of the codes can be used in SA to comply with the limit state design principles.

Simpson's rule is a simple, but accurate, method that is used to calculate all integrals in this chapter. The method is used by dividing the tower height into small elements (size of the FEM mesh or smaller) and then calculating the function at the centroid of each of these elements. The integral is then computed by multiplying each function value by the element size and then summing all the values. Mathematically the method can be described as follows:

$$\int_0^h f(y)\,dx = \sum_0^n \frac{h}{n} f(y) \tag{5.1}$$

Where,
y is the function variable
h is the height of the tower
n is the number of elements over the height of the tower

5.2. Loads

The direct wind pressure load described in Chapter 3 should be changed from a three dimensional wind pressure to a one dimensional line load for the analytical calculations. There are two methods that can be used to calculate the line load:

ASCE 7-10 Method

The velocity wind pressure as a function of tower height is calculated in section 3.2.2. The method can be extended to produce a line load. This is done by first determining a force coefficient for the shape and roughness of the structure. The force coefficients prescribed by the ASCE for different structures are given in Table 5-1. The velocity wind pressure can then be multiplied with the force coefficient and the projected area of the tower, to produce a line load. The necessary equations are given below:

$$F(y) = q_z(y)C_f(y)A_f(y) \tag{5.2}$$

Where,

y is the height of interest

$q_z(y)$ is the velocity wind pressure at height y

$C_f(y)$ is the force coefficient from Table 5-1

$A_f(y)$ is the projected area of the tower normal to the wind direction

Table 5-1: Force coefficients (ASCE 7-10, 2010)

Cross-Section	Type of Surface	h/D		
		1	7	25
Square (wind normal to face)	All	1.3	1.4	2.0
Square (wind along diagonal)	All	1.0	1.1	1.5
Hexagonal or octagonal	All	1.0	1.2	1.4
Round ($D\sqrt{q_z} > 2.5$) ($D\sqrt{q_z} > 5.3$, D in m, q_z in N/m^2)	Moderately smooth	0.5	0.6	0.7
	Rough (D'/D = 0.02)	0.7	0.8	0.9
	Very rough (D'/D = 0.08)	0.8	1.0	1.2
Round ($D\sqrt{q_z} \leq 2.5$) ($D\sqrt{q_z} \leq 5.3$, D in m, q_z in N/m^2)	All	0.7	0.8	1.2

Modified SANS method

To be able to make a direct comparison between the FEM result and analytical method, another method is used to calculate the direct wind pressure. The circumferential wind pressure used for the FEM is used to derive the line load. This is done by calculating the wind force acting normal to each element, and then calculating its component acting in the direction of the wind flow.

The shear force, V(y) and moment, M(y), as a function of tower height, is given by:

$$V(y) = \int_y^h F(y)dy + F_{Turbine} \tag{5.3}$$

$$M(y) = \int_y^h F(y).(h-y)dy + M_{Turbine} \quad (5.4)$$

Where,

F(y) is the direct wind force on the tower at height y

h is the tower height

y is the height of interest

$F_{Turbine}$ is the thrust force induced by the turbine

$M_{Turbine}$ is the overturning moment induced by the turbine

5.3. Design of reinforcing steel

The reinforcing steel is designed according to the ACI 307-98, that describes the design of reinforced concrete chimneys. The code uses the strength method for design, rather than the ULS design method.

The following assumptions are made by the code (ACI 307, 1998):

- Maximum concrete strain is 0.003
- Maximum steel strain is 0.07
- Design strength of a section in terms of moment will be taken as the nominal moment resistance multiplied by a strength reduction factor equal to 0.70 for vertical strength

The following equations, in conjunction with Figure 5-1, are used to calculate the nominal moment resistance of the tower:

$$K_1 = \frac{P_u}{rtf_c'} = 1.7Q\lambda + 2\varepsilon_m K_e \omega_t Q_1 + 2\omega_t \lambda_1 \quad (5.5)$$

Where,

P_u is the factored vertical load

f_c' is the cylinder compression strength of the concrete

r is the average radius of the section

t is the thickness of the section

The following angles and variables are shown in Figure 5-1:

$$\lambda = \tau - n_1\beta \quad \text{(Radians)} \quad (5.6)$$

$$Q_1 = \frac{\sin\psi - \sin\mu - (\psi-\mu)\cos\alpha}{1-\cos\alpha} \quad (5.7)$$

$$\lambda_1 = \mu + \psi - \pi \quad (5.8)$$

$$\cos\tau = 1 - \beta_1(1-\cos\alpha) \quad (5.9)$$

$$\cos\psi = \cos\alpha - \left(\frac{1-\cos\alpha}{\varepsilon_m}\right)\left(\frac{f_y}{E_s}\right) \geq -1.0 \quad (5.10)$$

$$\cos\mu = \cos\alpha + \left(\frac{1-\cos\alpha}{\varepsilon_m}\right)\left(\frac{f_y}{E_s}\right) \leq 1.0 \quad (5.11)$$

Where,

α is half the central angle subtended by neutral axis

β is half of the opening angle

β_1 is $0.85 - 0.05\left(\frac{f_c' - 27.6}{6.9}\right) \geq 0.65$

$$K_e = \frac{E_s}{f_y} \quad (5.12)$$

$$\omega_t = \frac{\rho_t f_y}{f_c'} \quad (5.13)$$

Where,

E_s is Young's modulus for steel

f_y is the steel yield strength

ρ_t is the ratio of the total vertical reinforcement to total area of concrete

n_1 is the number of openings entirely in compression zone

$$\varepsilon_m = 0.07\left(\frac{(1-\cos\alpha)}{(1+\cos\alpha)}\right) \leq 0.003 \quad (5.14)$$

$$M_n = P_u r K_3 \quad (5.15)$$

$$K_3 = \cos\alpha + \frac{K_2}{K_1} \quad (5.16)$$

$$K_2 = 1.7QR + \varepsilon_m K_e \omega_t Q_2 + 2\omega_t K \quad (5.17)$$

Q is the reinforcing stress level correction factor. It takes account of the reinforcing, not effective due to the position of the neutral axis, and the triangular stress strain diagram of the section. Q values for different values of α are given in Table 5-2.

Table 5-2: Q values for different angles of α

α ≤ 5 deg	$Q = (-0.523 + 0.181\alpha - 0.0154\alpha^2) + (41.3 - 13.2\alpha + 1.32\alpha^2)\left(\frac{t}{r}\right)$
5 deg < α ≤ 10 deg	$Q = (-0.154 + 0.01773\alpha + 0.00249\alpha^2) + (16.42 - 1.980\alpha + 0.0674\alpha^2)\left(\frac{t}{r}\right)$
10 deg < α ≤ 17 deg	$Q = (-0.488 + 0.076\alpha) + (9.758 - 0.640\alpha)\left(\frac{t}{r}\right)$
17 deg < α ≤ 25 deg	$Q = (-1.345 + 0.2018\alpha - 0.004434\alpha^2) + (15.83 - 1.676\alpha + 0.03994\alpha^2)\left(\frac{t}{r}\right)$
25 deg < α ≤ 35 deg	$Q = (0.993 - 0.00258\alpha) + (-3.27 + 0.0862\alpha)\left(\frac{t}{r}\right)$
α > 35 deg	$Q = 0.89$

$$Q_2 = \frac{(\psi-\mu)(1+2\cos^2\alpha)+0.5(4\sin 2\alpha+\sin 2\psi-\sin 2\mu)-4\cos\alpha(\sin\alpha+\sin\psi-\sin\mu)}{(1-\cos\alpha)} \quad (5.18)$$

$$K = \sin\psi + \sin\mu + (\pi - \psi - \mu)\cos\alpha \quad (5.19)$$

$$R = \sin\tau - (\tau - n_1\beta)\cos\alpha - \left(\frac{n_1}{2}\right)[\sin(\gamma + \beta) - \sin(\gamma - \beta)] \quad (5.20)$$

Where,

M_n is the nominal moment strength of the section

γ is half the angle between the center lines of the two openings and for no openings, $n_1 = \gamma = \beta = 0$; for one opening in the compression zone, $n_1 = 1, \gamma = 0$; for two openings in compression zone, $n_1 = 2$. This is useful when accounting for the door opening at the bottom of the tower.

The calculation procedure can be summarized by 5 steps if the following variables are known: r, t, f_c', β, γ, P_u and M_u. P_u and M_u are the factored vertical load and the factored moment.

Step 1) Assume a value for the total vertical steel ratio ρ_t.

Step 2) By trial and error, find the value of α that satisfies equation 5.5

Step 3) Substitute this value of α in equation 5.15 and calculate M_n.

Step 4) If $\varphi M_n < M_u$, increase ρ_t, If $\varphi M_n > M_u$, decrease ρ_t

Step 5) Repeat Step 2 to 4 until $\varphi M_n = M_u$

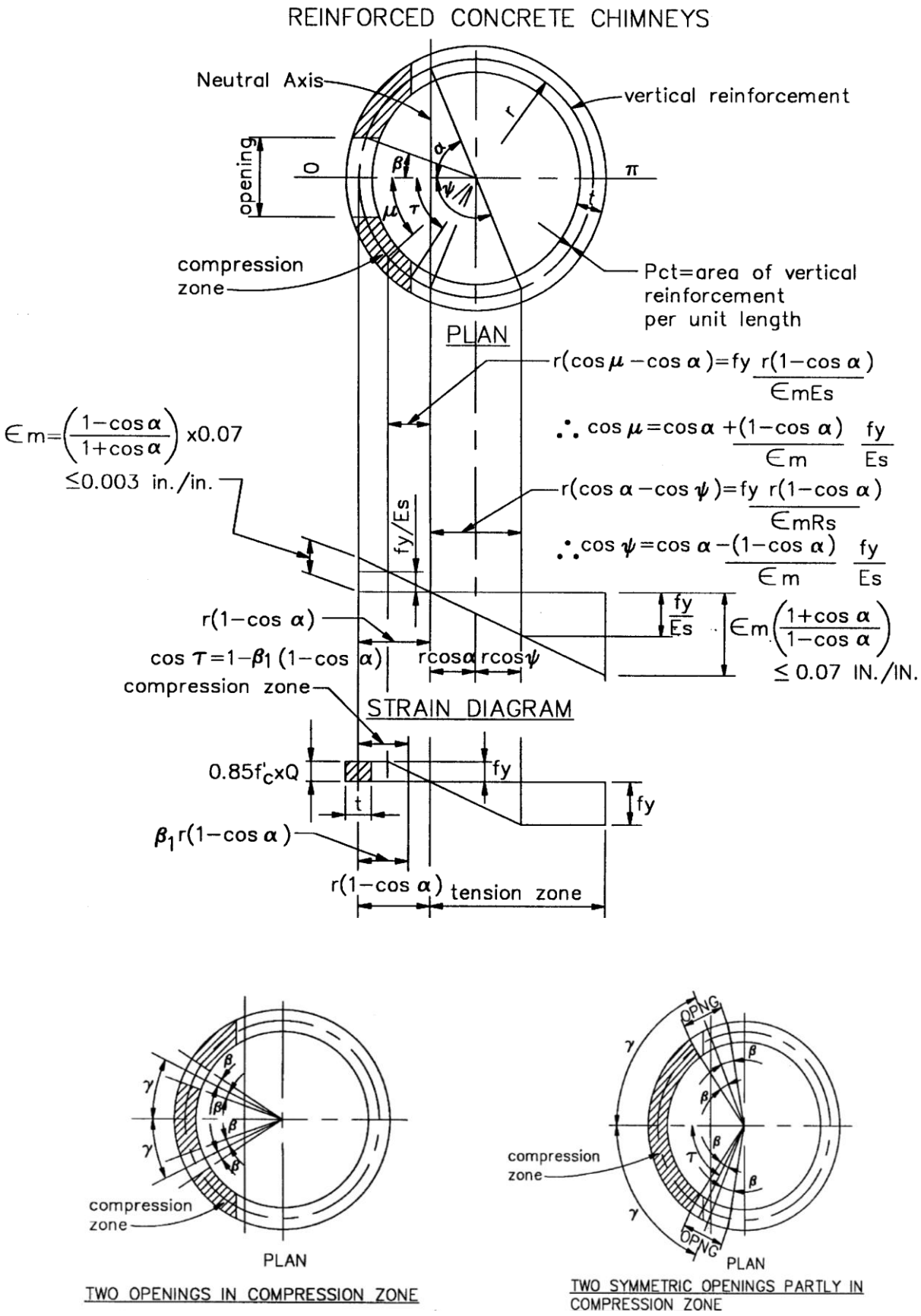

Figure 5-1: Stress-strain diagram for reinforced concrete tower with openings (ACI 307, 1998)

5.4. Shear strength and torsion resistance

The shear and torsion resistance of the tower is calculated according to the ACI 318-11 design code. The code is published by the American Concrete Institute and covers the proper design and construction of buildings of structural concrete (ACI 318, 2011). The tower is subjected to axial, moment, shear and torsion forces. The method discussed in this section will take account of the different forces to calculate the shear and torsion strength of the tower. As mentioned earlier, American design codes use the strength method instead of the ULS method generally used in SA.

The nominal shear strength of a concrete column is decomposed into the shear strength of the concrete itself and the shear strength provided by shear reinforcing. The factored design shear strength is given by:

$$V_u = \phi V_c + \phi V_s \tag{5.21}$$

Where,

V_c is the shear strength provided by the concrete

V_s is the shear strength provided by shear reinforcing

ϕ is the strength reduction factor. (For shear and torsion = 0.75)

The bending moment force can, to a certain extent, influence the shear strength of a column. This is due to the fact that the bending moment will cause parts of the section to crack, thus reducing the shear capacity of the concrete. The following equation takes into account the effects of the longitudinal reinforcing, as well as the magnitude of the moment and shear forces, to calculate the shear resistance of the concrete.

$$V_c = \left(\lambda\sqrt{f_c'} + 120\rho_w \frac{V_u d}{M_u}\right)\frac{b_w d}{7} \leq 0.3\lambda\sqrt{f_c'} b_w d \tag{5.22}$$

With, $\frac{V_u d}{M_u} \leq 1$

Where,

$\rho_w = \frac{A_s}{b_w d}$

A_s is the total area of the longitudinal reinforcing steel

V_u is the factored shear at the section considered

M_u is the factored moment occurring simultaneously with V_u

λ is taken as 1.0

d is the effective depth of the reinforcing

$b_w d$ is the effective shear area

The code recommends that for circular sections d should be taken as 0.8D where D is the diameter of the column. The effective shear area should be taken as $0.8A_g$ where A_g is the gross area of the column.

A torsion force will cause shear stresses in the section that will add to the normal shear force on the one side of the section and subtract on the other side. The code gives the following guideline to calculate the resistance of columns subjected to both shear and torsion forces.

For hollow sections:

$$\frac{V_u}{b_w d} + \frac{T_u p_h}{1.7 A_{oh}^2} \leq \phi \left(\frac{V_c}{b_w d} + 0.66\sqrt{f_c'} \right) \tag{5.23}$$

Where,

p_h is the perimeter of the centerline of the outermost closed torsional reinforcing

A_{oh} is the area enclosed by the centerline of the outermost closed transverse torsional reinforcement

The code also states that if the wall thickness of the section is less than $\frac{A_{oh}}{p_h}$ the second term in the equation should be changed to $\frac{T_u}{1.7 A_{oh}}$.

5.5. Deflection

The deflection of the tower can be accurately calculated by analytical methods in the uncracked state. The material behaviour becomes nonlinear when cracking takes place and the analytical methods will under estimate the deflection. The method described in this section can thus be used in the SLS condition, before significant cracking occurs. The method can also be used for a concrete tower that has a post tension force large enough to avoid the formation of cracks. One problem that has to be solved to be able to calculate the maximum deflection of the structure, is the equivalent stiffness of the reinforced concrete section. The stiffness of the section is a combination of the steel's stiffness and the concrete's stiffness. The section stiffness cannot simply be calculated by combining the stiffness of the two materials in their respective ratios, as this will average the effect of the steel stiffness over the whole section and cause the moment lever arm of the steel to be incorrect. The problem is solved by using the method of section transformation.

5.5.1. Transformed-section method for composite materials

A material that is composed out of more than one material is considered as a composite material. A reinforced concrete beam combines concrete and steel in such a manner as to utilize the strengths of both materials. Reinforced concrete can thus be seen as a composite material. The flexure formulas used to describe the behaviour of beams are derived for beams consisting of a homogeneous material and can thus not directly be used for a composite material. The transformed-section method transforms a composite section to a section consisting out of only one material. This is done by realizing that for a

composite beam the total cross-section area will remain a plane when a bending moment is applied to the beam. If the material has linear-elastic behaviour, Hooke's law applies and the stress in the section is given by $\sigma = E\varepsilon$. The Young's modulus of steel can be changed to that of the concrete, if the steel's section dimensions are changed to account for the difference in stiffness. It is important that when changing the dimensions of the steel reinforcing, the moment lever arm must still correspond to the original moment lever arm before the stiffness was altered. A transformation factor, n, is defined to convert the area of the steel to an equivalent area of concrete. The transformation factor is given by:

$$n = \frac{E_{st}}{E_{conc}} \tag{5.24}$$

After the reinforcing steel has been converted to an equivalent concrete area, the whole section consists out of one homogeneous material and the normal flexural formulas for calculating the deflection of a beam can be used.

5.5.2.Moment area method for deflection

The moment area method is a tool that is used to derive the slope, rotation and deflection of beams and frames. The moment area method was developed by Charles Greene in 1873. The method is based on two theorems called the moment area theorems.

Theorem 1 states that the change in slope between the tangents to the elastic curve at any two points is equal to the area under the M/EI diagram between the two points, provided that the elastic curve is continuous between the two points.

$$Slope = \frac{Area\ of\ bending\ moment\ diagram\ between\ points\ A\ and\ B}{EI}$$

Or mathematically:

$$\theta_{AB} = \int_A^B \frac{M}{EI} dx \tag{5.25}$$

Where,
M is the moment
EI is the flexural stiffness
θ_{AB} is the change in slope between points A and B
A, B are points on the elastic curve

Theorem 2 states that the vertical deviation of the tangent at a point A on an elastic curve, with respect to the tangent which is extended from another point B, equals the moment of the area under the M/EI diagram between those two points. This moment is computed about the point at which the deviation is desired, provided that the elastic curve is continuous between the two points. Mathematically the theorem is given by:

$$t_{A/B} = \int_A^B \frac{M}{EI} \bar{x}\, dx \tag{5.26}$$

Where,

$t_{A/B}$ is the deviation of a tangent at point B with respect to the tangent at point A.

$\bar{x}$ is the centroid of M/EI diagram measured horizontally from point A

The deflection of the tower along the height of the tower is thus given by:

$$\Delta(y) = \int_0^y \frac{M(y)}{E(y)\, I(y)} (h - y)\, dy \tag{5.27}$$

Where,

M(y) is the bending moment at height y

E(y) is Young's modulus of the transformed section at a height y

I(y) is the moment of inertia of the transformed section at a height y

5.6. Second order effects (P-Delta)

Slender structures that undergo relatively large deformations are prone to second order effect. One of the most common second order effects, is the P-Delta effect. The P-Delta effect occurs in all structures that are subjected to axial loads. The effect is usually negligibly small in rigid structures and is thus ignored in the analysis of the structure. When a structure undergoes large deformations, the axial load has an eccentricity and causes second order moments to arise. These moments can be significant in slender structures subjected to large axial forces. A wind turbine tower is slender and is subjected to a large axial force, caused by the turbine weight at the top of the tower. The own weight of a concrete tower will also cause second order moments in the deformed state. The effect is schematized in Figure 5-2.

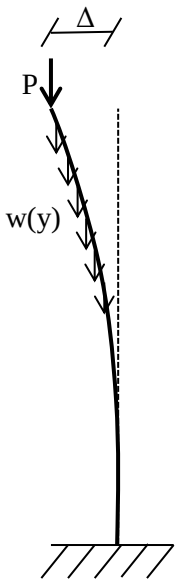

Figure 5-2: P-Delta effect on tower

The additional overturning moment of both the turbine weight and tower's own weight is calculated by using the maximum deflection of the tower and the deflection curve of the tower. Mathematically it can be calculated by the following equation:

$$M_{add} = \int_0^h w(y)\Delta(y)\,dy + P\Delta \tag{5.28}$$

Where,

w(y) is the function describing the own weight of the tower.

Δ(y) is the deflection function

P is the turbine weight

5.7. Fatigue design according to Model Code 2010

The fatigue life of the tower is checked using the Model code 2010. The code makes provision for high strength concrete subjected to a large number of cycles (>10^8). The method is based on the characteristic S-N curves of the reinforcing steel and concrete. The process that is followed to calculate the fatigue strength, is discussed below:

Reinforcing steel

The fatigue requirement will be met if the calculated maximum acting stress range, $\Delta\sigma_{Ss}$, satisfies the following requirement:

$$\gamma_{Ed}\ \Delta\sigma_{Ss} \leq \frac{\Delta\sigma_{Risk}(n)}{\gamma_{s,fat}} \tag{5.29}$$

Where,

$\Delta\sigma_{Ss}$ is the maximum steel stress range under the acting fatigue load

n is the foreseen number of load cycles in the design life of the structure

$\Delta\sigma_{Risk}(n)$ is the stress range relevant to n cycles obtained from the characteristic fatigue strength function given by the code

γ_{Ed} is the partial load factor for fatigue (Taken as 1.10 by the code)

$\gamma_{s,fat}$ is the partial material factor for steel (Taken as 1.15 by the code)

The characteristic fatigue curve is given by the following equation:

$$log(\Delta\sigma_{Risk}(n)) = \log(\Delta\sigma^*_{Risk}) - \frac{1}{k_1}\log\left(\frac{n}{N^*}\right) \qquad for\ n \le N^* \tag{5.30}$$

$$log(\Delta\sigma_{Risk}(n)) = \log(\Delta\sigma^*_{Risk}) - \frac{1}{k_2}\log\left(\frac{n}{N^*}\right) \qquad for\ n > N^* \tag{5.31}$$

The parameters of the S-N curves for different reinforcing bars, are given in Table 5-3 and the generic fatigue strength curve is shown in Figure 5-3.

Table 5-3: Parameters of S-N curves for reinforcing steel (embedded in concrete) (CEB-FIB, 2010)

	N^*	Stress exponent		$\Delta\sigma_{Risk}$ (MPa)	
		k_1	k_2	at N^* cycles	At 10^8 cycles
Straight and bent bars D ≥ 25φ					
φ ≤ 16 mm	10^6	5	9	210	125
φ > 16 mm	10^6	5	9	160	95
Marine environment	10^7	3	5	65	40
Where, φ is the reinforcing bar diameter D is the diameter of mandrel					

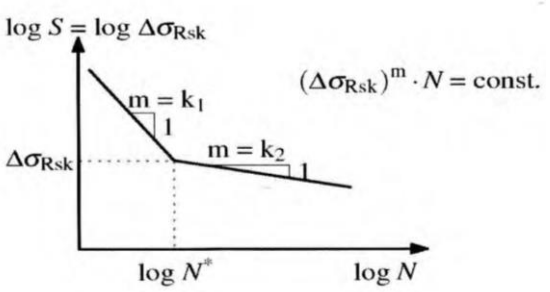

Figure 5-3: Generic characteristic fatigue strength curves (S-N curves) for steel (CEB-FIB, 2010)

Concrete

The fatigue requirements for concrete are given below:

$n \leq N$

Where,

n is the foreseen number of load cycles in the design life of the structure

N is the number of resisting stress cycles, to be calculated from the fatigue strength functions given below.

For concrete in compression:

For $S_{c,min} > 0.8$, the S-N relation for $S_{c,min} = 0.8$ is valid. For $0 \leq S_{c,min} \leq 0.8$ the following equations should be used:

$$\log N_1 = \left(12 + 16S_{c,min} + 8S_{c,min}^2\right)\left(1 - S_{c,max}\right) \quad (5.32)$$

$$\log N_2 = 0.2 \log N_1 (\log N_1 - 1) \quad (5.33)$$

$$\log N_3 = \frac{\log N_2 (0.3 - 0.375 S_{c,min})}{\Delta S_c} \quad (5.34)$$

If,

(a) $\log N_1 \leq 6, then\ \log N = \log N_1$

(b) $\log N_1 > 6\ and\ \Delta S_c \geq 0.3 - 0.375 S_{c,min}, then\ \log N = \log N_2$

(c) $\log N_1 > 6\ and\ \Delta S_c < 0.3 - 0.375 S_{c,min}, then\ \log N = \log N_3$

Where,

$\sigma_{c,max}$ is the maximum compressive stress

$\sigma_{c,min}$ is the minimum compressive stress

$S_{c,max}$ is the maximum compressive stress level

$S_{c,min}$ is the minimum compressive stress level

$S_{c,max} = \frac{\gamma_{Ed}\, \sigma_{c,max}\, \eta_c}{f_{ck,fat}}$

$S_{c,min} = \frac{\gamma_{Ed}\, \sigma_{c,min}\, \eta_c}{f_{ck,fat}}$

ΔS_c is the stress level range

$\Delta S_c = S_{c,max} - S_{c,min}$

The fatigue reference compression strength, $f_{ck,fat}$ is calculated below:

$$f_{ck,fat} = 0.85 \beta_{cc}(t) \left[\frac{1}{\gamma_c}\left(f_{ck}\left(1 - \frac{f_{ck}}{25 f_{ck0}}\right)\right)\right] \quad (5.35)$$

Where,

f_{ck} is the characteristic cylinder compression strength of the concrete

f_{ck0} is the reference strength (10 MPa)

γ_c is the material partial factor for concrete (1.5)

$\beta_{cc}(t)$ is a function describing the strength deployment of concrete with time

$$\beta_{cc}(t) = exp\left(s\left[1 - \left(\frac{28}{t}\right)^{0.5}\right]\right) \tag{5.36}$$

Where,

t is the concrete age in days at the time fatigue loading starts

s is the coefficient which depends on the strength class of the cement (s = 0.2 for CEM 52.5 N)

The stress gradient for concrete in the compression zone of a cracked section is taken into account by η_c:

$$\eta_c = \frac{1}{1.5 - 0.5\left(\frac{|\sigma_1|}{|\sigma_2|}\right)} \tag{5.37}$$

Where,

η_c is the averaging factor of concrete stresses in the compression zone considering the stress gradient.

$|\sigma_1|$ is the lower absolute value of the compressive stress within a distance of 300 mm from the surface under the relevant load combination of actions.

$|\sigma_2|$ is the larger absolute value of the compressive stress within a distance of 300 mm from the surface under the same load combination as for which $|\sigma_1|$ was determined.

The S-N curves for concrete given by the equations above are shown in Figure 5-4.

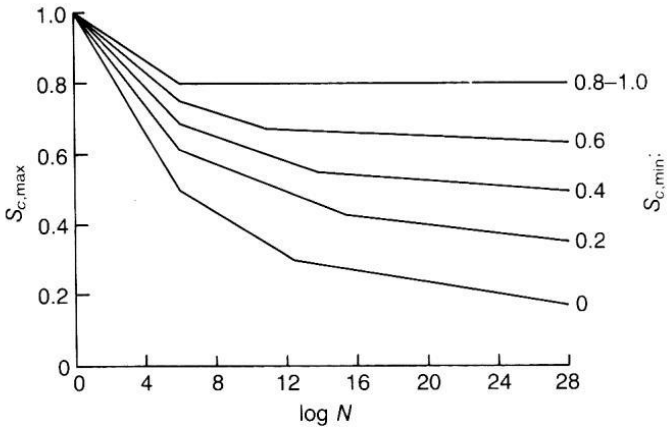

Figure 5-4: S-N curves for concrete (CEB-FIB, 2010)

5.8. Fundamental frequency of the tower

There are many analytical methods for calculating a structure's fundamental frequency, but very few of these methods can incorporate a varying section area, varying stiffness and lumped mass all together. Energy methods are of the few methods that can incorporate all the varying properties of the tower to calculate the fundamental frequency. The principle of conservation of energy forms the basis of all energy methods. The principle states that the total energy of a closed system will stay constant in the absence of losses like friction, damping etc. In practice, there will always be energy losses, but these losses are negligibly small in many cases and thus an accurate answer can still be achieved by neglecting them. The total energy of a closed vibrating system can be categorized into potential energy and kinetic energy and has the following property:

$$\frac{d}{dt}(K_e + P_e) = 0 \tag{5.38}$$

Where,

K_e is the total kinetic energy of the system

P_e is the total potential energy of the system

Rayleigh's energy method uses the conservation of energy principle to calculate the fundamental frequency of a structure. The kinetic energy of the system is the energy of the vibrating motion and is calculated from the velocity. The potential energy is given by the strain energy of the tower. The first step in Rayleigh's method is to assume a displacement function for the structure. The displacement function can then be used to calculate the kinetic and potential (strain) energy. The accuracy of the method largely depends on the accuracy of the assumed deflection function. A generic equation for the fundamental frequency of a beam is derived below:

Assuming harmonic vibration and that the displacement function for the structure is given by:

$$y(x,t) = Y(x)\sin(\omega t + \alpha) \tag{5.39}$$

Where,

Y(x) is the assumed deflection curvature of the tower, then

the kinetic energy of the beam is given by:

$$T = \frac{1}{2}mv^2 = \frac{1}{2}\int_0^h \dot{y}^2 dm = \frac{1}{2}\int_0^h \dot{y}^2\, m(x)\, dx \tag{5.40}$$

Where,

$\dot{y}$ is the first derivative of the displacement function

m(x) is the section mass per meter at height x

h is the height of the tower

Accounting for the lumped turbine mass the maximum kinetic energy is given by:

$$T_{max} = \frac{\omega^2}{2}\left[\int_0^h m(x)\, Y(x)^2\, dx + M_t\ Y(h)^2\right] \tag{5.41}$$

Where,

M_t is the turbine mass

The potential energy of the beam is the work done by deforming the beam. By assuming elastic deformation and neglecting the work done by shear force, the potential energy for the beam is given by:

$$U = \frac{1}{2}\int_0^h M\, d\theta = \frac{1}{2}\int_0^h \left(EI\frac{d^2y}{dx^2}\right)\frac{d^2y}{dx^2}\, dx \tag{5.42}$$

The maximum potential (strain) energy is given by:

$$U_{max} = \frac{1}{2}\int_0^h E(x)\, I(x)\left[Y^{"}(x)\right]^2\, dx \tag{5.43}$$

Where,

E(x) is Young's modulus for the transformed section at height x

I(x) is the moment of inertia for the transformed section at height x

Y"(x) is the second derivative of the displacement function

According to the conservation of energy principle, $T_{max} = U_{max}$ and thus the fundamental frequency is:

$$\omega^2 = \frac{\int_0^h E(x)\, I(x)\left[Y^{"}(x)\right]^2\, dx}{\int_0^h m(x)\, Y(x)^2\, dx + M_t\, Y(h)^2} \tag{5.44}$$

It is important to note that Rayleigh's method yields an upper-bound solution for the fundamental frequency of the tower. The assumed displacement function introduces additional constraints which increase the stiffness of the system and thus leads to a slightly higher fundamental frequency than that of the real structure. There are many deflection curves available for cantilever beams - two of the common curves are given below:

$$F_1(x) = a\left[1 - \cos\left(\frac{\pi x}{2h}\right)\right] \tag{5.45}$$

$$F_2(x) = a\left[\frac{3x^2}{2h^2} - \frac{1}{2}\frac{z^3}{h^3}\right] \tag{5.46}$$

Where,

a is a constant describing the maximum deflection of the tower. a is left as a constant throughout the frequency calculations.

5.9. Foundation flexibility effect on tower fundamental frequency

The analytical method discussed in the previous section does not make provision for the flexibility of the foundation. This effect can be accounted for by using a method proposed by Berger-Abam engineers (LaNier, 2004). The method involves separating the vibration frequencies into a rigid body base rotation frequency, rigid body base translation frequency and the tower flexure frequency. The different frequencies can then be combined with the following equation:

$$\frac{1}{f^2} = \frac{1}{f_r^2} + \frac{1}{f_t^2} + \frac{1}{f_f^2} \tag{5.47}$$

Where,

f is the combined tower frequency

f_r is the rigid body base rotation frequency

f_t is the rigid body base translation frequency

f_f is the tower flexure frequency calculated in section 5.8.

The rigid body base rotation frequency can be calculated by defining a new deflection curve for the rigid body motion. The frequency can then be calculated with the same method used to calculate the flexural frequency in section 5.8. The rigid body translation frequency can directly be calculated. The results are given below:

Base rotation:

$$Y_1(x) = \frac{b\,h}{K_r} z \tag{5.48}$$

$$U1_{max} = \frac{(bh)^2}{2K_r} \tag{5.49}$$

$$T1_{max} = \frac{1}{2}\left[\int_0^h m(x)\, Y1(x)^2\, dx + M_t\ Y1(h)^2\right] \tag{5.50}$$

$$f_r = \frac{1}{2\pi}\sqrt{\frac{U1_{max}}{T1_{max}}} \tag{5.51}$$

Where,

b is a constant

K_r is the rotation stiffness of the foundation

Base translation

$$f_t = \frac{1}{2\pi}\sqrt{\frac{K_h}{M}} \tag{5.52}$$

Where,

K_h is the translation stiffness of the foundation

M is the mass of the whole system

The modified tower fundamental frequency is then given by:

$$f = \sqrt{\frac{f_r{}^2 f_t{}^2 f_f{}^2}{f_r^2 f_f^2 + f_t^2 f_f^2 + f_r^2 f_t^2}} \tag{5.53}$$

Chapter 6: Results

6.1. Introduction

In this chapter the results of both the FEM and analytical model, are discussed. All the results are calculated according to the methods discussed in Chapter 4 and Chapter 5. They are then evaluated according to the appropriate structural guidelines to determine the structural integrity of the tower. The calculations that are done for both the FEM and analytical model, will be compared to determine the accuracy of the analytical method.

6.2. FEM verification

In this report the FEM is seen as the most accurate representation of the structural behaviour of the actual tower. All other methods will be compared to the FEM to determine their accuracy. It is thus important to verify the accuracy of the FEM. The first method used to verify the FEM is to compare the applied forces to the FEM reaction forces. The percentage error for both the SLS and ULS are given in Table 6-1. The percentage error in equilibrium is very small and it can therefore be said with relative certainty that the forces are correctly applied in the FEM.

Table 6-1: Percentage error for equilibrium

	SLS (%)	**ULS (%)**
Overturning moment	0.11	0.09
Shear force	-0.01	-0.07
Axial force	-0.14	-0.12
Torsion moment	-0.18	-0.19

The convergence of the model is another method that is used to verify the FEM. To ensure that the final solution is a well converged solution, the relative energy variation of each step has to be less than $1x10^{-5}$ and the relative out of balance force has to less than $1x10^{-3}$. This criterion is met for all load steps and thus a well converged solution is obtained.

The final check that is done, is to visually inspect the tower's deflected shape. The structural shape of the tower is very basic and it is thus possible to visualize the shape of the deformed tower. This serves as another method of ensuring the FEM is an accurate representation of the actual structure.

6.3. Deflection

Deflections are traditionally computed for the SLS. Large deflections of the tower top at the SLS will cause the efficiency of the turbine to decrease and thus these deflections must be limited. There is no deflection limit for the ULS, as long as the structure has sufficient strength to avoid collapse. The maximum deflection in the SLS and ULS is given in Table 6-2. Wind turbine manufacturers usually specify the maximum deflection of the tower under serviceability loads. These limits could not be obtained from the manufacturers and thus the ACI 307-98 is used. The code specifies that the lateral

deflection of the top of a concrete tower prior to the application of load factors, should not exceed the following:

$$Y_{max}=3.33h \quad (6.1)$$

Where,

Y_{max} = maximum lateral deflection (mm)

h = chimney height (m)

Table 6-2: Top of tower deflection

	SLS	**ULS**
FEM Deflection at crack initiation (mm)	168 (At 75% of load)	155 (At 30% of load)
FEM Maximum deflection (mm)	549	1808
ACI 307 limit for deflection	333	-

The tower's deflection at the moment when the concrete starts to crack, is also given in Table 6-2. This is an important parameter, because, until this point the reinforced concrete has behaved like a homogeneous material. As the concrete cracks, it loses its tensile strength and the material stops behaving like a homogeneous material. The tensile forces are now almost exclusively resisted by the steel. This causes a reduction in stiffness and thus the deflection increases significantly. The reduction in stiffness as the concrete starts to crack can clearly be seen in Figure 6-1.

The deflection of the tower exceeds the maximum lateral deflection prescribed by the ACI 307. The deflection can be reduced by increasing the reinforcing steel. The amount of extra reinforcing to limit the deflection, will depend on the deflection limit prescribed by the turbine manufacturer.

Cracks start to form at a slightly smaller lateral deflection for the ULS than for the SLS. This is due to the fact that for the ULS, the own weight partial load factor is taken as 0.9 and for the SLS it is taken as 1.0. The own weight is beneficial for resisting the overturning moment as it creates a compressive, "pre-tension", force in the concrete.

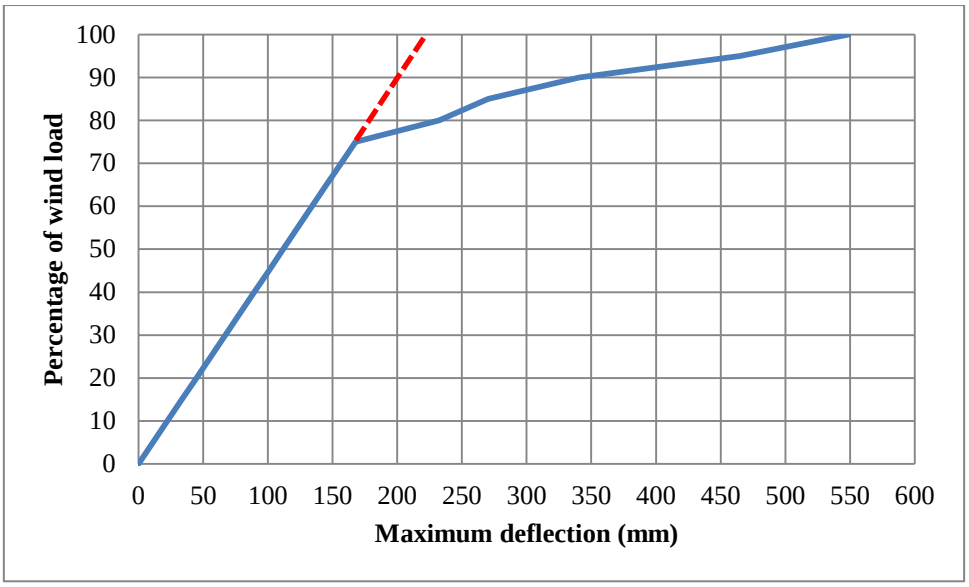

Figure 6-1: Maximum deflection as a function of applied wind load at the SLS

The analytical method for calculating the deflection of the tower, as discussed in section 5.5, is used to calculate the maximum deflection at the SLS. The deflection calculated by the analytical method at the SLS is 60% less than the deflection computed by the FEM. This is due to the fact that the concrete starts to crack at 75% of the total SLS wind load. The analytical method is only applicable for the uncracked state, and thus the stiffness is overestimated by the method in the cracked state. If the deflection line of the uncracked tower is extended (dotted red line) to where it reaches 100% of the load, then the deflection at this point corresponds to that of the analytical method. The analytical method estimates the deflection within 1.8% of the FEM value, when 75% of the total load is applied. It is thus clear that the analytical method is an accurate method for calculating the deflection of the tower while the concrete is uncracked.

A concrete section that is fully cracked on its tension side, will have a rigidity of anywhere from one-third to three-fourths of its uncracked full section rigidity (McCormac & Brown, 2014). The results for the analytical deflection are given in Table 6-3 for different percentages of concrete stiffness. By assuming that the concrete's modulus of elasticity is 33.3% of the original uncracked stiffness, the deflection is calculated within 4.7% of the FEM deflection. A more rigorous method for determining the stiffness reduction of the concrete due to the formation of cracks is given in section 6.12.

Table 6-3: Analytical method deflection calculated with different concrete stiffness

	Analytical method (mm)	Error (%) *
Uncracked section at 75% of load	165	-1.79
Uncracked section at 100% of load	220	-59.93
Cracked section - $0.75E_c$	281	-48.82
Cracked section - $0.33E_c$	523	-4.74

*Error when compared to FEM

6.4. Crack pattern and crack width

The tower is normally reinforced and therefore cracks must form in the concrete for the reinforcing steel to be effective. The number of cracks and crack width should, however, be limited in the SLS to avoid loss of stiffness which would reduce the fundamental frequency of the tower. The cracked tower for the SLS and the ULS is shown in Figure 6-2 and Figure 6-3 respectively.

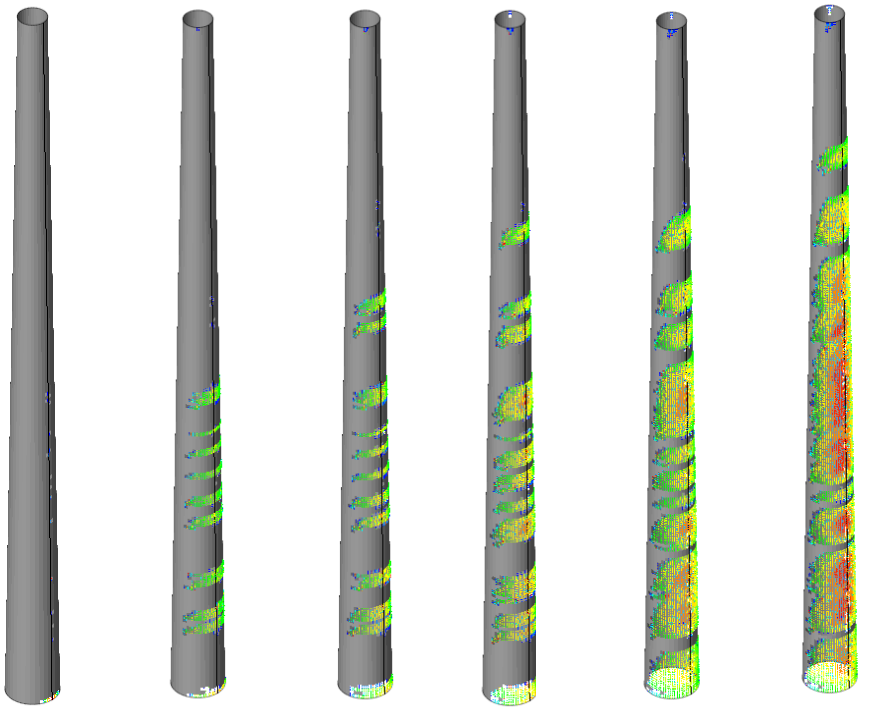

Figure 6-2: SLS crack pattern as a function of total wind load applied

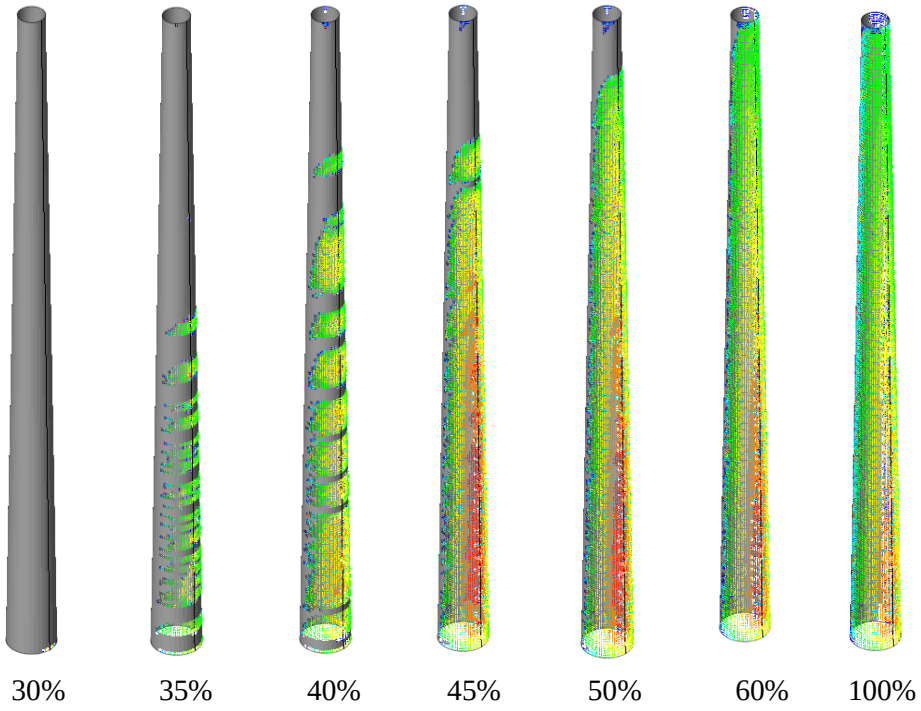

Figure 6-3: ULS crack pattern as a function of total applied wind load

The formation of cracks in the SLS starts at approximately 75% of the total wind load and for the ULS at 30%. The maximum crack width is computed from the FEM for both models and is given in Table 6-4. The recommended crack width specified by the SABS 0100 and ACI 224 codes is also given in Table 6-4 (ACI 224, 2007). The SLS crack width calculated by the FEM is larger than the largest crack width allowed by both codes. The crack width should thus be reduced by either increasing the reinforcing steel size, thus reducing the tensile stress in the reinforcing, or by decreasing the spacing of the bars.

Table 6-4: Comparison between computed crack width and code limits

FEM*	
SLS	0.446
ULS	1.590
SABS 0100-1*	
General	0.3
Aggressive environment	0.004 x Cover = 0.16
ACI 224*	
Dry air	0.41
Moist air, soil	0.30
Deicing chemicals	0.18
Seawater and seawater spray	0.15
Use in water-retaining structures	0.10

*All crack widths is given in mm

There are various analytical methods for calculating the crack width in concrete structures, but most deal with rectangular beams or slabs. If the stress in the reinforcing steel is known, the ACI 224 gives a method for approximating the maximum crack width. It is important to note that there are many factors affecting the crack width of a concrete member and that crack width calculations are merely an approximation and may differ substantially from the actual crack width. The method recommended by the ACI is given below:

$$w = 2\frac{f_s}{E_s}\beta\sqrt{d_c^2 + \left(\frac{s}{2}\right)^2} \tag{6.2}$$

Where,

w is the maximum crack width

f_s is the reinforcing steel stress

E_s is the modulus of elasticity of the reinforcing steel

β is the ratio of the distance between the neutral axis and tension face to the distance between the neutral axis and the centroid of the reinforcing steel (taken as approximately $1.0 + 0.08d_c$)

d_c is the thickness of the concrete cover

s is the bar spacing

The crack width calculated by the ACI method is 0.672 mm. This is higher than the 0.446 mm computed by the FEM and can be seen as a conservative approximation. It is interesting to note that by reducing the bar spacing by half, the crack width is reduced by 55% with the ACI method. This is thus a cost effective method of reducing the crack width of the concrete without increasing the percentage reinforcing steel.

6.5. Concrete stress

6.5.1. Compression stress

The FEM is used to compute the compression stress in the concrete at the ULS and SLS. By applying the partial material safety factor to the concrete compression strength, the compression stress should not exceed 63.3 MPa at the ULS. The compression stress in the tower, as a function of tower height, is given in Figure 6-4. The figure clearly shows that the stress in the concrete is well below this compression stress limit for the ULS. A large stress jump can be seen at foundation level. The most likely reason for this, is the fixed boundary condition enforced at the base of the tower. The tower is fixed against rotation and displacement in all three dimensions. The Poisson effect will cause the concrete to expand perpendicular to the principal compression stress direction. The rigid boundary condition restricts this expansion and causes a large stress concentration at the support. In practice, the tower-foundation interface will allow some expansion and the stress concentrations will not be as significant.

It is possible to optimize the wall thickness of the tower due to the large strength reserve still available. Another method to optimize the concrete usage, is to use a lower strength class of concrete. By reducing the wall thickness or the concrete strength class, the stiffness is also reduced, which will cause a reduction in the fundamental frequency of the tower. This calls for an iterative process where the tower is first designed for strength and then checked for its dynamic properties. If the tower frequency is too high and reserve strength is available, the stiffness can be reduced by the methods stated above, and if the frequency is too low, the stiffness can be increased. The concrete compression stress is not explicitly calculated with the analytical method, but is dealt with in section 6.6 where the moment capacity of the section is calculated.

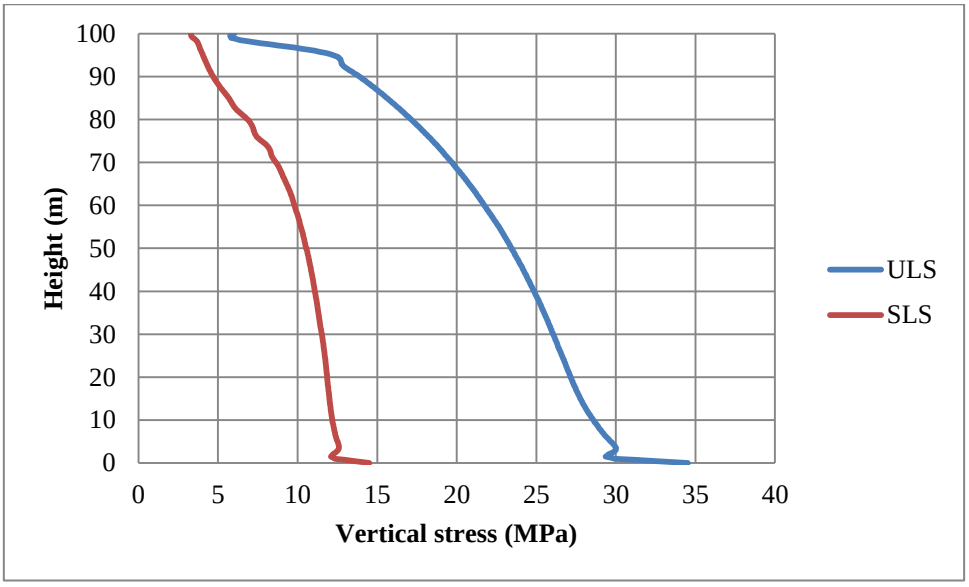

Figure 6-4: Concrete vertical compression stress for ULS and SLS

6.5.2.Shear stress

The maximum shear stress is first computed using the FEM. For a cylindrical cantilever beam, like the tower, the maximum shear stress occurs at the position of the neutral axis. The shear stress is computed one diameter length away from the ends of the tower. This is done to avoid stress concentrations caused by the boundary conditions at the base and concentrated loads at the top. These stress concentrations should be investigated in the final detailed design of the tower to ensure that localized cracking does not occur. The maximum shear stress computed is 3.70 MPa and occurs at the position of the neutral axis, one diameter length from the top of the tower. The shear stress is less than the concrete's combined shear and torsion resistance of 5.41 MPa and therefore shear reinforcing is not required.

The maximum principal stress occurring in the FEM, is investigated to determine the combined effect that moment, axial, torsion and shear forces have on the compression stress in the concrete. The maximum principal compression stress located at the base of the tower on the compression side, is

almost identical to the maximum vertical stress. The effects of shear on the compression side of the tower are thus negligibly small.

Table 6-5: FEM maximum shear and principal stress

	Stress (MPa)
Maximum shear stress*	3.70
Maximum vertical compression stress	36.533
Maximum principal compression stress	36.607

* Stress is computed one diameter length from ends of tower at the position of the neutral axis.

The concrete shear strength is also calculated according to section 5.4 and the results are given in Table 6-6. The ultimate shear stress calculated by the analytical method is significantly lower than that computed by the FEM. One reason for this can be that in the FEM, a large percentage of the section is cracked. This reduces the effective area resisting shear force and thus increases the shear stress in the remaining effective area.

The horizontal reinforcing in the tower that prevents cracking due to ovalization and temperature gradients, will act as shear reinforcing as well. This is ignored in the shear resistance calculation given above and thus the resistance calculated, is conservative.

Table 6-6: Maximum concrete shear stress

	Stress (MPa)
Ultimate shear stress (Including torsion): $V_u = \frac{V_u}{b_w d} + \frac{T_u}{1.7 A_{oh}}$	0.90
Concrete shear resistance: $V_c = \phi \left(\lambda \sqrt{f_c'} + 120 \rho_w \frac{V_u d}{M_u}\right) \frac{b_w d}{7}$	6.60
Combined shear and torsion resistance: $V_{st} = \phi \left(\frac{V_c}{b_w d} + 0.66 \sqrt{f_c'}\right)$	5.41

6.6. Reinforcing steel stress

The reinforcing steel stress is computed by the use of the FEM for both the SLS and ULS. The steel stress should not exceed the limit stress given in Table 6-7. The limit values in the table are calculated by applying the appropriate partial material factor to the characteristic yield stress of the reinforcing steel. The ULS tensile stress of the reinforcing steel, as a function of height, is given in Figure 6-5. The stress is given for the outside layer of reinforcing, as well as the inside layer. As expected, due to the longer lever-arm, the stress is slightly higher in the outside layer. The maximum tensile stress of the reinforcing at the base is just below the allowed stress and is thus completely optimized. The stress reduces to approximately 100 MPa at the top of the tower and it would thus be possible to gradually reduce the percentage reinforcing with height. The reinforcing steel's compression stress, as a function

of height, is given in Figure 6-6. The stress is well below the factored compression strength of the reinforcing. The percentage steel can, however, not be reduced as it is required for tensile resistance when the wind direction changes. The stress jumps at foundation level for both the tensile stress and compression stress, is due to the boundary conditions already discussed above.

Table 6-7: Factored reinforcing steel strength

	SABS 0100 allowable (MPa)	FEM - ULS (MPa)	FEM - SLS (MPa)
Tensile reinforcing steel strength	391.3	390.03	103.00
Compressive reinforcing steel strength	-327.3	-118.35	-52.70

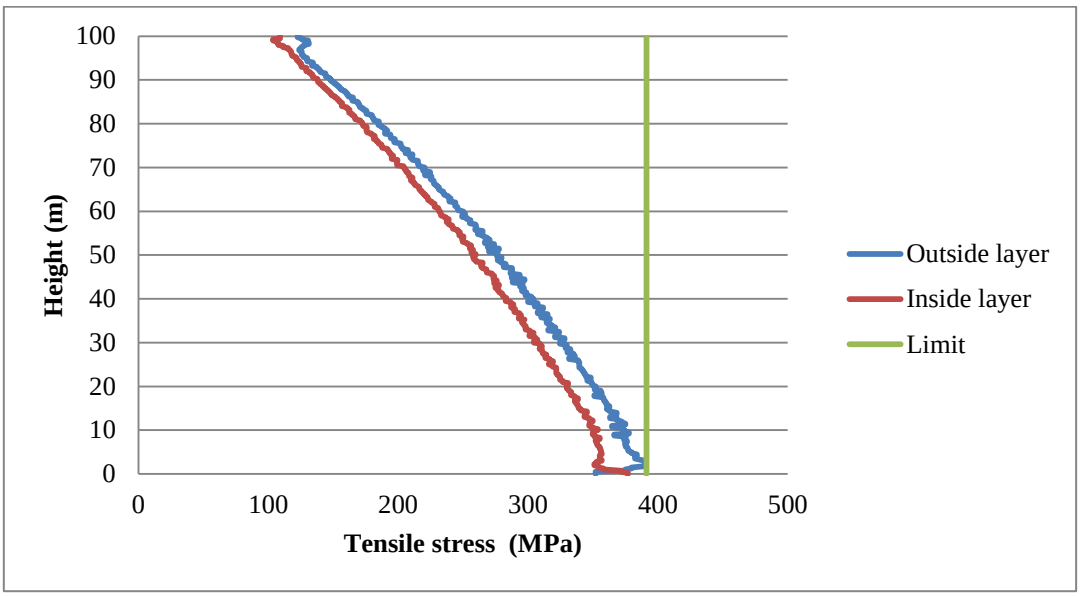

Figure 6-5: Reinforcing tensile stress

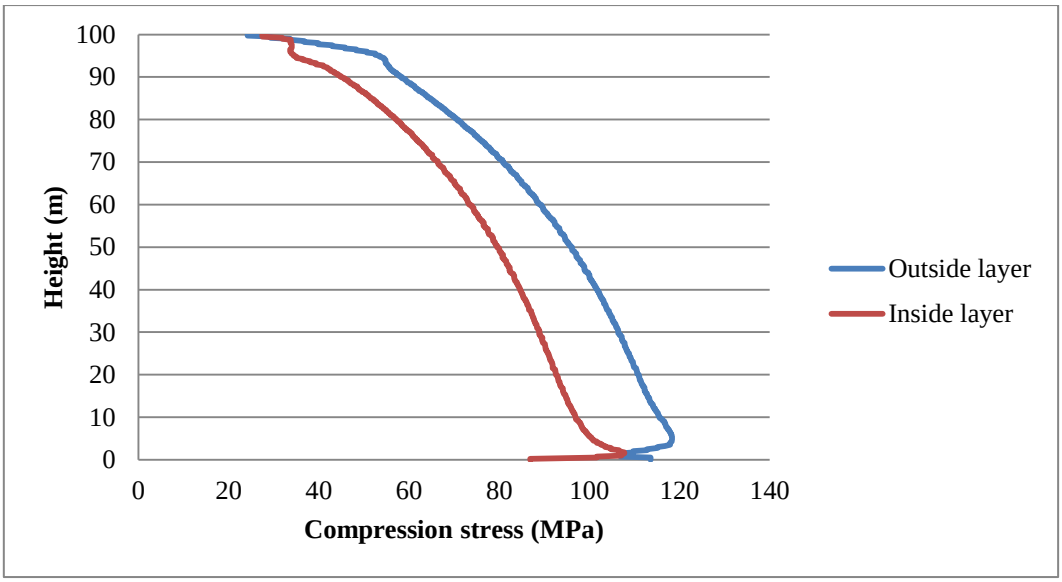

Figure 6-6: Reinforcing compression stress

The percentage reinforcing steel is also calculated according to the ACI 307-98 discussed in section 5.3 - the results are given in Table 6-8. The calculated reinforcing steel according to the ACI method is 13% less than that required by the FEM. A direct comparison between the two methods, however, is not possible as they use two different design methods. The FEM is computed using limit state design and the ACI method is calculated using strength design. The two methods use different partial material factors and it is therefore difficult to make a direct comparison. It is however clear that the ACI method will serve as a good starting point for the design of the reinforcing steel.

Table 6-8: Percentage reinforcing calculated by analytical method.

α (Degrees)*	32.44
Calculated amount of reinforcing required	4400 mm^2/m per layer**
Amount of reinforcing required by FEM	5068 mm^2/m per layer**
Under estimation of analytical method (%)	13.18

*See section 5.3
**2 Vertical layers of reinforcing

6.7. Fatigue

The fatigue life of the tower is evaluated according to the Model Code 2010. The fatigue stress range of the concrete and reinforcing steel is determined by the FEM. The tower is first analyzed under the serviceability loads to allow cracking to occur. The serviceability loads are then reduced by the variable fatigue loads and the structure is analyzed again by using the structural state at the end of the SLS analysis, as an initial state. The difference in stress between the two analyses is then compared to determine the maximum stress range in the concrete and reinforcing. The stress as a function of height for both the concrete and reinforcing are given in Figure 6-7 and Figure 6-8 respectively. The large stress variations above 75 m in Figure 6-8, are due to crack formation in the concrete. The concrete is fully cracked below 75 m and thus the tensile force that is resisted by the concrete, is transferred to the reinforcing steel. Above 75 m, the formation of cracks in the concrete is only starting to take place, and thus in certain areas the tensile force has already been transferred to the reinforcing and in other areas it is still resisted by both the reinforcing and the concrete. This causes the large stress variations. Both figures show stress concentrations at foundation level, due to the boundary conditions discussed above. A summary of the fatigue calculations is given in Table 6-9.

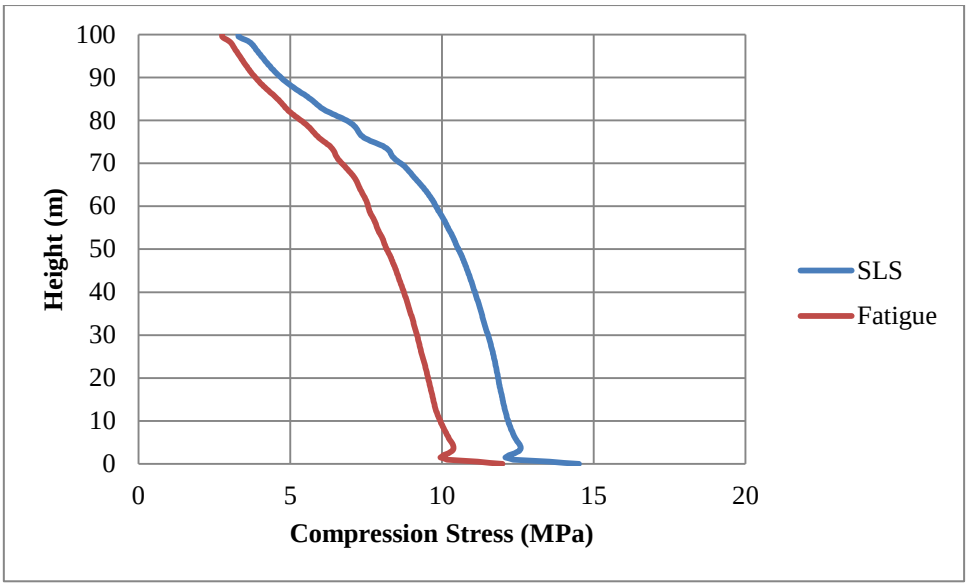

Figure 6-7: Compression stress range of concrete under fatigue loading

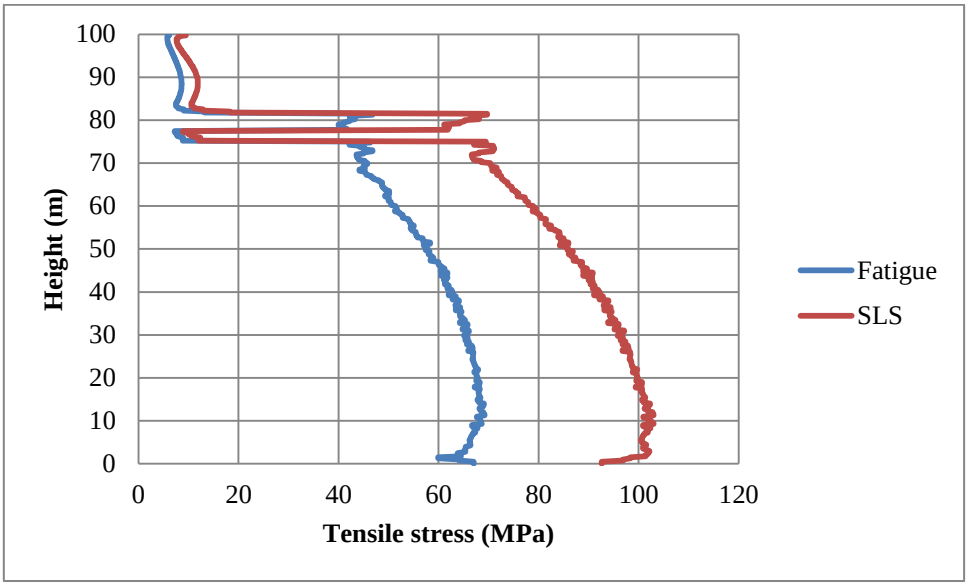

Figure 6-8: Tensile stress range of reinforcing steel under fatigue loading

Table 6-9: Summary of fatigue calculations

Concrete	
Maximum stress, $\sigma_{c,max}$	14.52 MPa
Minimum stress, $\sigma_{c,min}$	12.00 MPa
Calculated maximum load cycles, N	5.065×10^{34}
Applied number of load cycles, n	5.29×10^{8}
n < N, thus the concrete will not fail due to fatigue	

Reinforcing steel	
Maximum stress variation, $\Delta\sigma_{Ss}$	33.83 MPa
$\Upsilon_{ED}\Delta\sigma_{Ss}$	37.22 MPa
$\Delta_{Risk}(n)/\Upsilon_{s,fat}$	89.52 MPa
$\Upsilon_{ED}\Delta\sigma_{Ss} < \Delta_{Risk}(n)/\Upsilon_{s,fat}$, thus the reinforcing steel will not fail due to fatigue	

It is clear from the table that the fatigue limit state will not govern in this project. However the fatigue loads used for the calculations are obtained from computer simulations done by the NREL. The actual fatigue life of the tower can only be accurately determined once the actual fatigue loads of a specific turbine is procured from the turbine manufacturer.

6.8. P-Delta effect

The magnitude of second order effects on the tower is determined by turning on geometric nonlinearity for the FEM and then analyzing the tower at the ULS. The overturning moment is increased by 7.71% due to the P-Delta effect. This increase causes the reinforcing steel's tensile stress to be higher than the allowed maximum stress. The percentage reinforcing should thus be increased to reduce the tensile stress in the reinforcing steel to 391.3 MPa. The stresses in the tower do not increase by the same percentage as the load increases, due to the nonlinear nature of the structure. The increases in stress for the concrete and reinforcing are given in Table 6-10.

Table 6-10: Summary of FEM stress due to P-Delta effect

	ULS	ULS with P-Delta effect	Increase (%)
Overturning moment (MNm)	220.80	237.82	7.71
Concrete compression stress (MPa)	34.52	36.03	4.20
Reinforcing tension stress (MPa)	390.03	416.48	6.35
Reinforcing compression stress (MPa)	118.35	125.05	5.35

The additional moment is also calculated analytically by the method described in section 5.6. To be able to make a direct comparison between the two methods, the maximum deflection computed by the FEM is used to calculate the additional moments with the analytical method. The additional moment is calculated analytically by dividing the tower into a 1000 elements. The integral is then solved by using the method explained in section 5.1. The results for the analytical method are given in Table 6-11.

Table 6-11: Additional moment calculated by analytical method

	Own weight	Turbine weight	Total
Additional moment (MNm)	8.127	6.089	14.215
FEM ULS deflection (mm)	1808		
FEM P-Delta deflection (mm)**	1930		
Percentage increase in tension steel stress (%)	4.71*		

*Calculated from required area of reinforcing steel
**Deflection curve F1 is used. See section 5.8

The analytical method underestimates the additional moment by 16.5%. The most likely reason for this is that the analytical method uses an approximation of the actual deflection curve. The deflection curve has a direct effect on the accuracy of the calculated additional moment and thus any deviation from the actual curve will cause an error.

6.9. Global buckling of tower

Buckling is a mode of failure generally resulting from structural instability, due to compressive action on a structural member. Buckling is characterized by the sudden failure of a compression element. It is therefore important to ensure that buckling does not happen, as there will be no warning that the structure is on the brink of collapse. A wind turbine tower is subjected to compression stress caused by the own weight of the turbine, the turbine overturning moment, the turbine thrust force and the own weight of the tower itself. A buckling analysis is done for the FEM to determine the critical buckling load of the tower. The critical buckling load is computed as 3.76 times the ULS load. Buckling is thus not a critical design consideration.

6.10. Fundamental tower frequency

In this section a sensitivity analysis is done to determine the effect that soil stiffness and the formation of cracks in the concrete can have on the fundamental frequency of the tower. The FEM is used to do an eigenvalue analysis of the uncracked tower with the tower base being fixed for rotation and translation. The model is then modified and a series of eigenvalue analyses is done to determine the effect of different factors on the tower frequency. All the analyses are then compared to this uncracked rigid foundation frequency.

6.10.1. Rigid foundation with tower concrete not cracked

The FEM without foundation was used with the tower completely fixed at its base to determine the modal frequencies of the tower. The mode shapes and Eigen frequencies of the first 10 modes are given in Figure 6-9. The tower is symmetrical around the XY and ZY planes and thus certain mode shapes will occur twice at almost the same frequency. Mode shapes that are the same but occurring around different axes are grouped together in Figure 6-9. The working frequency of turbines was discussed in section 2.8 for variable speed turbines. The turbine loads used in this project is derived for a constant speed turbine. To be consistent with the rest of the design, it is assumed that the turbine rotates at a constant speed when the working frequency is calculated. In practice, the turbine will almost certainly be a variable speed turbine and the procedure described in section 2.8 should be used to calculate the working frequency. The turbine's rotational speed as well as the working frequency is given in Table 6-12.

Table 6-12: Working frequency of turbine

	Operation speed - 1P (rpm)	1P (Hz)	3P (Hz)	Working frequency	
				1.1P (Hz)	2.7P (Hz)
3.6 MW Constant speed	13.2	0.220	0.660	0.242	0.594

Mode 1: 0.445 Hz
Mode 2: 0.446 Hz

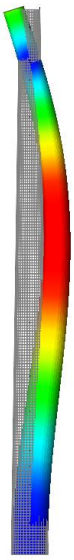

Mode 3: 2.418 Hz
Mode 4: 2.423 Hz

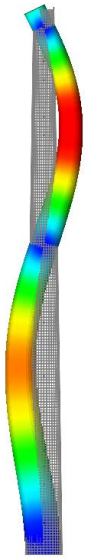

Mode 5: 6.490 Hz
Mode 6: 6.504 Hz

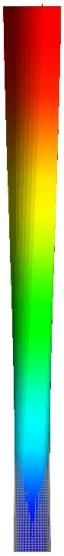

Mode 7: 7.884 Hz

Mode 8: 10.296 Hz

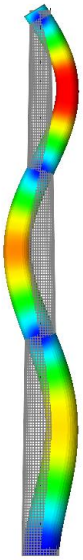

Mode 9: 12.308 Hz
Mode 10: 12.332 Hz

Figure 6-9: Mode shapes of tower not cracked with rigid foundation

The tower's frequency is also calculated using Rayleigh's method discussed in section 5.8. The method uses the deflection curve of the tower to calculate the fundamental frequency of the tower. The actual deflection curve is compared to the two approximate curves discussed earlier to determine their accuracy. The normalized deflection curves are given in Figure 6-10.

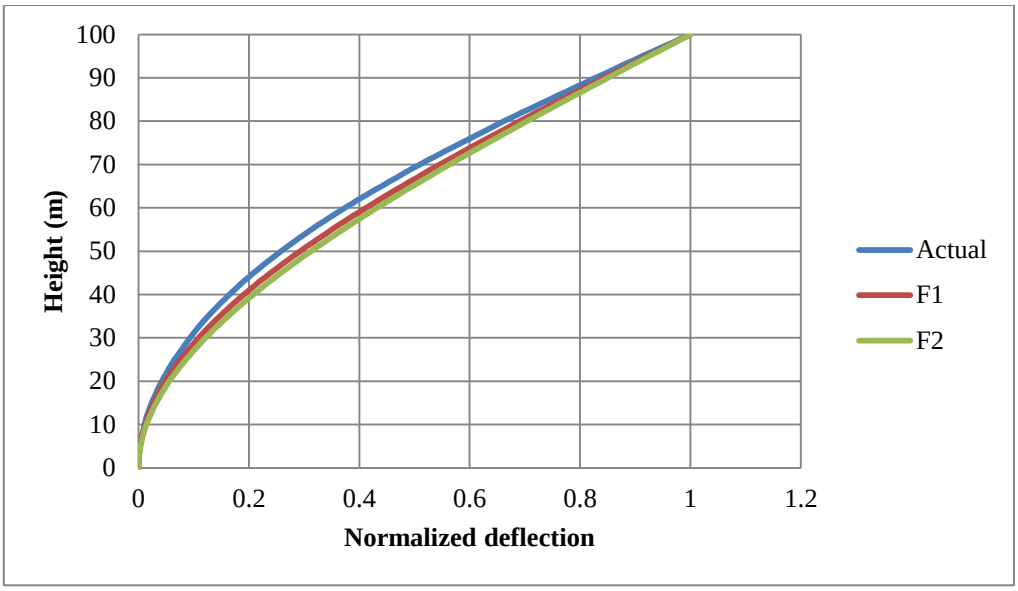

Figure 6-10: Normalized deflection curves

Curve fitting is done to determine the equation describing the actual deflection of the tower. The fitted curve given below has a standard error of 0.000539 and a coefficient of determination of 0.999997.

$$\Delta(y) = a + b.y + c.y^2 + d.y^3 + ey^4 \quad (6.3)$$

Where,

y is the height of interest

a = -1.64 x10^{-3}

b = 6.42 x10^{-4}

c = 6.38 x10^{-5}

d = 8.01 x10^{-7}

e = -5.01 x10^{-9}

The accuracy of Rayleigh's method and its sensitivity to the assumed deflection curve, are calculated by comparing the fundamental frequency obtained by both approximate deflection curves and actual deflection curve to the frequency obtained by the FEM. The results are given in Table 6-13.

Table 6-13: Comparison of Rayleigh's method to FEM

	Fundamental frequency (Hz)	Percentage error (%)
FEM	0.445	-
Actual deflection curve	0.424	-4.72
F1	0.454	2.02
F2	0.463	4.04

It is interesting that the approximate function F1 gives a more accurate answer than the actual deflection function. One reason for this may be that when the equations for Rayleigh's method were derived, it was assumed that the potential energy of the shear strain is negligibly small. If the potential energy due to shear strain is considered, the fundamental frequency will increase slightly. For a stiffer structure the shear strain will start to play a more dominant role and thus by ignoring it, the fundamental frequency will be underestimated. The actual deflection curve is more stiff than the approximate curves and thus the shear strain ignored, is more significant, hence the underestimation of the frequency.

6.10.2. Rigid foundation with concrete cracked

The formation of cracks in concrete reduces the stiffness of the concrete in tension. To determine the effect that this stiffness reduction has on the fundamental frequency of the tower, a structural analysis is done followed by an eigenvalue analysis. The eigenvalue analysis uses the tangent stiffness matrix of the last step of the structural analysis. This is done for both the ULS and SLS - the results are given in Table 6-14 and Table 6-15.

Table 6-14: SLS FEM tower mode frequencies with concrete cracked

Mode shape	1	2	3	4	5	6	7	8	9	10
Uncracked	0.445	0.446	2.418	2.423	6.490	6.504	7.884	10.296	12.308	12.332
SLS (Hz)	0.241	0.325	1.460	1.882	4.246	5.210	5.846	8.310	9.230	9.754
Reduction (%)	45.84	27.13	39.62	22.33	34.58	19.90	25.85	19.29	25.01	20.90

From Table 6-14 it is clear that the fundamental frequency of the tower is significantly reduced by the formation of cracks in the concrete. The reduction causes the frequency to fall outside the working frequency of the tower and will thus cause the tower to resonate. It is interesting to note that the first mode frequency is reduced much more than the second mode frequency, although they have the same mode shape. The reason for this is that the first mode coincides with the deflection direction of the tower in the SLS. The second mode is perpendicular to the applied wind load. This causes less concrete to be cracked in the tension zone of mode two, thus increasing the stiffness in this direction.

Table 6-15: ULS FEM tower mode frequencies with concrete cracked

Mode shape	1	2	3	4	5	6	7	8	9	10
Uncracked	0.445	0.446	2.418	2.423	6.490	6.504	7.884	10.296	12.308	12.332
ULS (Hz)	0.228	0.260	1.310	1.477	3.537	3.991	4.911	6.826	7.484	8.798
Reduction (%)	48.76	41.70	45.82	39.04	45.50	38.64	37.71	33.70	39.19	28.66

Although a much larger percentage of the concrete is cracked in the ULS, the fundamental frequency of the tower is reduced by only 3% from the SLS. The reason being that for both the ULS and the SLS, the tension zone is cracked. The tension zone, and hence the percentage of cracked concrete, is larger for the ULS. This will cause the deflection of the mode shape to increase, but will only slightly decrease the mode frequency when compared to the SLS. The reduction of the second mode shape is much more than the reduction observed at the SLS. At the ULS, the area of cracked concrete has extended to a point where it coincides with the tension zone of the second mode shape, thus reducing the mode frequency.

Rayleigh's method does not take into account the formation of cracks in the concrete. To simulate the stiffness reduction of the cracked concrete, Young's modulus of the concrete is reduced and the same method is used to calculate the fundamental frequency. The analytical frequency is then compared to the cracked FEM frequency that was computed by applying SLS loads to the tower. The results are given in Table 6-16.

Table 6-16: Rayleigh's method with reduced concrete stiffness to simulate cracked concrete

Deflection curve	Mode 1 - $0.75E_c$ (Hz)	Mode 1 - $0.33E_c$ (Hz)	Error - $0.75E_c$ (%)*	Error - $0.33E_c$ (%)*
Actual	0.37	0.27	55.49	14.04
F1	0.40	0.29	66.54	21.39
F2	0.41	0.30	69.82	23.51

*Compared to cracked SLS FEM fundamental frequency

Despite the stiffness of the concrete being reduced by as much as 66%, all the curves still overestimate the fundamental tower frequency. The actual curve gave the best results by estimating the cracked mode frequency within 14% of the FEM frequency.

6.10.3. Flexible foundation with concrete not cracked

The flexibility of the foundation can have a significant effect on the calculated fundamental frequency of the tower. The FEM with foundation that is schematized in section 4.8, is used to determine the mode frequencies of the tower supported on different soil types. The spring stiffness is changed according to the specific soil type being modelled. The results for various soil types are given in Table 6-17.

Table 6-17: Reduction in fundamental frequency due to different soil types

	Fundamental frequency (Hz)		
Soil type*	**Rigid foundation**	**Spring supported**	**% Reduction**
Soft clay	0.445	0.27283	38.69
Clay	0.445	0.32035	28.01
Fine sand	0.445	0.34268	22.99
Sand	0.445	0.36129	18.81
Coarse sand	0.445	0.36694	17.54
Gravel	0.445	0.37835	14.98

* See section 4.7

The percentage reduction in frequency given in Table 6-17 is quite severe. Wind turbine foundations are, however, not constructed on untreated soil. Extensive soil preparation is done before the foundation is constructed. The preparation can include various base layers, compacting techniques and even pile foundations if the soil stiffness is still undesirable. The analysis does, however, emphasize the importance of a detailed geotechnical survey to determine the soil stiffness, as an overestimation of the soil stiffness may cause severe vibrations and or even resonance of the structure. As an alternative, if it is known that the foundation will influence the frequency, the tower's frequency has to be adjusted so that the combined frequency falls within the allowable operating frequency range.

Rayleigh's method is modified in section 5.9 to take account of the foundation flexibility. This method is compared to the FEM results to determine the accuracy of this model. The results obtained by the modified Rayleigh method for different soil types are given in Table 6-18. All three deflection curves are used to calculate the fundamental frequency. The percentage error is calculated to determine which curve approximates the frequency the most accurate. It is interesting that the actual deflection curve that was the least accurate when calculating the fundamental frequency of the tower with rigid foundation, gives the most accurate results for a tower with flexible foundation. As discussed above, the stiffer deflection curves give a lower fundamental frequency due to the shear energy ignored. This underestimation is beneficial when computing the frequency of a tower with flexible foundation. The actual deflection curve approximates the fundamental frequency within 5% of the FEM results for all the soil types. The method is therefore an excellent analytical method for determining the frequency of a tower with a flexible foundation.

Table 6-18: Comparison of fundamental frequencies of different soil types

	Fundamental frequency (Hz)				Percentage error (%)		
Soil type[1]	**FEM**	**Analytical F1[2]**	**F2[2]**	**Actual[3]**	**F1**	**F2**	**Actual**
Soft clay	0.273	0.288	0.290	0.279	5.42	6.26	2.38
Clay	0.320	0.344	0.348	0.330	7.28	8.51	2.93
Fine sand	0.343	0.374	0.379	0.356	9.13	10.62	3.96
Sand	0.361	0.397	0.403	0.376	9.96	11.65	4.12
Coarse sand	0.367	0.404	0.411	0.382	10.23	11.98	4.18
Gravel	0.378	0.419	0.426	0.395	10.80	12.70	4.31

[1] See section 4.7
[2] Based on deflection curves from section 5.8
[3] Based on actual deflection curve

6.10.4. Flexible foundation with tower concrete cracked

This section calculates the reduction in fundamental frequency when the concrete is cracked and the tower is supported on sandy soil. This is an absolute worst case scenario and the probability that both these factors will be present in a well design turbine tower, is low. It does show, however, that for an accidental load case where the concrete is cracked and the foundation is flexible, the fundamental frequency can be reduced as much as 64%. This will almost certainly lead to resonance of the tower and ultimately structural failure. The FEM results are given in Table 6-19.

Table 6-19: Mode frequencies for cracked tower with foundation on sand

Mode shape	1	2	3	4	5	6	7	8	9	10
Uncracked	0.445	0.446	2.418	2.423	6.490	6.504	7.884	10.296	12.308	12.332
ULS - Sand (Hz)	0.161	0.185	1.079	1.098	3.074	3.284	4.286	5.479	6.226	6.545
Reduction (%)	63.82	58.52	55.38	54.68	52.63	49.51	45.64	46.79	49.42	46.93

6.11. Four node element vs eight node element

The effect that the number of nodes per curved shell element have on the accuracy of the results is investigated by analyzing the same model with 4 node elements and then with 8 node elements. The analysis time is also computed to determine if the increase in accuracy can justify the increase in analysis time.

Table 6-20: Comparison between 4 node and 8 node elements

	Error (%)*
Maximum reinforcing tension stress	3.43
Maximum reinforcing compression stress	0.59
Maximum concrete compression stress	1.42
Maximum deflection	1.62
Increase in analysis time	56.39

*Error when 4 node results are compared to 8 node results

The results obtained by using 8 node curved shell elements are slightly more accurate, but the analysis time increased by 56% making it difficult to justify the increase in accuracy.

6.12. Correction factor for tower frequency and deflection in cracked state

This section proposes an analytical model for calculating the maximum deflection and fundamental frequency of the tower in the cracked state. The analytical model is compared to four different FEM's to evaluate its accuracy. The FEM discussed in Chapter 4 is used with four different percentages of reinforcing steel to model the tower with different degrees of cracking.

It is found that for all four FEM's, crack formation starts when the tower deflection is between 0.14% and 0.16% of the tower height. This serves as a guide when deciding if the tower should be modelled in the cracked or uncracked state with the analytical method.

The proposed analytical model assumes that the concrete in the tension zone of the section is cracked and that it has no stiffness in tension. The stiffness reduction is incorporated into the analytical methods discussed in Chapter 5 by reducing the concrete's modulus of elasticity. This is shown mathematically below:

$$E_{reduced} = E_c \left(\frac{x}{D}\right) \tag{6.4}$$

Where,

$E_{reduced}$ is the cracked concrete's modulus of elasticity for the section
D is the tower diameter
x is the length of the compression zone

The position of the neutral axis can be calculated using the method described in section 5.3. The compression zone length is then computed by subtracting the neutral axis position from the diameter of the tower.

The results for the analytical model are compared to that of the FEM in Table 6-21. From the table it is clear that the modified analytical model gives conservative results when compared to the FEM. The model estimates the deflection within 21% of the FEM deflection. It is thus a valuable method for calculating the deflection of the tower in the cracked state.

Table 6-21: Results for analytical deflection in cracked state

Layout #	Vertical Steel per layer (mm^2/m)	Maximum reinforcing steel stress (MPa)	FEM maximum deflection (mm)	Analytical deflection-uncracked (mm)	Modified analytical model 1	
					Deflection – cracked (mm)	Error * (%)
1	4401	443.9	2015	516	2447	21.48
2	5068	390.0	1808	507	2173	20.22
3	6545	309.7	1489	489	1738	16.76
4	7919	260.3	1292	472	1470	13.81

* Error when compared to FEM deflection

The fundamental frequency calculated by the modified analytical model is compared to the results obtained from the FEM in Table 6-22. The analytical method estimated the cracked fundamental frequency of the tower within 5% of the frequency computed by the FEM. The modified analytical model is thus an excellent method for computing the fundamental frequency of the tower in the cracked state and may even be accurate enough to use in the detailed design stage.

Table 6-22: Results for analytical tower frequency in cracked state

Layout #	Vertical Steel per layer (mm^2/m)	Fundamental frequency (Hz)		Error* (%)
		FEM - cracked	Modified analytical method - cracked	
1	4401	0.204	0.215	5.36
2	5068	0.216	0.228	5.11
3	6545	0.241	0.252	4.14
4	7919	0.262	0.271	3.26

* Error when compared to FEM frequency

The process for calculating the deflection and natural frequency of the tower is summarized below:

1. Determine if tower is cracked : $deflection > \frac{0.16}{100}.(Height\ of\ tower)$
2. Determine position of neutral axis: section 5.3
3. Determine compression zone length: $(Tower\ diameter) - (neutral\ axis\ position)$
4. Calculate reduced modulus of elasticity for concrete: equation 6.4
5. Calculate cracked deflection by using reduced modulus of elasticity: section 5.5
6. Calculate cracked fundamental frequency using reduced modulus of elasticity: section 5.8

It is important to note that these models are calibrated using the tower investigated in this report and that care should be taken when applying them to towers falling outside the scope of the investigation. Differences in height, reinforcing layout and level of loading may all affect the cracked deflection.

Chapter 7: Conclusion and recommendations

Concrete wind turbine towers play a vital role in ensuring the continuous development of large scale wind turbines. The lack of knowledge on the design of concrete wind turbine towers in SA gave rise to this research project. The aim of this project is to investigate and highlight important aspects of the design process of a reinforced concrete wind turbine tower. The tower is designed using nonlinear finite element modelling as a design tool to accurately design the tower for various loads and load cases. An analytical design method is developed that can be used in the preliminary design stage. Finally the importance of the soil-structure interaction is investigated through a sensitivity analysis. The findings of the project are given below:

7.1. Tower deflection

It is important that the displacement at the top of the tower is limited to avoid the efficiency of the turbine to decrease. It is found that the formation of cracks has a significant effect on the stiffness of the tower. This stiffness reduction leads to a large increase in the maximum deflection of the tower. It is found that the percentage reinforcing steel required for the ULS may not necessary be sufficient to limit the deflection of the tower in the SLS. Alternatively, the tower geometry could be adjusted to limit its deflection, but cracking leads to significantly non-proportional deflection increase beyond 75% of the SLS load, which indicates that an increase in the percentage of reinforcement may help.

The analytical method used to estimate the maximum deflection of the tower underestimated the deflection of the tower by 60% for the SLS. The reason is that the analytical method assumes that the concrete is uncracked. The modified analytical method, however, takes into account the stiffness reduction caused by the formation of cracks and gave conservative results when compared to the FEM. The overestimation of the modified analytical method was in the order of 21%. The method can thus successfully be used to compare different tower models in the preliminary design stage.

7.2. Crack formation in the concrete

The formation of cracks in the concrete is found to be one of the most important factors influencing the behaviour of the tower. The deflection, durability and dynamic behaviour of the tower are all strongly influenced by the formation of cracks. The crack width computed by the FEM indicates that the cracks may cause durability problems if the structure is situated in an aggressive environment. It is found that the reduction of the bar spacing is a cost effective method of reducing the crack width. The analytical method for estimating the maximum crack width gives conservative crack widths when compared to the FEM.

7.3. Reinforced high strength concrete

Concrete with cylinder compression strength of 80 MPa is used for the tower. It is found that the strength class can be reduced due to a large strength reserve available. The high stiffness of the high

strength concrete used may, however, be necessary to increase the tower's fundamental frequency to avoid resonance.

The stress in the concrete is dominated by normal stresses due to bending. It is found that the principal stress of the concrete is almost identical to the normal stress due to bending. The shear strength of the concrete is thus not as critical as the compression strength.

The analytical method for calculating the moment strength of the tower gives a good first estimate of the percentage reinforcing required. It does, however, underestimate the amount of reinforcing steel required with 13%.

7.4. Fatigue design

The Model code 2010 is identified as an appropriate code for evaluating the fatigue life of the tower due to the fact that the code makes provision for high cycle fatigue of high strength concrete. It is found that fatigue is not a critical design consideration for the tower designed in this project. The fatigue loads used for the calculations are, however, not actual turbine fatigue loads. To accurately evaluate the fatigue life of the tower it is necessary to use the actual fatigue loads for a specific turbine.

7.5. Second order effects

Second order effects increase the overturning moment of the tower by 7.7%. It is thus important to take account of the P-Delta effect when the structure is analyzed, as the increase in overturning moment may lead to an unsafe structure if it is ignored.

7.6. Dynamic behaviour

The sensitivity analyses done on the fundamental frequency of the tower emphasize the importance of modelling the actual structure and boundary conditions as accurately as possible when carrying out an Eigenvalue analysis. The fundamental frequency of the tower is reduced by 46% after the tower has cracked. This reduction leads to the tower frequency falling outside the working frequency of the turbine.

The soil stiffness has a significant influence on the tower's natural frequency. The frequency is reduced by 37% when the foundation is built on soft clay. It is, however, extremely unlikely that the foundation will be built on untreated soft soil. When the foundation is built on gravel, which is more realistic, the frequency is reduced by 15%. The preparation of the soil under the foundation will thus strongly influence the dynamic behaviour of the tower.

7.7. Future research and recommendations

This project investigated the basic design of a concrete wind turbine tower, but it will be valuable to do a complete detailed design in future. The detailed design should focus on aspects like stress concentrations at the foundation tower interface, at the turbine-tower interface and at the door frame. Precast construction holds many advantages and it will be beneficial to investigate the behaviour of precast segments and especially the behaviour of the joints connecting the segments. The design of the horizontal steel in the tower that prevents ovalization and temperature gradient cracks, is not investigated in this project and must be designed in future studies. It became clear while doing this project, that the formation of cracks in the concrete can have a significant effect on the behaviour of the tower and even make it difficult to predict the dynamic behaviour. Post-tensioned tower construction is suitable for dynamically loaded structures and will eliminate the formation of cracks in the concrete, if the post-tension force is sufficiently large. This has the benefit that it is possible to accurately compute the fundamental frequency of the tower. The durability of the structure will also be greatly increased. These advantages of post-tensioned concrete constructions may justify the cost increase of the method.

The most important aspect of future designs, however, is the procurement of actual turbine loads from the manufacturers. These loads will enable the researcher to do an accurate design that can serve as a design template of concrete wind turbine towers. This study showed the need and importance of a design code for concrete wind turbine towers.

Bibliography

3TIER. (2009). 3TIER Global Wind Dataset: Africa Validation. *White Paper*.

ACI 224. (2007). *Causes, Evaluation, and Repair of Cracks in Concrete Structures.* Farmington Hills: American Concrete Institute.

ACI 307. (1998). *Design and Construction of Reinforced Concrete Chimneys.* American Concrete Institute.

ACI 318. (2011). *Building Code Requirements for Structural Concrete.* American Concrete Institute.

Adhikari, S. (2010). Effect of wind on structure. *Structural engineering forum of India*.

ASCE 7-10. (2010). *Minimum Design Loads for Buildings and Other Structures.* American Society of Civil Engineers.

Bachmann et al, H. (1995). *Vibration Problems in Structures.* Berlin: Birkhauser Verlag.

Bamforth, P., & Chisholm, D. (2008). *Properties of Concrete for use in Eurocode 2.* The Concrete Centre.

Brughuis, F. (2004). *Large wind turbines: the higher the bette.* Netherlands: Advanced Tower Systems.

Buchholdt, H., & Moossavi Nejad, S. (2012). *Structural Dynamics for Engineers.* London: ICE.

Caldarone, M. A. (2009). *High-Strength Concrete: A practical guide.* New York, USA: Taylor & Francis.

Carucci, V. (2010). Resonance and Magnification in Piping System Vibration. *Carmagen Engineering*.

CEB-FIB. (2010). *Model Code 2010.* Switzerland: International Federation for Structural Concrete (fib).

Constantinescu, H., & Magureanu, C. (2011). Study of shear behaviour of high performance concrete using push-off tests. *Civil Engineering and Installations*.

Danza, H., Irassar, E., & Cabrera, O. (2002). High-strenght concrete with different fine aggregate. *Cement and Concrete Research*.

de Rábago, J. (2011). Precast concrete wind towers and offshore foundations: A huge market coming ahead. *Consolis*.

de Vries, E. (2012, June 27). *Close up - the E126, still the world's biggest turbine*. Retrieved June 13, 2014, from windpowermonthly: http://www.windpowermonthly.com/article/1138562/close---e126-worlds-biggest-turbine

Deep Resource. (2013, June 24). *DeepResource: Observing the world of geopolitics, energy and other resources* . Retrieved June 13, 2014, from http://deepresource.wordpress.com/2013/06/24/enercon-e-126/

Diana 9.4.4. (2012). Diana's user manual. In *Element Library Chapter 9.* The Netherlands: TNO-DIANA.

DNV, & Riso. (2002). *Guidelines for the design of wind turbines.* Denmark: Det Norske Veritas, Riso National Laboratory.

DNV/RISO. (2002). *Guidelines for design of wind turbines.* Denmark.

Dvorak, P. (2011). *windpowerengineering*. Retrieved June 4, 2014, from http://www.windpowerengineering.com/construction/challenges-in-moving-huge-and-heavy-components/

EN 1992-1-1: 2004. (n.d.). *Eurocode 2 Design of concrete structures-Part 1.1: General rules for buildings.* European Committee for Standardization.

Gaspar, R. (2012). *Concrete wind towers: a low-tech innovation for a high-tech sector.* X&Y Partners.

Gazetas, G. (1983). Analysis of machine foundation vibrations: state of the art. *Soil Dynamics and Earthquake Engineering*.

Giosan, I. (n.d.). Vortex Shedding Induced Loads on Free Standing Structures. *Structural Vortex Shedding Response Estimation Methodology and Finite Element Simulation*.

GWEC. (2013). *Global Wind Energy Report.* Global Wind Energy Council.

Hendriks, e. (2012). Guidelines for Nonlinear Finite Element Analysis of Concrete Structures. *Rijkswaterstaat Centre for Infrastructure*.

Hibbeler, R. (2008). *Mechanics of Materials.* Singapore: Pearson.

IEC. (2005). International Electrotechnical Commission 61400-1 - Third edition. *Wind turbines Part 1: Design requirements*.

Illston, J., & Domone, P. (2009). *Construction Materials.* New York: Spon Press.

Inneo Torres. (n.d.). Retrieved November 18, 2013, from Assembly Process: http://www.inneo.es/index.php/en/installation-process.html

International Electrotechnical Commission. (2005). IEC 61400-1 - Third edition. *Wind turbines Part 1: Design requirements*.

IRENA. (2012). RENEWABLE ENERGY TECHNOLOGIES: COST ANALYSIS SERIES. *International Renewable Energy Agency*.

LaNier, M. (2004). *LWST Phase I Project Conceptual Design Study: Evaluation of Design and Construction Approaches for Economical Hybrid Steel/Concrete Wind Turbine Towers.* Washington: National Renewable Energy Laboratory.

LaNier, M., & PE Berger/ABAM Engineers. (2004). *LWST Phase I Project Conceptual Design Study: Evaluation of Design and Construction Approaches for Economical Hybrid Steel/Concrete Wind Turbine Towers.* Colorado: National Renewable Energy Laboratory.

McCormac, C. J., & Brown, H. R. (2014). Design of Reinforced Concrete - Ninth Edition.

Model Code 2010. (2011). The International Federation for Structural Concrete.

NorthField, C. (n.d.). *Case studies NorthField construction*. Retrieved June 4, 2014, from http://www.northfield-construction.co.uk/case-studies.php?cat=3&study=5

Owens, G., & Addis, B. (2001). *Fultons`s concrete technology.* Cement and Concrete institute.

P&H. (2012). *Contact Us* . Retrieved June 12, 2014, from Earth Systems: http://earthsys.com/cm/Contact/Patrick%20and%20Henderson%20Contact%20Information.html

Ragan, P., & Manuel, L. (2007). Comparing Estimates of Wind Turbine Fatigue Loads using Time-Domain and Spectral Methods. *Wind Engineering*.

Ray, M. (2006). Analysis of wind shear models and trends in different terrains. *Renewable Energy Research Laboratory*.

Robberts, J., & Marshall, V. (2010). *Analysis and design of concrete structures.* Nuclear structural engineering.

SABS 0100-1. (2000). *Part 1: Design The structural use of concrete.* The South African Bureau of Standards.

SANS 10100-1: 2000. (n.d.). *The structural use of concrete - Part 1: Design.* South African National Standards.

SANS 10160-3. (2011). *Basis of structural design and actions for buildings and industrial structures Part 3: Wind actions.* SABS.

Szewczuk , S. (2012). *Review of the strategic wind energy activities in South Africa.* Pretoria, South Africa: CSIR Built Environment.

Techet, A. (2005). Vortex Induced Vibrations. *Massachusetts Institute of Technology*.

TRH 11. (2009). *Dimensional and mass limitations and other requirements for abnormal load vehicles.* Pretoria.

Tricklebank, A., & Magee, B. (2005). *Concrete towers for onshore and offshore wind farms.* UK: The concrete centre.

van Zyl, W. (2012). High strength concrete in Southern Africa. *University of Stellenbosch*.

Appendix A

FEM without foundation

The FEM used for all structural analysis is shown below:

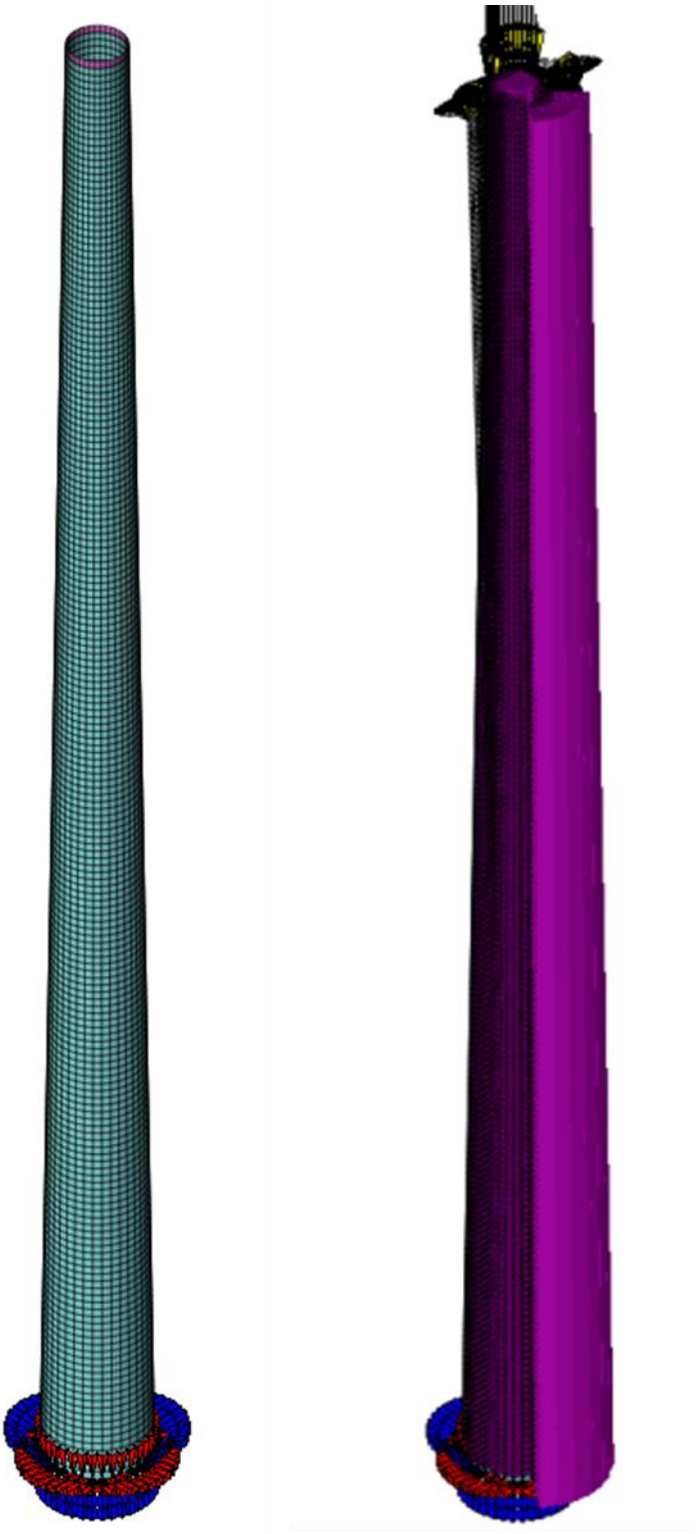

FEM model with and without loads

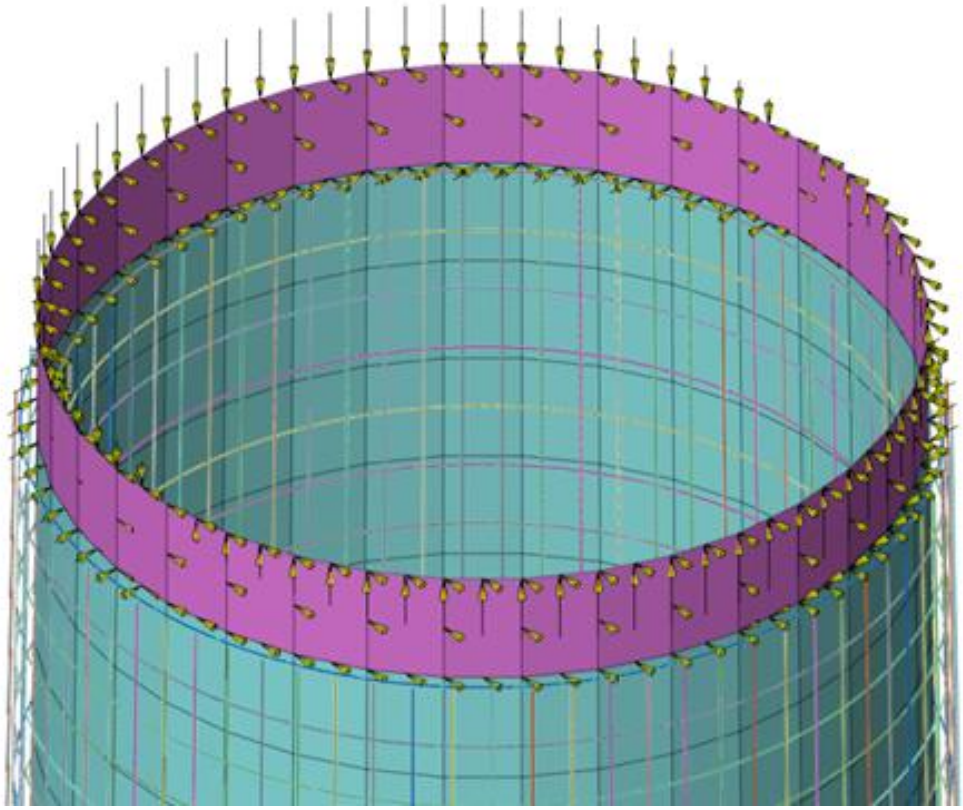

Steel ring with turbine loads applied to it

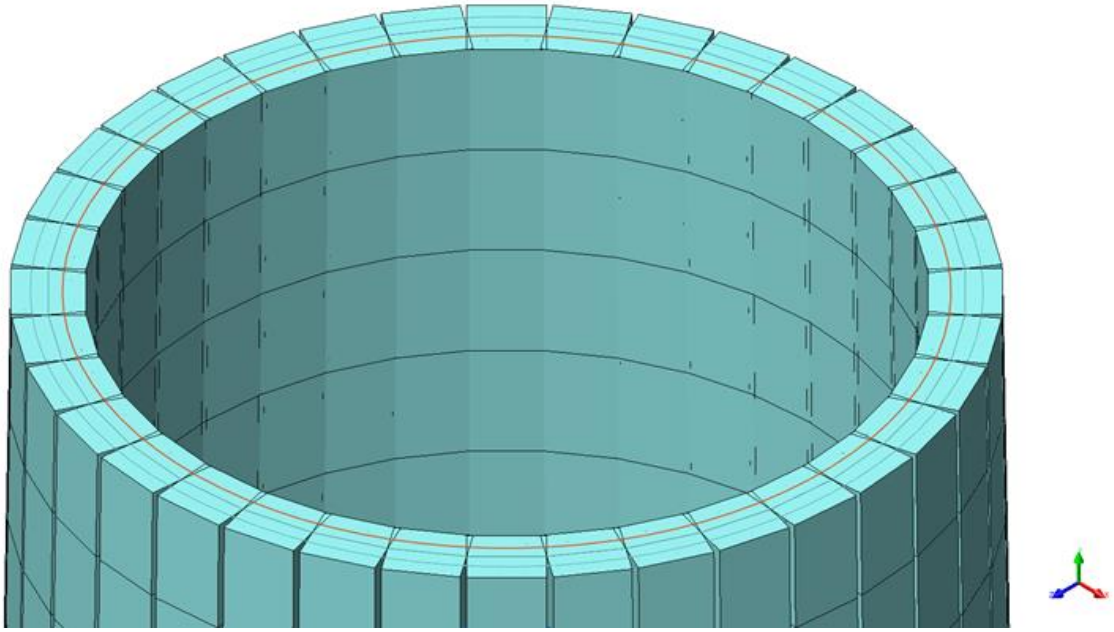

Rendered shell elements with layers of reinforcing visible

FEM with foundation

The FEM that is used to investigate the soil stiffness effect on the tower is shown below:

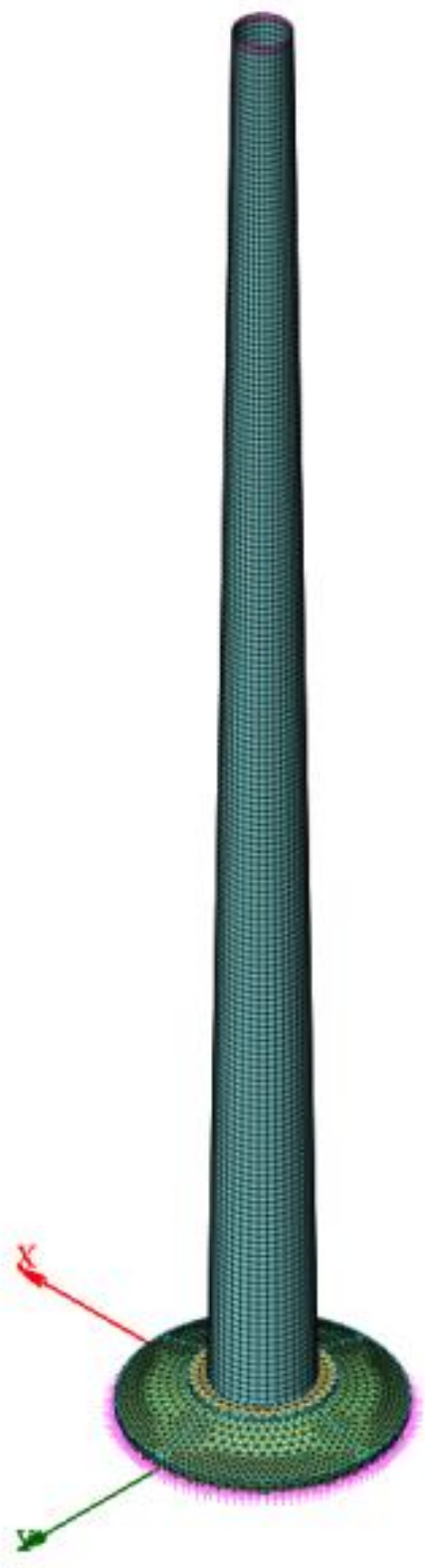

Tower with foundation

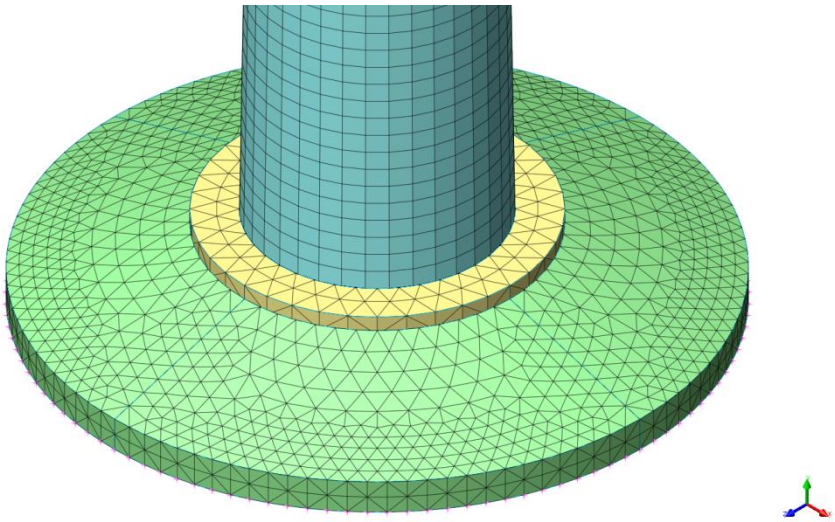

Foundation detail

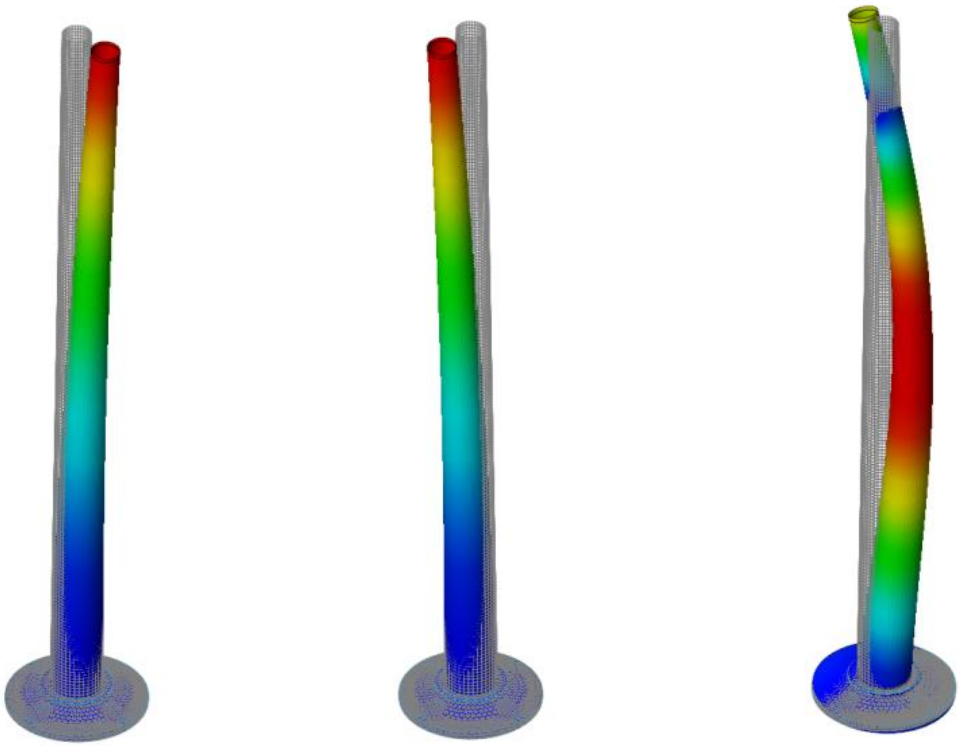

Mode 1 Mode 2 Mode 3

Mode shapes with foundation

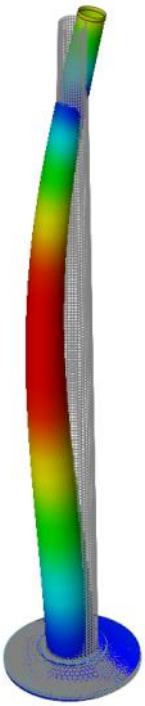

Mode 4

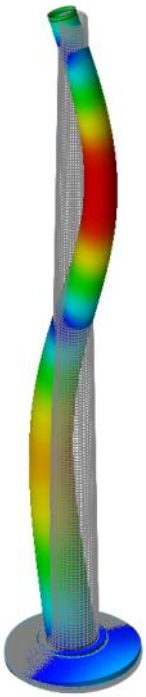

Mode 5

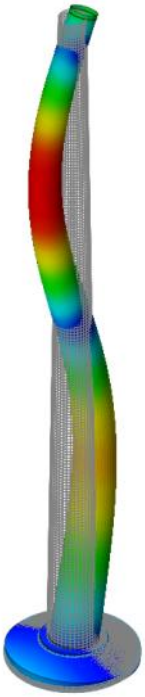

Mode6

Mode shapes with foundation

Mode7

Mode 8

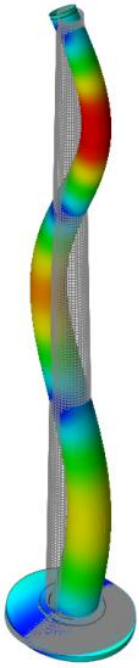

Mode 9

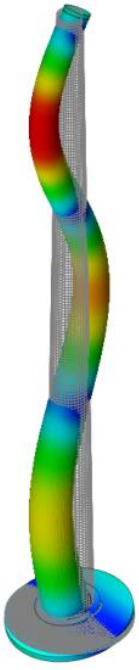

Mode 10

Mode shapes with foundation

Appendix B: 3TIER wind data

The 30 year wind data obtained from 3TIER is converted to an extreme 50 year wind speed by using a software program called Windographer. The results for three wind farms currently in operation are given below:

Dassiesfontein - 100m

Wind speed characteristics

Quantity	Value
Mean wind speed (m/s)	7.415
Weibull k	1.980

Results

Method	Vref (50 yr) (m/s)
Periodic Maxima	35.621
Method of Independent Storms	31.510
EWTS II (Exact)	31.667
EWTS II (Gumbel)	32.093
EWTS II (Davenport)	34.821

Cookhouse -100m

Wind speed characteristics

Quantity	Value
Mean wind speed (m/s)	8.050
Weibull k	1.946

Results

Method	Vref (50 yr) (m/s)
Periodic Maxima	35.210
Method of Independent Storms	28.528
EWTS II (Exact)	35.164
EWTS II (Gumbel)	35.637
EWTS II (Davenport)	38.642

Van Staden - 100m

Wind speed characteristics

Quantity	Value
Mean wind speed (m/s)	7.849
Weibull k	2.166

Results

Method	Vref (50 yr) (m/s)
Periodic Maxima	32.802
Method of Independent Storms	30.235
EWTS II (Exact)	29.916
EWTS II (Gumbel)	30.321
EWTS II (Davenport)	32.982

Appendix C: UK concrete center tower design

The UK concrete center did a preliminary design for a 100 m concrete pre-cast wind turbine tower.

The proposed design is given below:

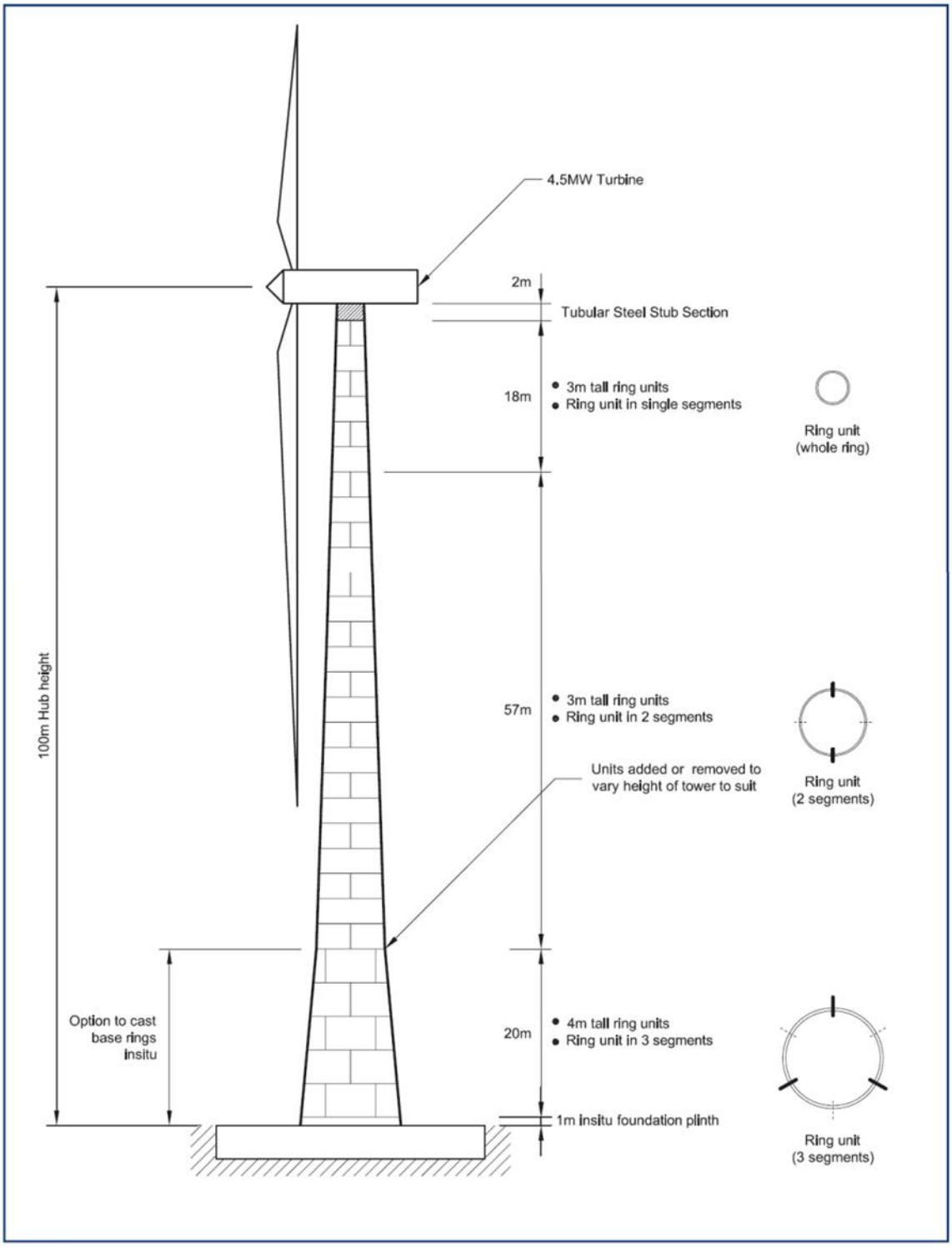

Preliminary design of 100 m concrete tower (Tricklebank & Magee, 2005)

Appendix D: Companies currently designing concrete towers

ACCIONA

Concrete tower segments assembled

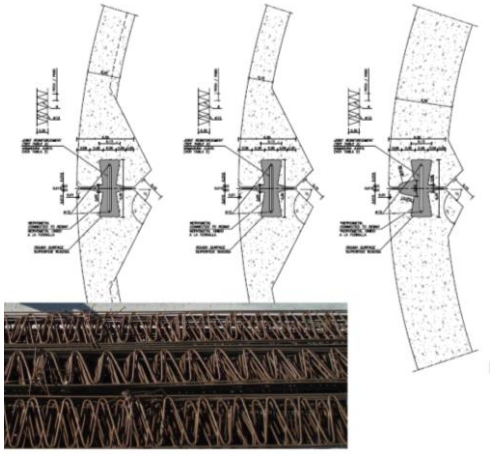

Vertical joint detail

Inneo Torres

Tower segments transported on normal truck

Max Bögl

Self-climbing crane

Advance Tower systems (ATS)

Rectangular pre-cast design

Hormifuste

Pre-cast factory

Enercon

Small pre-cast sections